FEBRUARY 2020 Ph.D in Engineering Physics YILDIZ BERK ATEŞ

REPUBLIC OF TURKEY

GAZİANTEP UNIVERSITY

GRADUATE SCHOOL OF NATURAL & APPLIED SCIENCES

THE INVESTIGATION OF THE EFFECTS OF VELOCITY DEPENDENT POTENTIAL IN THE SOLUTION OF WAVE EQUATION

Ph.D. THESIS

IN

ENGINEERING PHYSICS

BY

YILDIZ BERK ATEŞ

FEBRUARY 2020

THE INVESTIGATION OF THE EFFECTS OF VELOCITY DEPENDENT POTENTIAL IN THE SOLUTION OF WAVE EQUATION

Ph.D. Thesis

in

Engineering Physics

Gaziantep University

Supervisor

Prof. Dr. Eser OLĞAR

by

Yıldız BERK ATEŞ

February 2020

©2020[Yıldız BERK ATEŞ]

REPUBLIC OF TURKEY
GAZİANTEP UNIVERSITY

GRADUATE SCHOOL OF NATURAL & APPLIED SCIENCES

ENGINEERING PHYSICS

Name of the Thesis : The Investigation of the Effects of Velocity Dependent Potential in the Solution of Wave Equation

Name of the Student : Yıldız BERK ATEŞ

Exam Date : 06.02.2020

Approval of the Graduate School of Natural and Applied Sciences

Prof. Dr. A. Necmeddin YAZICI
Director

I certify that this thesis satisfies all the requirements as a thesis for the degree of Doctor of Philosophy.

Prof. Dr. Ramazan KOÇ
Head of Department

This is to certify that we have read this thesis and that in our opinion it is fully adequate, in scope and quality, as a thesis for the degree of Doctor of Philosophy.

Prof. Dr. Eser OLĞAR
Supervisor

Examining Committee Members	Signature
Prof. Dr. Hayriye TÜTÜNCÜLER	…………………..
Prof. Dr. Eser OLĞAR	…………………..
Assoc. Prof. Dr. M. Fatih HASOĞLU	…………………..
Assoc. Prof. Dr. Abdullah KABLAN	…………………..
Asst. Prof. Dr. Tuba DENKÇEKEN	…………………..

I hereby declare that all information in this document has been obtained and presented in accordance with academic rules and ethical conduct. I also declare that, as required by these rules and conduct, I have fully cited and referenced all material and results that are not original to this work.

Yıldız BERK ATEŞ

ABSTRACT

THE INVESTIGATION OF THE EFFECTS OF VELOCITY DEPENDENT POTENTIAL IN THE SOLUTION OF WAVE EQUATION

BERK ATEŞ, Yıldız

Ph.D in Engineering Physics

Supervisor: Prof. Dr. Eser OLĞAR

February 2020

88 pages

In this thesis, the effect of the velocity-dependent potential is taken into consideration in order to obtain the solution of Schrödinger equation (SE) for different physical potentials. By choosing form factors as three different cases such as $\varepsilon(r) = \gamma\rho_0, \varepsilon(r) = \gamma r$ and $\varepsilon(r) = \gamma r^2$, the velocity-dependent potential is determined and the energy eigenvalues and eigenfunction are obtained for any quantum numbers n and l. During all calculations, the well-known method Nikiforov-Uvarov (NU) method is used. It is seen that by taking $\gamma = 0$, the obtained results are reduced to results of velocity-independent potential case which are in good agreement with those of in literature. The variations of energy eigenvalues are tabulated and graphed with respect to quantum numbers *n* and *l.*

Key Words: Velocity-Dependent Potentials, Analytical Solution, Numerical Solution, Nikiforov-Uvarov Method.

ÖZET

HIZA BAĞLI POTANSİYELLERİN DALGA DENKLEMLERİ ÜZERİNE ETKİSİNİN ARAŞTIRILMASI

BERK ATEŞ, Yıldız

Doktora Tezi, Fizik Mühendisliği

Danışman: Prof. Dr. Eser OLĞAR

Şubat 2020

88 sayfa

Bu tez çalışmasında, Schrödinger dalga denkleminin farklı fiziksel potansiyeller için çözümünü elde etmek için, hıza bağlı potansiyelin etkisi dikkate alındı. Form faktörü $\varepsilon(r) = \gamma\rho_0, \varepsilon(r) = \gamma r$ ve $\varepsilon(r) = \gamma r^2$ gibi üç farklı durumda seçerek hıza bağlı potansiyel heaplandı ve herhangi bir kuantum durumuna karşılık gelen enerji özdeğerleri ve özfoksiyonları elde edilmiştir. Tüm hesaplamalar boyunca, yaygın olarak kullanılan Nikiforov-Uvarov metodu kullanılmıştır. Form faktörü $\gamma = 0$ olarak alındığında elde edilen sonuçlar, hıza bağlı olmayan potansiyel formuna indirgenerek literatürle iyi uyum içerisinde olduğu görüldü. Enerji değişimleri kuantum sayıları n ve l ye göre tablo ve grafik haline getirildi.

Anahtar Kelimeler: Hıza bağlı Potansiyeller, Analitik çözüm, Nümerik Çözüm, Nikiforov-Uvarov Method.

"Dedicated to my dear doughter Cemre ATEŞ and my mother

Ayşe berk"

ACKNOWLEDGEMENTS

First of all I would like to thank my supervisor Prof. Dr. Eser OLĞAR for his support and advices during my thesis. Secondly, I wish to thank my mother, Ayşe BERK and my husband, Mehmet Ali ATEŞ for his support during all my Ph.D. education and thank my daughter Cemre ATEŞ to give me joy of life.

TABLE OF CONTENTS

Page

ABSTRACT .... **v**

ÖZET .... **vii**

ACKNOWLEDGEMENTS .... **viii**

TABLE OF CONTENTS .... **ix**

LIST OF TABLES .... **xi**

LIST OF FIGURES .... **xiii**

CHAPTER 1 .... **1**

INTRODUCTION **1**

CHAPTER 2 .... **6**

THEORY OF VELOCITY-DEPENDENT POTENTIAL **6**

2.1 Velocity-Dependent Potential 6

2.2 Schrödinger Equation With Velocity-Dependent Potential 6

2.3 Nikiforov-Uvarov Method 7

CHAPTER 3 .... **10**

APPLICATIONS TO PHYSICAL POTENTIALS **10**

3.1 Case 1: State of form factor $\varepsilon(r) = \gamma\rho_0$ 10

3.1.1 Harmonic Oscillator 11

3.1.2 Coulomb potential 13

3.1.3 Hulthen Potential 17

3.1.4 Kratzer Potential 21

3.1.5 Mie potential 24

3.1.6 Cornell Potential 27

3.1.7 Woods-Saxon Potential 31

3.1.8 Pöschl-Teller Potential 34

3.2 Case 2: State of form factor $\varepsilon(r) = \gamma r$ 38
3.2.1 Harmonic Oscillator 39
3.2.2 Coulomb Potential 42
3.2.3 Hulthen Potential 45
3.2.4 Kratzer Potential 49
3.2.5 Mie Potential 52
3.2.6 Cornell Potantial 55
3.2. 7 Woods-Saxon Potential 58
3.2.8 Pöschl-Teller Potential 61
3.3 Case 3: State of form factor $\varepsilon(r) = \gamma r^2$ 64
3.3.1 Harmonic Oscillator 64
3.3.2 Hulthen Potential 68
3.3.3 Woods-Saxon Potential 72
3.3.4 Pöschl-Teller Potential 74
CHAPTER 4 .... Hata! Yer işareti tanımlanmamış.
CONCLUSION .... Hata! Yer işareti tanımlanmamış.
REFERENCES **82**
CURRICULUM VITAE **88**

LIST OF TABLES

Page

Table 3.1 The energy eigenvalues of the Coulomb potential in Case 1 under $\gamma = 0.02, \mu = 1/2, \hbar = 1, A = 50, \rho_0 = 4.$ 16

Table 3.2 The energy eigenvalues of the Hulthen potential in Case 1 under $\gamma = 0,5$ $\mu = 1/2, \hbar = 1, K = 0.006, \kappa = 10, \rho_0 = 0.1.$ 20

Table 3.3 The energy eigenvalues of the Kratzer potential in Case 1 under $A = -0.5$ $B = 0.1, C = -0.05, \gamma = 50, m = 1/2, \hbar = 1, \rho_0 = 0.5.$ 23

Table 3.4 The energy eigenvalues of the Mie potential in Case 1 under $m = 1/2,$ $a = 10, \gamma = 5, V_0 = 5, \rho_0 = -2.$ 26

Table 3.5 The energy eigenvalues of theCornell potential in Case 1 under $\delta = -5,$ $\mu = 1/2, \alpha = 5, \hbar = 1, \rho_0 = 1, b = 1.3, \gamma = 0.01, a = -0.5.$ 30

Table 3.6 The energy eigenvalues of the Woods-Saxon potential in Case 1 under $\gamma = 0.05, m = 1/2, \hbar = 1, V_0 = 0.06, \beta = 2, \rho_0 = -5.$ 34

Table 3.7 The energy eigenvalues of the Pöschl-Teller potential in Case 1 under $\gamma = 0.6, m = 1/2, \hbar = 1, V_0 = 0.5, \delta = -0.03, \rho_0 = 10.$ 38

Table 3.8 The energy eigenvalues of the Harmonic oscillator potential in Case 2 $w = 10, \alpha = -0.48, \delta = 2, \gamma = -25, m = 1/2, \hbar = 1.$ 41

Table 3.9 The energy eigenvalues of the Coulomb potential in Case 2 under $\gamma = 0.02, \delta = -2, \mu = 1/2, \hbar = 1, A = 50.$ 44

Table 3.10 The energy eigenvalues of the Hulthen potential in Case 2 under $K = 0.06, \kappa = 10, \gamma = 0.5, \delta = -0.05, m = 1/2\hbar = 1.$ 48

Table 3.11 The energy eigenvalues of the Kratzer potential in Case 2 under $A = -0.05, B = 0.1, C = -0.05, \gamma = 50, \delta = 0.3, m = 1/2, \hbar = 1.$ 51

Table 3.12 The energy eigenvalues of the Mie potential in Case 2 under

$m = 1/2, a = 10, \gamma = 5, V_0 = 0.06, \hbar = 1$. 54
Table 3.13 The energy eigenvalues of the Cornell potential in Case 2 under $\delta = -5, m = 1/2, \alpha = 5, \hbar = 1, b = 1.3, \gamma = 0.01, a = -0.05$. 57
Table 3.14 The energy eigenvalues of the Woods-Saxon potential in Case 2 under $m = 1/2, \gamma = 0.05, \hbar = 1, V_0 = 0.06, \delta = -0.005$. 60
Table 3.15 The energy eigenvalues of the Pöschl-Teller potential in Case 2 under $\gamma = 0.6, \delta = -0.03, m = 1/2, \hbar = 1, V_0 = 0.5$. 63
Table 3.16 The energy eigenvalues of the Harmonic oscillatör potential in Case 3 under $w = 10, \alpha = -0.48, \delta = 0,5, \gamma = -25, m = 1/2, \hbar = 1$. 67
Table 3.17 The energy eigenvalues of the Hulthen potential in Case 3 under $K = 0.06, \kappa = 10, \gamma = 0.5, \delta = -0.05, m = 1/2, \hbar = 1$. 71
Table 3.18 The energy eigenvalues of the Woods –Saxon potential in Case 3 under $m = 1/2, \gamma = 0.05, \hbar = 1, V_0 = 0.06$. 73
Table 3.19 The energy eigenvalues Pöschl-Teller potential in Case 3 under $\gamma = 0.6$, $m = 1/2, \hbar = 1, V_0 = 0.5, \alpha = -0.004$. 77

LIST OF FIGURES

Page

Figure 3.1 Harmonic oscillator potential for w=10, m=1⁄2. 11

Figure 3.2 Coulomb potential for A=50. 14

Figure 3.3 The graph of energy eigenvalues of the Coulomb potential in Case 1 for $\gamma = 0.02, \mu = 1/2, \hbar = 1, A = 50, \rho_0 = 4$. 17

Figure 3.4 Hulthen potential for $K = 0.06; \kappa = 10$. 18

Figure 3.5 The graph of energy eigenvalues of the Hulthen potential in Case 1 for $\gamma = 0,5, \mu = 1/2, \hbar = 1, K = 0.006, \kappa = 10, \rho_0 = 0.1$. 20

Figure 3.6 Kratzer potential for $A = -0.05, B = 0.1; C = -0.05$ **Hata! Yer işareti tanımlanmamış.**

Figure 3.7 The graph of energy eigenvalues of the Kratzer potential in Case 1 for $A = -0.5, B = 0.1, C = -0.05, \gamma = 50, m = 1/2, \hbar = 1, \rho_0 = 0.5$. 23

Figure 3.8 Mie Potential for $a = 10, V_0 = 0.06$ 24

Figure 3.9 The graph of energy eigenvalues of the Mie potential in Case 1 for $m = 1/2, a = 10, \gamma = 5, V_0 = 5, \rho_0 = -2$. 26

Figure 3.10 Cornell potential for $b = 1.3, a = -0.5$ 27

Figure 3.11 The graph of energy eigenvalues of the Cornell potential in Case 1 for $\delta = -5, \mu = 1/2, \alpha = 5, \hbar = 1, \rho_0 = 1, b = 1.3, \gamma = 0.01, a = -0.5$... 30

Figure 3.12 Woods-Saxon potential for $V_0 = 0.06, \beta = 2, q = 1$. 31

Figure 3.13 The graph of energy eigenvalues of Woods-Saxon potential in Case 1 for $\gamma = 0.05, m = 1/2, \hbar = 1, V_0 = 0.06, \beta = 2, \rho_0 = -5$. 34

Figure 3.14 Pöschl-Teller potential for $V_0 = 0.5, q = 1$. 35

Figure 3.15 The graph of energy eigenvalues of the Pöschl-Teller potential in Case1 for $\gamma = 0.6, m = 1/2, \hbar = 1, V_0 = 0.5, \delta = -0.03, \rho_0 = 10$. 38

Figure 3.16 The graph of energy eigenvalues of the Harmonic oscillator potential in

Case 2 for $w = 10, \alpha = -0.48, \delta = 2, \gamma = -25, m = 1/2, \hbar = 1$. ……………..42

YÖK

Figure 3.17 The graph of energy eigenvalues of the Coulomb potential in Case 2 for $\gamma = 0.02, \delta = -2, \mu = 1/2, \hbar = 1, A = 50$. 44
Figure 3.18 The graph of energy eigenvalues of the Hulthen potential in Case 2 for $K = 0.06, \kappa = 10, \gamma = 0.5, \delta = -0.05, m = 1/2, \hbar = 1$. 49
Figure 3.19 The graph of energy eigenvalues of the Kratzer potentialin Case 2 for $A = -0.05, B = 0.1, C = -0.05, \gamma = 50, \delta = 0.3, m = 1/2, \hbar = 1$. 52
Figure 3.20 The graph of energy eigenvalues of Mie potential in Case 2 for $m = 1/2,\ a = 10, \gamma = 5, V_0 = 0.06, \hbar = 1$. 54
Figure 3.21 The graph of energy eigenvalues of Cornell potentialin Case 2 for $\delta = -5, m = 1/2, \alpha = 5, \hbar = 1, b = 1.3, \gamma = 0.01, a = -0.05$. 58
Figure 3.22 The graph of energy eigenvalues of Woods- Saxon potential in Case 2 for $\gamma = 0.05, \hbar = 1, V_0 = 0.06, \delta = -0.005$. 61
Figure 3.23 The graph of energy eigenvalues of Pöschl-Teller potential in Case 2 for $\gamma = 0.6, \delta = -0.03, m = 1/2, \hbar = 1, V_0 = 0.5$. 64
Figure 3.24 The graph of energy eigenvalues of Harmonic oscillator potential in Case for $w = 10, \alpha = -0.48, \delta = 0,5, \gamma = -25, m = 1/2, \hbar = 1$. 68
Figure 3.25 The graph of energy eigenvalues of Hulthen potential in Case 3 for $K = 0.06, \kappa = 10, \gamma = 0.5, \delta = -0.05, m = 1/2, \hbar = 1$. 71
Figure 3.26 The graph of energy eigenvalues of Woods-Saxon potential in Case 3 for. $m = 1/2, \gamma = 0.05, \hbar = 1, V_0 = 0.06$. 74
Figure 3.27 The graph of energy eigenvalues of Pöschl-Teller potential in Case 3 for $\gamma = 0.6, m = 1/2, \hbar = 1, V_0 = 0.5, \alpha = -0.004$. 78

LIST OF SYMBOLS

δ	Delta
γ	Gamma
ε	Epsilon
ξ	XI
λ	Lamda
μ	Mu
τ	Tau
σ	Sigma
ω	Omega
κ	Kappa
φ	Phi
ħ	Tshe
α	Alpha
θ	Theta

CHAPTER 1

INTRODUCTION

The eigenvalue problem plays an important role in order to analyze many physical systems in branches of physics such as quantum mechanics, nuclear physic and atomic and molecular physic,….etc. The energy spectrum of most of these systems is determined by using the solution of second order differential wave equation called Schrödinger equation. Generally, it is possible to obtain the solution of wave equation for all physical potentials describing some physical interaction. When it is considered in content are second order differential equation, it is well known that the exact solution of Schrödinger equation for physical potentials is limited to few number of potentials. In the presence of complex potentials, it is difficult to obtain the analytic solution. Therefore only the approximate solution can be obtained. In order get rid of this problem, some analytical methods and approximation are proposed. The common methods and approximations are WKB approximation [1], time independent Perturbation method [2], Variational method [3], Supersymetric quantum mechanics [4], 1/N expansion [5] … etc.

One type of the solution of wave equation in quantum physics is the bound state solution which is a special quantum state of a particle subject to a potential that the corresponding particle has a tendency to localize in some regions of space. For example, the bound state solution of Schrödinger equation in the presence of Hulthen potential is solved by using Nikoforov-Uvarov method [6], the shifted 1/N expansion [7] method and Supersymetric quantum mechanics (SUSY) method [8-11]. Any l-state solution of Schrödinger equation for Hulthen potential is determined in [12] by framework of Asymptotic Iteration method (AIM) [13-15]. Similar to these applications, the bound state solutions for other potentials are studied with different methods such as Kratzer potential [16-19], Mie potential [20-22], the Coulomb potential [23], Harmonic oscillator [23], Woods-Saxon [24-25] and Pöschl-Teller potential [26, 27].

One of the interesting applications of Schrödinger equation in physics is the effects of velocity-dependent potential in the wave equation. In recent years, the spectrum analysis of Schrödinger equation in the presence of velocity-dependent potential has drawn great attention of researchers. The velocity-dependent potential was first derived to analyze scattering of meson from the complex nuclei in nuclear physic [28]. In the atomic physic, the velocity dependent potential was used to demonstrate the scattering of electrons from the oxygen and neon atoms [29]. At the same time, the solution of radial Schrödinger equation by velocity-dependent potential is used for describing particles with a position-dependent effective mass [30, 31]. Although the solution of the Schrödinger equation with velocity-dependent potential holds an important place in many different fields of physics, the exact analytical solution for such an equation is only possible with the angular momentum l=0 for some potential models. For this reason the effect of isotropic velocity-dependent potentials on the energy spectrum has been studied using different methods as analytically and approximately [32-39].

In reference [40], the bound state solution of Schrödinger equation was calculated for condition of s-wave case by using the formal scattering theory. The availability of scattering theory is given with two analytical evidences. One of the is using directly non-local velocity-dependent potential and the other proof is equivalent non-local but energy dependent. The energy spectrums of Schrödinger equation are obtained analytically and numerically for velocity-dependent potential has the form of a square-well.

Additionally the bound state solution of Schrödinger equation is investigated in the p-wave state by framework formal the scattering theory with using general function of velocity-dependent term [41].

Jaghoub studied the solution of the Schrödinger equation with an isotropic velocity-dependent potential which has the form of a constant perturbing potential and perturbing Harmonic oscillator under a local square-well potential field in the presence of general function of form factor by using perturbation theory [42].

The exact bound state solution of the Schrödinger equation was evaluated in presence of velocity-dependent perturbing potential for different value of form factor which are $\varepsilon(r) = \gamma\rho_0$ and $\varepsilon(r) = \gamma r^2$ [43]. In this study, although the wave function is obtained analytically, the eigenvalues is determined only numerically.

Additional to this study, the solution of wave equation with velocity-dependent potential by using perturbation method for general functional form of form factor is done by Jaghoub [44]. Developed model has been applied for the changes in the scattering phase-shift and wave function by considering the velocity-dependent interaction as a small perturbation. In order to test the validity of the obtained model, it was applied to fully soluble model for nucleon-nucleon scattering. The results were in good agreement with those of the fully soluble model.

The eigenvalues and eigenfunction of Morse potentials in the framework of velocity-dependent effects are investigated for any quantum states of l by considering the cases of form factor as $\varepsilon(r) = \gamma\rho_0$ and $\varepsilon(r) = \gamma r^2$ [45]. The corresponding energy spectrum are derived analytically only for $\varepsilon(r) = \gamma\rho_0$ and numerically for $\varepsilon(r) = \gamma r^2$ in the context of Asymptotic Iteration method (AIM).

Also, Bayrak and collaborators [46] extended their model to Coulomb and Harmonic oscillator potentials in order to get the solution of radial Schrödinger equation including an isotropic velocity -dependent potentials. In a similar way, only the analytical solution was calculated only for the case of $\varepsilon(r) = \gamma\rho_0$.

The velocity-dependent potential is used to produce the single-particle energy levels for general function of form factor in [47]. At the same time the single-particle energy states of neutrons were calculated and compared with the experimental data, in order to show the truth of their model.

The single-particle energy spectrums are evaluated for some closed shell heavy and super heavy nuclei by using a form of an effective velocity-dependent nucleon-nucleus potential [48]. Although a general analytical solution is derived for velocity-dependent potential, the numerical values of the single-particle energy have been calculated by using general function of form factor.

The velocity-dependent potential is reproduced to define the dynamics of a rigid body in a rotating frame, and this potential has been associated to electromagnetic analogs in [49]. In this study, the form factor is considered as a general function and rigid body problem is formed in the presence of effect of velocity-dependent potential.

The static potential of an electron interacting is display with an atom by a sum of two Debye-Huckel or Yukawa functions, using velocity-dependent potential with a regularized Yukawa form factor [50]. In spite of the authors focused on a general solution, numerical values of energy were calculated by making different approaches to general function of the velocity-dependent potential term.

In [51], the analytic solution of Schrodinger equation with Morse potential is present when velocity-dependent potentials has a general form factor function. Moreover, energy spectrums of neutrons are obtained for any quantum states by using perturbation method for a general function of velocity dependent term and a constant form. The obtained results are compared with experimental data.

Another study on Morse potential is included in [52]. The corresponding eigenfunctions is determined to approximate a nonlocal or velocity-dependent nucleon-nuclear potential by using Hartree-Fock calculations.

When all studies related to energy- dependent potential are concluded it can be seen that the analytic solution of potentials are limited to a few potential for the form factor is not constant. The solution of Schrödinger equation in the case of constant form factor can be obtained easily by any method. In non-constant form factor case, the form factor is considered as a function and the corresponding energy spectrum are calculated by using perturbation expansion. In the view of these studies, our aim is to increase the number of solved velocity-dependent potentials in physics. During the study, the Nikiforov-Uvarov method is used to overcome this deficiency in literature. In this context, the solution of Schrödinger equation by taking into account of velocity-dependent effect for different states of form factor, the Harmonic oscillator, Coulomb, Hulthen, Kratzer, Mie, Cornell, Wood-Saxon and Pöschl-Teller potentials are considered. The energy eigenvalues of these potentials have been calculated for all states of form factor. The solution of some potential were obtained analytically and for some of them numerically. The obtained results were compared with literature and energy graphs were drawn.

This thesis consists of 4 chapters. The organization of the thesis is as follows. In Chapter 1, the information about thesis and a brief description of velocity-dependent potential are presented in addition to literature survey. The theory of velocity-dependent potential and NU method are given in Chapter 2. The application of Schrödinger equation for velocity-dependent potential such as Harmonic oscillator, Coulomb, Kratzer, Mie, Hulthen, Cornell, Woods-Saxon and Pöschl-Teller potentials are presented in Chapter 3. Finally, conclusions and noteworthy results are discussed in the last chapter.

CHAPTER 2

THEORY OF VELOCITY-DEPENDENT POTENTIAL

The definition of velocity-dependent potential is presented in this chapter. Using this definition, the radial part of Schrödinger equation is formed when the part of form factor is considered in the potential.

2.1 Velocity-Dependent Potential

Kisslinger potential, namely the effect of velocity-dependent potential is determined as terms of del and gradient operators as,

$$\nabla(\varepsilon(r)\nabla\psi) = \varepsilon(r)\nabla^2\psi + \nabla\varepsilon(r).\nabla\psi \tag{2.1}$$

where ψ is a three-dimensional wave function and $\varepsilon(r)$is an isotropic function of the radial variable *r*. In equation, the first term on the right is actually a kinetic energy term and for this reason the name velocity-dependent potential, which associated with the kinetic energy term in the Schrödinger equation. This potential, which correctly predicted the predominantly p-wave nature of the pion-nucleon scattering, was produced by Kisslinger [28]. The form function $\varepsilon(r)$ can be taken to represent the nuclear density. As a result, the second term in Eq. (2.1) is sensitive to the diffuse edge in nuclei which is especially important in light ones [40].

2.2 Schrödinger Equation with Velocity-Dependent Potential

The velocity-dependent potential is a superposition of the $V_{eff}(r)$ and the isotropic velocity-dependent $V_{total}(r,p)$ potentials which has form [28],

$$V_{total}(r,p)=V_{eff}(r)+\frac{\hbar^2}{2m}\left[\varepsilon(r)\nabla^2+\vec{\nabla}\varepsilon(r).\vec{\nabla}\right] \tag{2.2}$$

Where, $V_{eff}(r)=\frac{l(l+1)}{r^2}+V(r)$ with the corresponding physical potential $V(r)$, $\hbar$ is the Planck constant, m is the mass of the particle. The radial Schrödinger equation in terms of Eq. (2.12) may be written as,

$$\left[-\frac{\hbar^2}{2m}\nabla^2+V_{total}(r,p)\right]R(r)=ER(r) \tag{2.3}$$

for a particle with energy E moving under the isotropic velocity-dependent potential. Substituting Equation (2.2) into Eq. (2.3) yields,

$$\left[-\frac{\hbar^2}{2m}\nabla^2+V_{eff}(r)+\frac{\hbar^2}{2m}\left(\varepsilon(r)\nabla^2+\vec{\nabla}\varepsilon(r).\vec{\nabla}\right)\right]R(r)=ER(r). \tag{2.4}$$

In the presence of effective potential, the Schrödinger equation in Equation (2.4) is transformed to

$$\left[-\frac{\hbar^2}{2m}\nabla^2+\frac{l(l+1)}{r^2}+V(r)+\frac{\hbar^2}{2m}\left(\varepsilon(r)\nabla^2+\varepsilon'(r).\vec{\nabla}\right)\right]R(r)=ER(r). \tag{2.5}$$

which is the required Schrödinger equation form including velocity-dependent potential function.

2.3 Nikiforov-Uvarov Method

Nikiforov-Uvarov (NU) is a method of solving the second order linear equations with special functions. The energy spectrums of many physical systems have been investigated Nikiforov-Uvarov method [53-59]. This method, the non-relativistic Schrödinger equation or similarly in used frequently in the solution of independent second order differential equations the method. In this method, it is necessary to express any Schrödinger equation or second order differential equation as follows.

$$\psi_n''(s)+\frac{\tilde{\tau}(s)}{\sigma(s)}\psi_n'(s)+\frac{\tilde{\sigma}(s)}{\sigma^2(s)}\psi_n(s)=0 \tag{2.6}$$

Where $\sigma(s)$ and $\tilde{\sigma}(s)$ are polynomials, at most of second degree, and $\tilde{\tau}(s)$ is a first-degree polynomial. To make the application of the NU method simpler and more direct, we introduce a more compact presentation of the idea. In order to do this, the Equation (2.6) is rewritten as follows [23].

$$\psi_n''(s)+\left(\frac{c_1-c_2 s}{s(1-c_3 s)}\right)\psi_n'(s)+\left(\frac{-\xi_1 s^2+\xi_2 s-\xi_3}{s^2(1-c_3 s)^2}\right)\psi_n(s)=0, \tag{2.7}$$

in which the wave function is in form of

$$\psi_n(s)=\phi(s)\,y_n(s). \tag{2.8}$$

Comparing Equation (2.7) with Equation (2.6), following identifications are obtained

$$\tilde{\tau}(s)=c_1-c_2 s,\quad \sigma(s)=s(1-c_3 s),\quad \tilde{\sigma}(s)=-\xi_1 s^2+\xi_2 s-\xi_3. \tag{2.9}$$

With these equations the necessary parameters for the solution of the equation are derived.

(i) The relevant constant

$$\begin{aligned}
c_4 &= \frac{1}{2}(1-c_1)\\
c_5 &= \frac{1}{2}(c_2-2c_3)\\
c_6 &= c_5^2+\xi_1\\
c_7 &= 2c_4c_5-\xi_2\\
c_8 &= c_4^2+\xi_3\\
c_9 &= c_3c_7+c_3^2c_8+c_6\\
c_{10} &= c_1+2c_4+2\sqrt{c_8}\\
c_{11} &= c_2-2c_5+2\left(\sqrt{c_9}+c_3\sqrt{c_8}\right)\\
c_{12} &= c_4+\sqrt{c_8}\\
c_{13} &= c_5-\left(\sqrt{c_9}+c_3\sqrt{c_8}\right)
\end{aligned} \tag{2.10}$$

(ii) The essential polynomial functions

$$\begin{aligned}
\pi(s) &= c_4+c_5 s-\left[\left(\sqrt{c_9}+c_3\sqrt{c_8}\right)s-\sqrt{c_8}\right],\\
k &= -(c_7+2c_3c_8)-2\sqrt{c_8c_9},\\
\tau(s) &= c_1+2c_4-(c_2-2c_5)s-2\left[\left(\sqrt{c_9}+c_3\sqrt{c_8}\right)s-\sqrt{c_8}\right].
\end{aligned} \tag{2.11}$$

(iii) The energy equation

$$\lambda=c_2 n-(2n+1)c_5+(2n+1)\left(\sqrt{c_9}+c_3\sqrt{c_8}\right)+n(n-1)c_3+c_7+2c_3c_8+2\sqrt{c_8c_9}. \tag{2.12}$$

(iv) The wave function

$$\rho(s) = s^{c_{10}}\left(1-c_3 s\right)^{c_{11}},$$
$$\phi(s) = s^{c_{12}}\left(1-c_3 s\right)^{c_{13}},\ c_{12}>0,\ c_{13}>0, \tag{2.13}$$
$$y_n(s) = P_n^{(c_{10},c_{11})}\left(1-2c_3 s\right),\ c_{10}>-1,\ c_{11}>-1,$$

where $P_n^{(\mu,\nu)}(x),\ \mu>-1,\ \nu>-1$, and $x\in[-1,1]$ are Jacobi polynomials with

$$P_n^{(\alpha,\beta)}(1-2s) = \frac{(\alpha+1)_n}{n!}\,{}_2F_1(-n,1+\alpha+\beta+n;\alpha+1;s), \tag{2.14}$$

and $N_{n\kappa}$ is a normalization constant. Also, the above wave functions can be expressed in terms of the hypergeometric function as following,

$$\psi_{n\kappa}(s) = N_{n\kappa}s^{c_{12}}\left(1-c_3 s\right)^{c_{13}}\,{}_2F_1(-n,1+c_{10}+c_{11}+n;c_{10}+1;c_3 s) \tag{2.15}$$

where $c_{12}>0,\ c_{13}>0$ and $s\in[0,1/c_3],\ c_3\neq 0.$

In the rather more special case of $c_3=0$, the wave functions can be written in form of the Laguerre function as following,

$$\psi_{n\kappa}(s) = N_{n\kappa}s^{c_{12}}e^{c_{13}s}L_n^{c_{10}-1}(c_{11}s).$$

CHAPTER 3

APPLICATIONS TO PHYSICAL POTENTIALS

In this chapter, the effect of velocity-dependent potentials on the solution of SE has been investigated and energy spectrums are obtained for well-known physical potentials. For the first time, here the solution of the radial Schrödinger equation with the Harmonic oscillator, Coulomb, Hulthen, Kratzer ,Mie, Cornell, Woods-Saxon and Pöschl-Teller potentials including velocity dependent are obtained for any quantum states for different form factor by using the Nikiforov-Uvarov method. The corresponding energy eigenvalues are calculated in the presence of velocity-dependent potentials.

The applications in this section will be discussed in three different categories. These are;

i) $\varepsilon(r) = \gamma\rho(r) = \gamma\rho_0$

ii) $\varepsilon(r) = \gamma\rho(r) = \gamma r$

iii) $\varepsilon(r) = \gamma\rho(r) = \gamma r^2$

3.1 Case 1: State of form factor $\varepsilon(r) = \gamma\rho_0$

In this case, by taking form factor $\varepsilon(r) = \gamma\rho(r) = \gamma\rho_0$ the Schrödinger equation in Equation. (2.14) becomes,

$$R''[r] + \frac{2}{r(-1+\gamma\rho_0)}R'[r] - \frac{\left(-2E_n mr^2 + l(l+1)\hbar^2 + 2mr^2V[r]\right)}{r^2\hbar^2(-1+\gamma\rho_0)}R[r] = 0. \tag{3.2}$$

By considering different examples of $V(r)$, equation is reduced to the eigenvalue equation to be.

3.1.1 Harmonic Oscillator

The meaning of Harmonic oscillator [59] is around an average value at one or more characteristic frequencies in physical systems. The Harmonic oscillator is a model for many physical systems, describing it's a natural movement by harmonic equation. For example acoustic vibration of solid, vibration motion of molecules, electro-magnetic waves, etc. The graph of the potential is given in Figure 3.1.

The Harmonic oscillator potential is given by

$$V[r]=\frac{1}{2}m\omega^2 r^2,$$

where ω is the angular velocity.

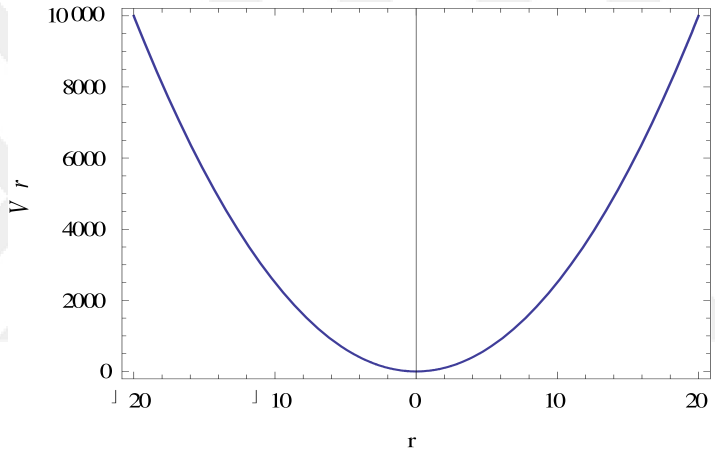

Figure 3.1 Harmonic oscillator potential for *w*=10, *m*=1⁄2.

By substituting $V[r]$ in Equation (3.1), the Schrödinger equation becomes

$$R''[r]+\frac{2}{r(1-\gamma\rho_0)}R'[r]+\left[\frac{\left(2E_n r^2\mu-mr^4w^2\mu-l(l+1)\hbar^2\right)}{r^2\hbar^2(1-\gamma\rho_0)}\right]R[r]=0. \tag{3.2}$$

By performing the change of new variable $r\to\alpha\tau$ and substituting into the Equation (3.2), the equation is transformed to

$$\frac{(1-\gamma\rho_0)}{\alpha^2}R''[\tau]+\frac{2}{\alpha^2\tau}R'[\tau]+\frac{\left(2E_n\alpha^2\mu\tau^2-mw^2\alpha^4\mu\tau^4-l(l+1)\hbar^2\right)}{\alpha^2\tau^2\hbar^2}R[\tau]=0. \tag{3.3}$$

Similarly using the transformation, $\tau\to\sqrt{s}$ Equation. (3.3) becomes,

$$U''[s]+\frac{(3-\gamma\rho_0)U'[s]}{2s(1-\gamma\rho_0)}+\frac{\left(s\alpha^2\mu\left(-2E_n+sw^2\alpha^2\mu\right)+l(1+l)\hbar^2\right)U[s]}{4s^2\hbar^2(-1+\gamma\rho_0)}=0. \tag{3.4}$$

By comparing Equation (3.4) with Eq. (2.5) then following parameters are obtained,

$$\xi_1=-\left(mw^2\alpha^4\mu\right)/\left(4(-1+\gamma\rho_0)\hbar^2\right)$$
$$\xi_2=\left(-2E_n\alpha^2\mu\right)/\left(4(-1+\gamma\rho_0)\hbar^2\right)$$
$$\xi_3=-\left(l(1+l)\hbar^2\right)/\left(4(-1+\gamma\rho_0)\hbar^2\right)$$

Other c_i terms are obtained using Equation (2.6) as follows,

$$\begin{aligned}
c_1&=3/\left(2(1-\gamma\rho_0)\right)\\
c_2&=0\\
c_3&=0\\
c_4&=\frac{1+2\gamma\rho_0}{-4+4\gamma\rho_0}\\
c_5&=0\\
c_6&=-\frac{mw^2\alpha^4\mu}{4(-1+\gamma\rho_0)\hbar^2},\\
c_7&=\frac{E_n\alpha^2\mu}{2(-1+\gamma\rho_0)\hbar^2}\\
c_8&=-\frac{l(l+1)}{4(-1+\gamma\rho_0)}+\frac{(1+2\gamma\rho_0)^2}{(-4+4\gamma\rho_0)^2}\\
c_9&=-\frac{mw^2\alpha^4\mu}{4(-1+\gamma\rho_0)\hbar^2}\\
c_{10}&=\frac{3}{2(1-\gamma\rho_0)}+\frac{2(1+2\gamma\rho_0)}{-4+4\gamma\rho_0}+2\sqrt{-\frac{l(l+1)}{4(-1+\gamma\rho_0)}+\frac{(1+2\gamma\rho_0)^2}{(-4+4\gamma\rho_0)^2}}\\
c_{11}&=\sqrt{-\frac{mw^2\alpha^4\mu}{(-1+\gamma\rho_0)\hbar^2}}\\
c_{12}&=\frac{1+2\gamma\rho_0}{-4+4\gamma\rho_0}+\sqrt{-\frac{l(l+1)}{4(-1+\gamma\rho_0)}+\frac{(1+2\gamma\rho_0)^2}{(-4+4\gamma\rho_0)^2}}\\
c_{13}&=-\frac{1}{2}\sqrt{-\frac{mw^2\alpha^4\mu}{(-1+\gamma\rho_0)\hbar^2}}.
\end{aligned} \tag{3.5}$$

Substituting these expressions into the energy equation of Equation (2.12), the energy equation is obtained as,

$$\lambda = (1+2n)\sqrt{\xi_1} - \xi_2 + 2\sqrt{\xi_1\left(\xi_3 + \frac{(1+\gamma\rho_0)^2}{(-4+4\gamma\rho_0)^2}\right)}, \tag{3.6}$$

and energy eigenvalues is

$$E_n = \frac{\begin{array}{l} 2(-1+\gamma\rho_0)(-\frac{1}{2}(1+2n)\sqrt{-\frac{mw^2\alpha^4\mu}{(-1+\gamma\rho_0)\hbar^2}} - \\ \frac{1}{4}\sqrt{-\frac{mw^2\alpha^4\mu\left(l(4-4\gamma\rho_0)+l^2(4-4\gamma\rho_0)+(1+\gamma\rho_0)^2\right)}{(-1+\gamma\rho_0)^3\hbar^2}})\hbar^2 \end{array}}{\alpha^2\mu}. \tag{3.7}$$

The corresponding wave function becomes,

$$R[n,r] = N_{ln}2\mathrm{e}^{-r\sqrt{\xi_1}} r^{1+\frac{1+\gamma\rho_0}{-4+4\gamma\rho_0}+\sqrt{\xi_3+\frac{(1+\gamma\rho_0)^2}{(-4+4\gamma\rho_0)^2}}} L_n^{-1+\frac{3-\gamma\rho_0}{2(1-\gamma\rho_0)}+\frac{2(1+\gamma\rho_0)}{-4+4\gamma\rho_0}+2\sqrt{\xi_3+\frac{(1+\gamma\rho_0)^2}{(-4+4\gamma\rho_0)^2}}}\sqrt{\xi_1}. \tag{3.8}$$

where N_{nl} is the normalization constant.

The obtained results are new which have not been reported before in available literature to the best of our knowledge. However, as a special case when $\gamma = 0$, then Equation (3.7) and Equation (3.8) are reduced to

$$E_n = \frac{\left(2\sqrt{\frac{w^2\alpha^4\mu^2}{\hbar^2}} + 4n\sqrt{\frac{w^2\alpha^4\mu^2}{\hbar^2}} + \sqrt{\frac{(1+2l)^2 w^2\alpha^4\mu^2}{\hbar^2}}\right)\hbar^2}{2\alpha^2\mu}.. \tag{3.9}$$

$$R[n,r] = N_{ln}2\mathrm{e}^{-r\sqrt{\xi_1}} r^{\frac{3}{4}+\sqrt{\frac{1}{16}+\xi_3}} L_n^{2\sqrt{\frac{1}{16}+\xi_3}}\sqrt{\xi_1}. \tag{3.10}$$

This result is consistent with these reported by Berkdemir [60] after matching the parameters.

3.1.2 Coulomb Potential

Coulomb potential deals an electron of charge moving in the Coulomb electrostatic field of the nucleus. The graph of the potential is drawn as a function in Figure 3.2. The Coulomb potential [59] is taken as

$$V[r] = -\frac{A}{r},$$

where A is the depth of the Coulomb potential.

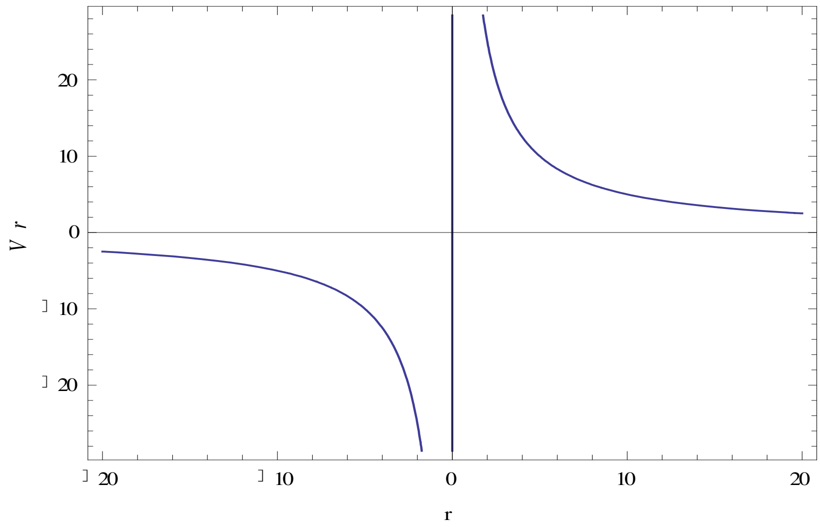

Figure 3.2 Coulomb potential for A=*50***.**

After the similar approach as for the Harmonic oscillator potential, then SE with Coulomb potential takes the form,

$$R''[r]+\frac{2}{r(1-\gamma\rho_0)}R'[r]-\frac{2\left(l+l^2-r\left(A+E_n r\right)\right)\mu}{r^2\hbar^2(1-\gamma\rho_0)}R[r]=0. \tag{3.11}$$

Now if a physical wave function $R(r)=\dfrac{U(r)}{r}$ is proposed then Equation (3.11) becomes,

$$(1-\gamma\rho_0)U''[r]+\frac{2\gamma\rho_0}{r}U'[r]-\frac{2\left(\left(l+l^2+r\left(A-E_n r\right)\right)\mu+\gamma\hbar^2\rho_0\right)}{r^2\hbar^2}U[r]=0. \tag{3.12}$$

To solve the above equation, after defining a variable of the form $r\rightarrow\alpha s$, Equation (3.12) yields,

$$U''[s]+\frac{2\gamma\rho_0}{s(1-\gamma\rho_0)}U'[s]-\frac{2\left(\left(l+l^2+s\alpha\left(A-E_n s\alpha\right)\right)\mu+\gamma\hbar^2\rho_0\right)}{s^2\hbar^2(1-\gamma\rho_0)}U[s]=0. \tag{3.13}$$

The followings are the parameters;

$$\xi_1=-\frac{2E_n\alpha^2\mu}{\hbar^2(1-\gamma\rho_0)}$$

$$
\begin{aligned}
\xi_2 &= \frac{-2A\alpha\mu}{\hbar^2\left(1-\gamma\rho_0\right)} \\
\xi_3 &= \frac{2\left(l\mu+l^2\mu+\gamma\hbar^2\rho_0\right)}{\hbar^2\left(1-\gamma\rho_0\right)} \\
c_1 &= 2\gamma\rho_0 / \left(1-\gamma\rho_0\right) \\
c_2 &= 0 \\
c_3 &= 0 \\
c_4 &= \frac{1}{2}\left(1-\frac{2\gamma\rho_0}{1-\gamma\rho_0}\right) \\
c_5 &= 0 \\
c_6 &= -\frac{2E_n\alpha^2\mu}{\hbar^2\left(1-\gamma\rho_0\right)} \\
c_7 &= \frac{2A\alpha\mu}{\hbar^2\left(1-\gamma\rho_0\right)} \\
c_8 &= \frac{2\left(l\mu+l^2\mu+\gamma\hbar^2\rho_0\right)}{\hbar^2\left(1-\gamma\rho_0\right)}+\frac{1}{4}\left(1-\frac{2\gamma\rho_0}{1-\gamma\rho_0}\right)^2 \\
c_9 &= -\frac{2E_n\alpha^2\mu}{\hbar^2\left(1-\gamma\rho_0\right)} \\
c_{10} &= 1+2\sqrt{\frac{2\left(l\mu+l^2\mu+\gamma\hbar^2\rho_0\right)}{\hbar^2\left(1-\gamma\rho_0\right)}+\frac{1}{4}\left(1-\frac{2\gamma\rho_0}{1-\gamma\rho_0}\right)^2} \\
c_{11} &= 2\sqrt{2}\sqrt{-\frac{E_n\alpha^2\mu}{\hbar^2\left(1-\gamma\rho_0\right)}} \\
c_{12} &= \frac{1}{2}\left(1-\frac{2\gamma\rho_0}{1-\gamma\rho_0}\right)+\sqrt{\frac{2\left(l\mu+l^2\mu+\gamma\hbar^2\rho_0\right)}{\hbar^2\left(1-\gamma\rho_0\right)}+\frac{1}{4}\left(1-\frac{2\gamma\rho_0}{1-\gamma\rho_0}\right)^2} \\
c_{13} &= -\sqrt{2}\sqrt{-\frac{E_n\alpha^2\mu}{\hbar^2\left(1-\gamma\rho_0\right)}}.
\end{aligned}
\tag{3.14}
$$

the energy equation can be obtained for the Coulomb potential as,

$$
\begin{aligned}
\lambda = \sqrt{2}\left(1+2n\right)\sqrt{\frac{E_n\alpha^2\mu}{\hbar^2\left(-1+\gamma\rho_0\right)}}-\frac{2A\alpha\mu}{\hbar^2\left(-1+\gamma\rho_0\right)}+ \\
\sqrt{2}\sqrt{\frac{E_n\alpha^2\mu\left(8l\left(l+1\right)\mu+\hbar^2+\gamma\rho_0\left(-8l\left(l+1\right)\mu+2\hbar^2+\gamma\hbar^2\rho_0\right)\right)}{\hbar^4\left(-1+\gamma\rho_0\right)^3}}.
\end{aligned}
\tag{3.15}
$$

Ever since, the Equation (3.15) can not be solved analytically by using NU method; the numerical values of energy for *n* and *l* were obtained from energy equation with appropriate parameters $\gamma = 0.02, \mu = 1/2, \hbar = 1, A = 50, \rho_0 = 4,$ and these value was shown in Table 3.1. When the appropriate constants are selected for the parameters, energy spectrums and wave function of Coulomb potential have the same results as the literature in condition of form factor $\varepsilon(r) = 0.$ The graph of energy is presented as a function of *r* in Figure 3.3. It is seen from the figure, the energy values of Coulomb potential showed a parabolic increase negatively depending on the quantum number. Similarly, the energy increase negatively as the momentum number increases. Besides, it can be seen from the graph that energy gets its greatest value is E_n=*-3.01233* when *n=10* and l_1=1 and its smallest value is E_n=*-67.5973* in *n=1* and l_1=*1*. In addition, since the energy values are very close to each other in *n>8* quantum states, they showed a change around almost the same value. Also, this energy figure gives nearly a close result compared to non velocity-dependent potential.

The corresponding wave function

$$R[n,r] = \frac{1}{r}\left(\begin{array}{l} N_{ln}\, 2\sqrt{2}\mathrm{e}^{-\sqrt{2}r\sqrt{-\frac{E_n\alpha^2\mu}{\hbar^2(1-\gamma\rho_0)}}}\, r^{1+\frac{1}{2}\left(1-\frac{2\gamma\rho_0}{1-\gamma\rho_0}\right)+\sqrt{\frac{2\left(l\mu+l^2\mu+\gamma\hbar^2\rho_0\right)}{\hbar^2(1-\gamma\rho_0)}+\frac{1}{4}\left(1-\frac{2\gamma\rho_0}{1-\gamma\rho_0}\right)^2}} \\ L_n^{2\sqrt{\frac{2\left(l\mu+l^2\mu+\gamma\hbar^2\rho_0\right)}{\hbar^2(1-\gamma\rho_0)}+\frac{1}{4}\left(1-\frac{2\gamma\rho_0}{1-\gamma\rho_0}\right)^2}}\sqrt{-\frac{E_n\alpha^2\mu}{\hbar^2\left(1-\gamma\rho_0\right)}} \end{array} \right) \tag{3.16}$$

Table 3.1 The energy eigenvalues of the Coulomb potential in Case 1 under $\gamma = 0.02, \mu = 1/2, \hbar = 1, A = 50, \rho_0 = 4.$

State	l_1=*1*	l_2=*2*	l_3=*3*
n=1	-67.5973	-38.1415	-24.4966
n=2	-37.5467	-24.1499	-16.8499
n=3	-23.8496	-16.6517	-12.2957
n=4	-16.4795	-12.172	-9.36619
n=5	-12.0643	-9.2839	-7.37134
n=6	-9.21205	-7.31383	-5.95202
n=7	-7.26356	-5.91027	-4.90639
n=8	-5.87373	-4.87513	-4.11391
n=9	-4.84774	-4.0899	-3.49901
n=10	-4.06885	-3.48017	-3.01233

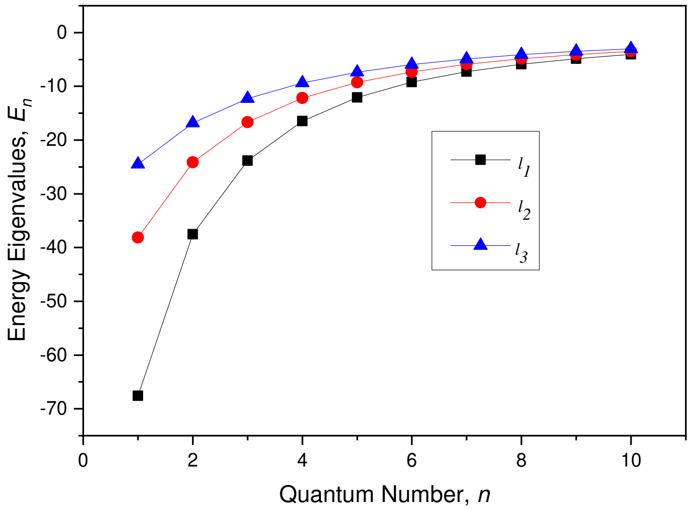

Figure 3.3 The graph of energy eigenvalues of the Coulomb potential in Case 1 under $\gamma = 0.02, \mu = 1/2, \hbar = 1, A = 50, \rho_0 = 4$.

In this figure, l_1, l_2, l_3 show the angular momentum for l_1=1, l_2=2, l_3=3 different values, respectively.

3.1.3 Hulthen Potential

The Hulthen potential [60] is very important exponential short range potential which behaves like a Coulomb potential for small values of r and decreases exponentially for large values of r. The Hulthen potential has been used in many branches of physic, such as atomic physic, nuclear physic, solid state physic and chemical physic. The graph of potential is presented in Figure 3.4. The Hulthen potential is given by,

$$V[r] = -\frac{e^{-\frac{r}{\kappa}} K}{\left(1 - e^{-\frac{r}{\kappa}}\right)\kappa},$$

where K and κ are the strength and the range parameter of the potential respectively.

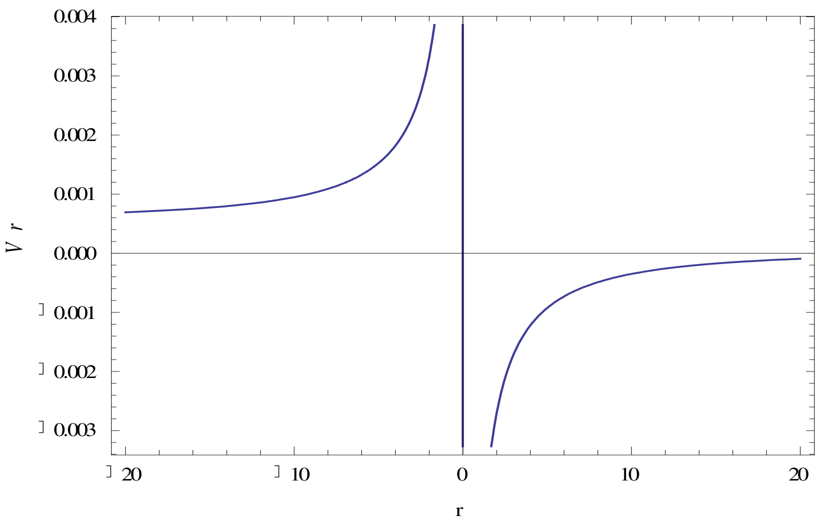

Figure 3.4 Hulthen potential for $K = 0.006, \kappa = 10$.

In order the obtain the energy eigenvalues of the Hulthen potential and the Schrödinger equation becomes,

$$R''[r] + \frac{1}{(1-\gamma\rho_0)}\left(-\frac{l(l+1)}{r^2} + \frac{2\left(E_n + \frac{K}{\left(-1+e^{r/\kappa}\right)\kappa}\right)\mu}{\hbar^2}\right)R[r] = 0. \tag{3.17}$$

By using Pekeris approximation [61] and then defining the new approximation,

$$\frac{l(l+1)}{r^2} \approx \frac{l(l+1)}{\left(1-e^{-\frac{r}{\kappa}}\right)^2 \kappa^2}$$

and substituting this expression into the Equation (3.17) yields

$$R''[r] + \frac{1}{(1-\gamma\rho_0)}\left(-\frac{l(l+1)}{\left(1-e^{-\frac{r}{\kappa}}\right)^2 \kappa^2} + \frac{2\left(E_n + \frac{K}{\left(-1+e^{r/\kappa}\right)\kappa}\right)\mu}{\hbar^2}\right)R[r] = 0 \tag{3.18}$$

By using transformation $r \to e^{-s\kappa}$ the Equation (3.18) becomes

$$R''[s] + \frac{1}{s}R'[s] + \frac{\left(2K(-1+s)s\kappa\mu - 2E_n(-1+s)^2\kappa^2\mu + l(l+1)\hbar^2\right)}{(-1+s)^2 s^2\hbar^2(-1+\gamma\rho_0)}R[s] = 0. \tag{3.19}$$

By using the parameters

$$
\begin{aligned}
&\xi_1 = -\left(2K\kappa\mu - 2E_n\kappa^2\mu\right)/\hbar^2\left(-1+\gamma\rho_0\right)\\
&\xi_2 = \left(-2K\kappa\mu + 4E_n\kappa^2\mu\right)/\hbar^2\left(-1+\gamma\rho_0\right)\\
&\xi_3 = -\left(-2E_n\kappa^2\mu + l\left(l+1\right)\hbar^2\right)/\hbar^2\left(-1+\gamma\rho_0\right)\\
&c_1 = -1, c_2 = -1, c_3 = -1, c_4 = 1\\
&c_5 = \frac{1}{2}, c_6 = \frac{1}{4}+\xi_1, c_7 = 1-\xi_2, c_8 = 1+\xi_3\\
&c_9 = \frac{1}{4}+\xi_1+\xi_2+\xi_3\\
&c_{10} = 1+2\sqrt{1+\xi_3}\\
&c_{11} = -2+2\left(-\sqrt{1+\xi_3}+\sqrt{\frac{1}{4}+\xi_1+\xi_2+\xi_3}\right)\\
&c_{12} = 1+\sqrt{1+\xi_3}\\
&c_{13} = \frac{1}{2}+\sqrt{1+\xi_3}-\sqrt{\frac{1}{4}+\xi_1+\xi_2+\xi_3},
\end{aligned}
\tag{3.20}
$$

it can be obtained the energy equation for the Hulthen potential as

$$
\begin{aligned}
\lambda = {} & 1+\frac{1}{2}\left(-1-2n\right)-n-\left(-1+n\right)n-\xi_2-2\left(1+\xi_3\right)+\\
& 2\sqrt{\left(1+\xi_3\right)\left(\frac{1}{4}+\xi_1+\xi_2+\xi_3\right)}+\left(1+2n\right)\left(-\sqrt{1+\xi_3}+\sqrt{\frac{1}{4}+\xi_1+\xi_2+\xi_3}\right).
\end{aligned}
\tag{3.21}
$$

The Equation (3.21) cannot be solved analytically by using NU method therefore the numerical solutions of energy of energy for n and l were calculated from energy equation with appropriate parameters $\gamma = 0.5, \mu = 1/2, \hbar = 1, K = 0.006, \kappa = 10,$ $\rho_0 = 0.1$. The values of energy were presented in Table 3.2. Energy spectrums and wave function of Hulthen potential give the similar results compared to the literature for value of $\varepsilon(r) = 0$ form factor. The graph of energy is plotted as a function of r in Figure 3.5. The energy values of Hulthen potential showed a decrease negatively depending on the increase quantum number, at the same time, energy decreases negatively when the angular momentum increases. Such as, E_n=*-0.00996143 in n=1* and $l_1=1$, E_n=*-0.0113747* in $n=2$ and $l_2=2$. As seen Figure 3.5 the energy changes of the Hulthen potential showed almost the same behavior in all quantum states. Therefore, changes of energy show the same act in different momentum states. Further, this graph gives approximately similar result compared to the literature for case $\varepsilon(r) = 0$.

The corresponding wave function becomes,

$$R[n,r] = N_{nl}\, r^{\frac{1}{2}\left(1-\frac{2\gamma\rho_0}{1-\gamma\rho_0}\right)+\sqrt{\frac{2\left(l\mu+l^2\mu+\gamma\hbar^2\rho_0\right)}{\hbar^2(1-\gamma\rho_0)}+\frac{1}{4}\left(1-\frac{2\gamma\rho_0}{1-\gamma\rho_0}\right)^2}} \tag{3.22}$$

$${}_2F_1\left(-n,1+-1+2\sqrt{1+\xi_3}+\sqrt{\frac{1}{4}+\xi_1+\xi_2+\xi_3})+n;2+2\sqrt{1+\xi_3};-r\right).$$

These results are new and have never been reported in the literature before to the best of our knowledge.

Table 3.2 The energy eigenvalues of the Hulthen potential in Case 1 under $\gamma = 0.5, \mu = 1/2, \hbar = 1, K = 0.006, \kappa = 10, \rho_0 = 0.1$.

State	*l_1=1*	*l_2=2*	*l_3=3*
n=1	-0.00996143	-0.0113747	-0.0125892
n=2	-0.0221315	-0.0251252	-0.0279842
n=3	-0.0389452	-0.0433183	-0.0478221
n=4	-0.0606469	-0.0661348	-0.0721385
n=5	-0.0873868	-0.0937471	-0.101059
n=6	-0.119252	-0.126288	-0.134712
n=7	-0.156295	-0.163853	-0.173211
n=8	-0.198545	-0.20651	-0.216647
n=9	-0.24602	-0.254306	-0.265091
n=10	-0.298732	-0.307273	-0.3186

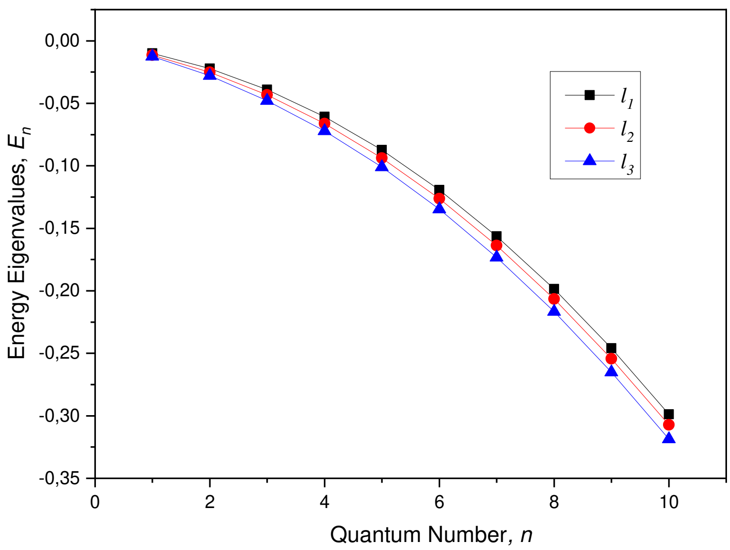

Figure 3.5 The graph of energy eigenvalues of the Hulthen potential in Case 1 for for $\gamma = 0.5, \mu = 1/2, \hbar = 1, K = 0.006, \kappa = 10, \rho_0 = 0.1$.

3.1.4 Kratzer Potential

Kratzer potential [62] has been used extensively so far in order to describe the molecular structure and interactions. The graph of potential is given in Figure 3.6. The Kratzer potential is

$$V[r] = A - \frac{B}{r} + \frac{C}{r^2},$$

where the parameters, A, B and C are constant which are related with Kratzer potential.

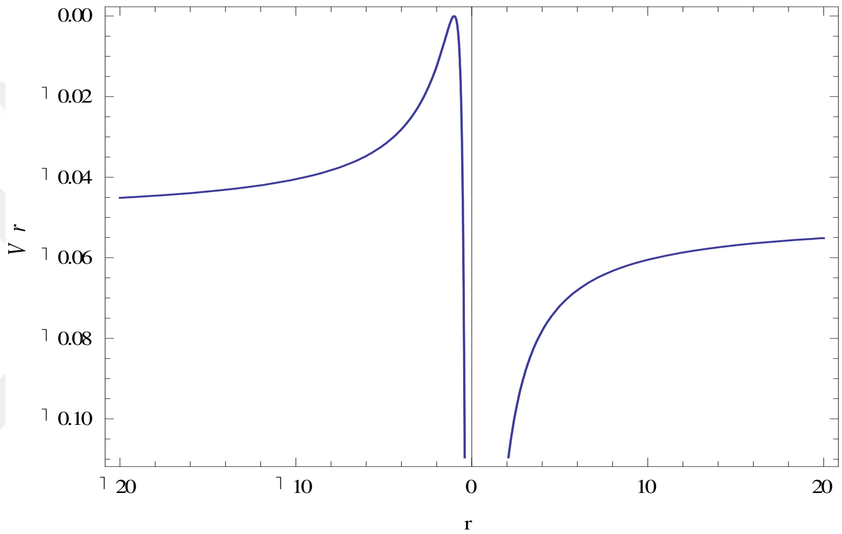

Figure 3.6 Kratzer potential for $A = -0.05, B = 0.1, C = -0.05$.

The SE with Kratzer potential takes the form,

$$R''[r] + \frac{-2}{r(-1+2\gamma\rho_0)}R'[r] + \frac{\begin{pmatrix} -(-2Am+2E_n m)r^2 + 2Bmr + \\ \hbar^2 l(l+1) + 2Cm \end{pmatrix}}{r^2\hbar^2(-1+2\gamma\rho_0)}R[r] = 0. \tag{3.23}$$

The corresponding parameters take the form

$$\xi_1 = (-2Am + 2E_n m)/(-1+2\gamma\rho_0)\hbar^2$$
$$\xi_2 = 2Bm/\hbar^2(-1+2\gamma\rho_0)$$
$$\xi_1 = (-2Am + 2E_n m)/(-1+2\gamma\rho_0)\hbar^2$$
$$c_1 = -2/(-1+2\gamma\rho_0)$$
$$c_2 = 0, c_3 = 0$$

$$
\begin{aligned}
c_4 &= \frac{1}{2} + \frac{1}{-1+\gamma\rho_0} \\
c_5 &= 0 \\
c_6 &= \xi_1 \\
c_7 &= -\xi_2 \\
c_8 &= \xi_3 + \left(\frac{1}{2} + \frac{1}{-1+2\gamma\rho_0}\right)^2 \\
c_9 &= \xi_1 \\
c_{10} &= \frac{2}{-1+2\gamma\rho_0} + 2\left(\frac{1}{2} + \frac{1}{-1+2\gamma\rho_0}\right) + 2\sqrt{\xi_3 + \left(\frac{1}{2} + \frac{1}{-1+2\gamma\rho_0}\right)^2} \\
c_{11} &= 2\sqrt{\xi_1} \\
c_{12} &= \frac{1}{2} + \frac{1}{-1+2\gamma\rho_0} + \sqrt{\xi_3 + \left(\frac{1}{2} + \frac{1}{-1+2\gamma\rho_0}\right)^2} \\
c_{13} &= -\sqrt{\xi_1},
\end{aligned}
\tag{3.24}
$$

the energy equations is obtained

$$
\lambda = \left(1+2n\right)\sqrt{\xi_1} - \xi_2 + 2\sqrt{\xi_1\left(\xi_3 + \left(\frac{1}{2} + \frac{1}{-1+2\gamma\rho_0}\right)^2\right)}. \tag{3.25}
$$

Since the analytical solution of the Equation (3.25) could not be achieved by using NU method, numerical solutions of energy are obtained for n and l. The results obtained are given in the Table 3.3 below with fixed parameters $A=-0.5, B=0.1, C=-0.05, \gamma=50, m=1/2, \hbar=1, \rho_0=0.5.$ Energy equation and wave function of Kratzer potential have the same results when compared with the literature in case of form factor $\varepsilon(r)=0.$ Besides, the values of energy are shown in Figure 3.6 as a function of *r*. In figure, the energy values of Kratzer potential increase negatively depending on the quantum number. It is seen in the graph, since the energy increases when $n>4$ quantum state this increase is almost the same for different momentum number and coincided at the same point. For this reason, it can be said that energy fluctuations also have the same act in different quantum state. For example E_n=*-0, 50001* for $n=9$ and $l_1=1$, $l_2=2$, $l_3=3$. Besides, this energy figure gives pretty much close results compared to the non-velocity-dependent potential in the literature.

The corresponding wave function is determined

$$R[n,r] = N_{ln}\, 2e^{-r\sqrt{\xi_1}}\, r^{\frac{1}{2}+\sqrt{\frac{1}{4}+\xi_3}}\, L_n^{2\sqrt{\frac{1}{4}+\xi_3}}\, \sqrt{\xi_1} \tag{3.26}$$

Table 3.3 The energy eigenvalues of the Kratzer potential in Case 1 under $A=-0.5, B=0.1, C=-0.05, \gamma=50, m=1/2, \hbar=1, \rho_0=0.5$.

State	$l_1=1$	$l_2=2$	$l_3=3$
n=1	-0.0500234	-0.0500208	-0.0500182
n=2	-0.0500108	-0.0500099	-0.0500091
n=3	-0.0500062	-0.0500058	-0.0500054
n=4	-0.050004	-0.0500038	-0.0500036
n=5	-0.0500028	-0.0500027	-0.0500026
n=6	-0.0500021	-0.050002	-0.0500019
n=7	-0.0500016	-0.0500015	-0.0500015
n=8	-0.0500013	-0.0500012	-0.0500012
n=9	-0.050001	-0.050001	-0.050001
n=10	-0.0500008	-0.0500008	-0.0500008

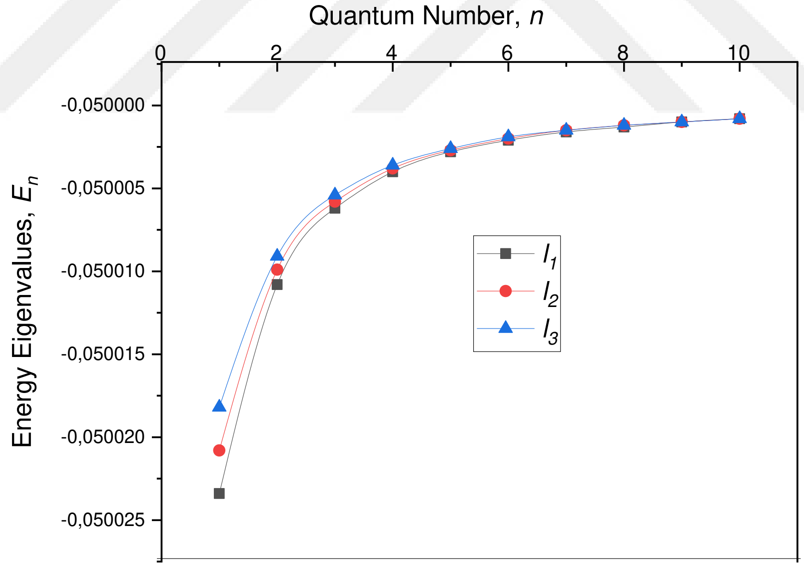

Figure 3.7 The graph of energy eigenvalues of the Kratzer potential in Case 1 under $A=-0.5, B=0.1, C=-0.05, \gamma=50, m=1/2, \hbar=1, \rho_0=0.5$.

3.1.5 Mie Potential

Mie-Type potential which belongs to a class of multi-parameter exponential potential has application in vibration and rotational spectroscopy in physical sciences because its interaction model comprises of both repulsive and attractive terms for short and large intermolecular distances respectively for some diatomic molecules [63].
Mie potential has the form

$$V[r] = V_0\left(\frac{1}{2}\left(\frac{a}{r}\right)^2 - \frac{a}{r}\right),$$

where a is the positive constant which is strongly repulsive at shorter distances.

And by substituting into Schrödinger Equation. (3.1) takes the form

$$R''[r] + \frac{2}{r(-1+\gamma\rho_0)}R'[r] - \frac{\left(-2E_n mr^2 + a^2mV_0 - 2amrV_0 + l(l+1)\hbar^2\right)}{r^2\hbar^2(-1+\gamma\rho_0)}R[r] = 0. \quad (3.27)$$

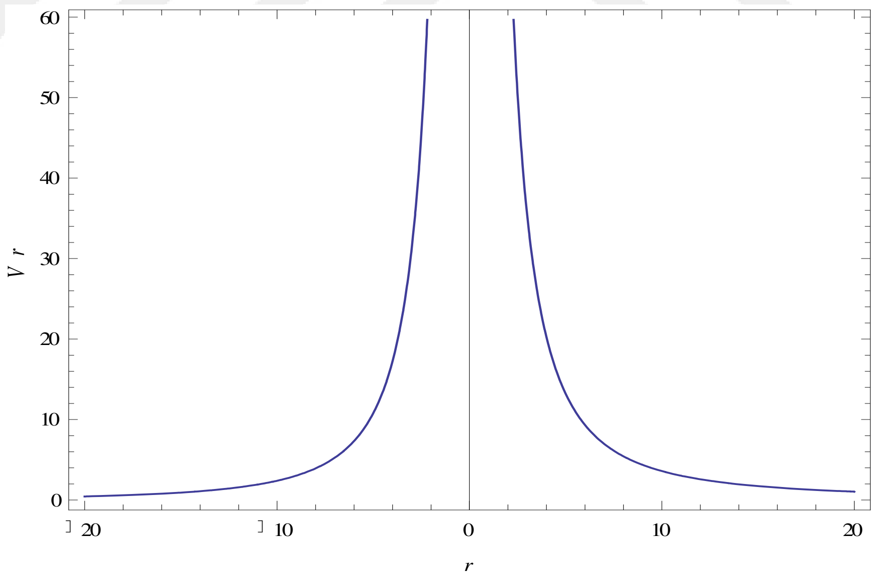

Figure 3.8 Mie Potential for $a = 10, V_0 = 0.5$.

By defining parameters value at this step are

$$\xi_1 = 2mE_n / \left(\hbar^2(-1+\gamma\rho_0)\right)$$

$$
\begin{aligned}
&\xi_2 = -2mV_0 a / \left(\hbar^2 \left(-1+\gamma\rho_0\right)\right) \\
&\xi_3 = -\left(\hbar^2 l\left(l+1\right) + a^2 m V_0\right) / \left(\hbar^2\left(-1+\gamma\rho_0\right)\right) \\
&c_1 = -2 / -\left(1+\gamma\rho_0\right), c_2 = 0, c_3 = 0 \\
&c_4 = \frac{1}{2}\left(1+\frac{2}{-1+\gamma\rho_0}\right), c_5 = 0 \\
&c_6 = \frac{2E_n m}{\left(-1+\gamma\rho_0\right)\hbar^2}, c_7 = \frac{2maV_0}{\hbar^2\left(-1+\gamma\rho_0\right)} \\
&c_8 = \frac{-\hbar^2 l\left(l+1\right) - ma^2V_0}{\hbar^2\left(-1+\gamma\rho_0\right)} + \frac{1}{4}\left(1+\frac{2}{-1+\gamma\rho_0}\right)^2 \\
&c_9 = \frac{2E_n m}{\left(-1+\gamma\rho_0\right)\hbar^2}, c_{10} = 1+2\sqrt{\frac{-\hbar^2 l\left(l+1\right) - ma^2V_0}{\hbar^2\left(-1+\gamma\rho_0\right)} + \frac{1}{4}\left(1+\frac{2}{-1+\gamma\rho_0}\right)^2} \\
&c_{11} = 2\sqrt{2}\sqrt{\frac{E_n m}{\hbar^2\left(-1+\gamma\rho_0\right)}} \\
&c_{12} = \frac{1}{2}\left(1+\frac{2}{-1+\gamma\rho_0}\right) + \sqrt{\frac{-\hbar^2 l\left(l+1\right) - ma^2V_0}{\hbar^2\left(-1+\gamma\rho_0\right)} + \frac{1}{4}\left(1+\frac{2}{-1+\gamma\rho_0}\right)^2} \\
&c_{13} = -\sqrt{2}\sqrt{\frac{E_n m}{\hbar^2\left(-1+\gamma\rho_0\right)}},
\end{aligned}
\tag{3.28}
$$

energy equation and corresponding wave equation are obtained by using Equation (2.8) and Equation (2.12)

$$
\begin{aligned}
\lambda = \sqrt{2}\left(1+2n\right)&\sqrt{\frac{E_n m}{\hbar^2\left(-1+\gamma\rho_0\right)}} + \frac{2maV_0}{\hbar^2\left(-1+\gamma\rho_0\right)} + \\
2\sqrt{2}&\sqrt{\frac{E_n m\left(-\frac{ma^2V_0 + l\left(l+l\right)\hbar^2}{\hbar^2\left(-1+\gamma\rho_0\right)} + \frac{1}{4}\left(1+\frac{2}{-1+\gamma\rho_0}\right)^2\right)}{\hbar^2\left(-1+\gamma\rho_0\right)}}.
\end{aligned}
\tag{3.29}
$$

The Equation (3.29) can not be solved analytically by using NU method; the numerical solutions of energy for n and l are given in Table 3.4 with suitable parameters $m = 1/2$, $a = 10, \gamma = 5, V_0 = 0.5, \hbar = 1, \rho_0 = -2$ and energy graphs is plotted as shown in Figure 3.8 for this values. Further, energy spectrum and wave function of Mie potential are compared to the literature and give the same results in case $\varepsilon(r)=0$. Looking at the energy change of Mie potential in figure, it shows a change similar to the energy change of Kratzer potential.

The corresponding wave function becomes,

$$R\left[n,r\right]=N_{nl}\,2\sqrt{2}\mathrm{e}^{-\sqrt{2}r\sqrt{\frac{E_n m}{\hbar^2(-1+\gamma\rho_0)}}}\,r^{1+\frac{1}{2}\left(1+\frac{2}{-1+\gamma\rho_0}\right)+\sqrt{\frac{-l(l+1)\hbar^2-a^2mV_0}{\hbar^2(-1+\gamma\rho_0)}+\frac{1}{4}\left(1+\frac{2}{-1+\gamma\rho_0}\right)^2}}$$
$$L_n^{2\sqrt{\frac{-l(1+l)\hbar^2-a^2mV_0}{\hbar^2(-1+\gamma\rho_0)}+\frac{1}{4}\left(1+\frac{2}{-1+\gamma\rho_0}\right)^2}}\sqrt{\frac{E_n m}{\hbar^2\left(-1+\gamma\rho_0\right)}}. \tag{3.30}$$

Table 3.4 The energy eigenvalues of the Mie potential in Case 1 under $m=1/2, a=10, \gamma=5, V_0=0,5, \rho_0=-2.$

State	$l_1=1$	$l_2=2$	$l_3=3$
n=1	-0.00127641	-0.0010222	-0.000820311
n=2	-0.000587506	-0.000503988	-0.000430766
n=3	-0.000336386	-0.000299217	-0.000264841
n=4	-0.000217607	-0.000197943	-0.00017914
n=5	-0.000152205	-0.000140571	-0.000129188
n=6	-0.0001124	-0.000104957	-0.0000975511
n=7	-0.0000863899	-0.0000813431	-0.0000762577
n=8	-0.0000684646	-0.0000648866	-0.0000612451
n=9	-0.0000555903	-0.0000529622	-0.0000502658
n=10	-0.0000460333	-0.0000440465	-0.0000419945

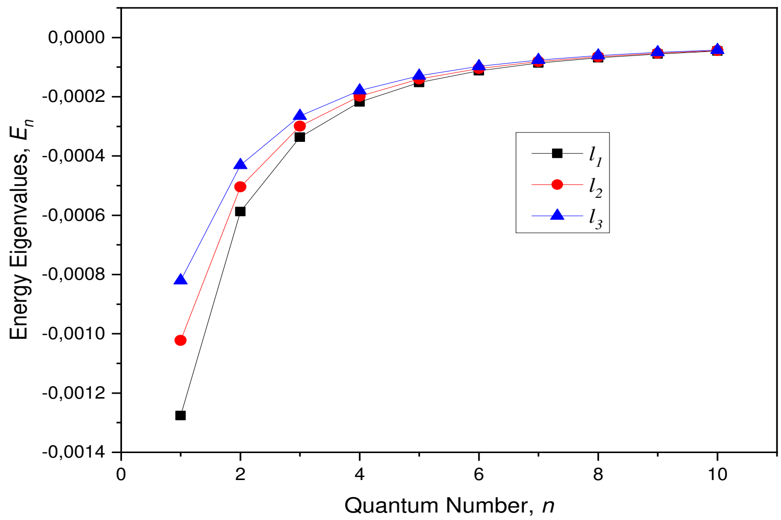

Figure 3.9 The graph of energy eigenvalues of the Mie potential in Case 1 for $m=1/2, a=10, \gamma=5, V_0=0.5, \rho_0=-2.$

3.1.6 Cornell Potential

The Cornell potential is a linear combination of the Coulomb and linear potentials the Cornell potential is [64]

$$V\left[r\right]=ar-\frac{b}{r},$$

where b is model parameter for the Coulomb strength and a is the string tension. The graph of potential is plotted as a function in Figure 3.9.

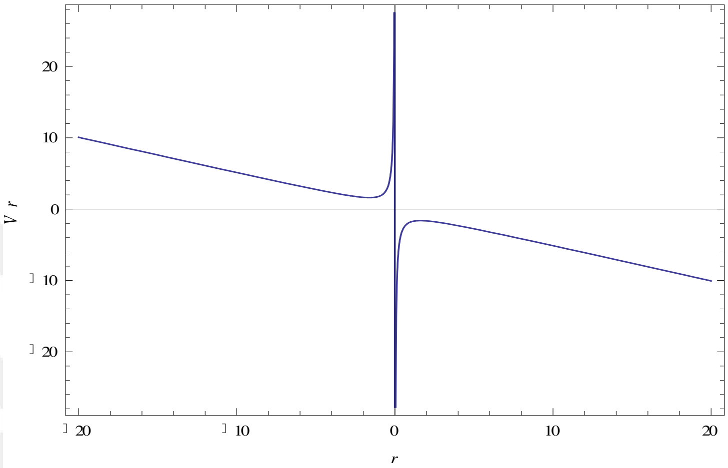

Figure 3.10 Cornell potential for $b=1.3, a=-0.5$.

The SE has the form

$$\begin{gathered}R''\left[r\right]+\frac{2}{r\left(-1+\gamma\rho_0\right)}R'\left[r\right]+\\ \frac{\left(-2mr\left(-b+r\left(E_n+ar\right)\right)+l\left(2m+\hbar^2\right)+l^2\left(2m+\hbar^2\right)\right)}{r^2\hbar^2\left(-1+\gamma\rho_0\right)}R\left[r\right]=0.\end{gathered}\tag{3.31}$$

And then by defining wave function $R[r]=\frac{U[r]}{r}$ the Equation (3.31) becomes

$$\begin{gathered}\frac{\left(r^2\hbar^2-r^2\gamma\hbar^2\rho_0\right)}{r^2\hbar^2}U''\left[r\right]+\frac{2\gamma\rho_0}{r}U'\left[r\right]+\\ \frac{1}{r^2\hbar^2}\begin{pmatrix}2mr\left(-b+r\left(E_n+ar\right)\right)-l\left(2m+\hbar^2\right)-\\ l^2\left(2m+\hbar^2\right)-2\gamma\hbar^2\rho_0\end{pmatrix}U\left[r\right]=0.\end{gathered}\tag{3.32}$$

By using transformation $r=\alpha\tau$ the Equation (3.32) becomes

$$U''[\tau]-\frac{2\gamma\tau\hbar^2\rho_0}{-\tau^2\hbar^2+\gamma\tau^2\hbar^2\rho_0}U'[\tau]+ \tag{3.33}$$
$$\frac{\left(-2m\alpha\tau\left(-b+\alpha\tau\left(E_n+a\alpha\tau\right)\right)+l\left(2m+\hbar^2\right)+l^2\left(2m+\hbar^2\right)+2\gamma\hbar^2\rho_0\right)}{-\tau^2\hbar^2+\gamma\tau^2\hbar^2\rho_0}U[\tau]=0.$$

In terms of a new variable $\tau = 1/s$ then Eq. (3.32) yields,

$$U''[s]+\frac{2-4\gamma\rho_0}{s(1-\gamma\rho_0)}U'[s]+ \tag{3.34}$$
$$\frac{\left(2l(1+l)m+\frac{2bm\alpha}{s}-\frac{2E_nm\alpha^2}{s^2}-\frac{2am\alpha^3}{s^3}+l(l+1)\hbar^2+2\gamma\hbar^2\rho_0\right)}{s^2\hbar^2(-1+\gamma\rho_0)}U[s]=0.$$

Due to the coefficients of $U[s]$ in the above equation, $\frac{1}{s}$, $\frac{1}{s^2}$ and $\frac{1}{s^3}$ do not provide solution of the equation by NU method, binomial expansion was made to these the coefficients. The binomial expansion is shown as follows [65]

$$(1+x)^n = 1+nx+\frac{n(n-1)}{2!}x^2+\frac{n(n-1)(n-2)}{3!}x^3+... \tag{3.35}$$

where n negative integer and x takes values $0 \le x < 1$.

By using expansion in the Eq. (3.34), the expansion of $\frac{1}{s}$ for $n=-1$ the expansion of $\frac{1}{s^2}$ for $n=-2$ and the expansion of $\frac{1}{s^3}$ for $n=-3$ in Equation (3.34) are obtained as follows

$$\begin{aligned}
&\frac{1}{s}\to\left(\frac{3}{\delta}-\frac{3s}{\delta^2}+\frac{s^2}{\delta^3}\right)\\
&\frac{1}{s^2}\to\left(\frac{6}{\delta}-\frac{8s}{\delta^2}+\frac{3s^2}{\delta^3}\right)\\
&\frac{1}{s^3}->\left(\frac{-2}{\delta}+\frac{9s}{\delta^2}-\frac{6s^2}{\delta^3}\right).
\end{aligned} \tag{3.36}$$

Substituting these expressions into the Equation (3.34), the corresponding equation is transformed to

$$U''[s]+\frac{(2-4\gamma\rho_0)}{s(1-\gamma\rho_0)}U'[s]+ \tag{3.37}$$

$$\frac{\left(\begin{array}{l}2l(1+l)m+s^2\left(\frac{2bm\alpha}{\delta^3}-\frac{6E_n m\alpha^2}{\delta^3}+\frac{12am\alpha^3}{\delta^3}\right)+\\ s\left(-\frac{6bm\alpha}{\delta^2}+\frac{16E_n m\alpha^2}{\delta^2}-\frac{18am\alpha^3}{\delta^2}\right)\\ +\frac{6bm\alpha}{\delta}-\frac{12E_n m\alpha^2}{\delta}+\frac{4am\alpha^3}{\delta}+l(l+1)\hbar^2+2\gamma\hbar^2\rho_0\end{array}\right)}{s^2\hbar^2(-1+\gamma\rho_0)}U[s]=0.$$

The corresponding parameters take the form

$$\xi_1=-\left(\frac{2bm\alpha}{\delta^3}-\frac{6E_n m\alpha^2}{\delta^3}+\frac{12am\alpha^3}{\delta^3}\right)/\left(\hbar^2(-1+\gamma\rho_0)\right)$$

$$\xi_2=\left(-\frac{6bm\alpha}{\delta^2}+\frac{16E_n m\alpha^2}{\delta^2}-\frac{18am\alpha^3}{\delta^2}\right)/\left(\hbar^2(-1+\gamma\rho_0)\right)$$

$$\xi_3=-\left(\frac{6bm\alpha}{\delta}-\frac{12E_n m\alpha^2}{\delta}+\frac{4am\alpha^3}{\delta}+l(l+1)\hbar^2+2\gamma\hbar^2\rho_0+2l(l+1)m\right)/(1-\gamma\rho_0)$$

$$c_1=(2-4\gamma\rho_0)/(1-\gamma\rho_0)$$

$$c_2=0,c_3=0,c_4=\frac{1}{2}\left(1-\frac{2-4\gamma\rho_0}{1-\gamma\rho_0}\right)$$

$$c_5=0,c_6=\xi_1,c_7=\xi_2$$

$$c_8=\xi_3+\frac{1}{4}\left(1-\frac{2-4\gamma\rho_0}{1-\gamma\rho_0}\right)^2,c_9=\xi_1,c_{10}=1+2\sqrt{\xi_3+\frac{1}{4}\left(1-\frac{2-4\gamma\rho_0}{1-\gamma\rho_0}\right)^2},c_{11}=2\sqrt{\xi_1} \tag{3.38}$$

$$c_{12}=\frac{1}{2}\left(1-\frac{2-4\gamma\rho_0}{1-\gamma\rho_0}\right)+\sqrt{\varepsilon 3+\frac{1}{4}\left(1-\frac{2-4\gamma\rho_0}{1-\gamma\rho_0}\right)^2},c_{13}=-\sqrt{\xi_1},$$

using Equation (2.12), the energy equation is obtained as,

$$\lambda=(1+2n)\sqrt{\xi_1}-\xi_2+2\sqrt{\xi_1\left(\xi_3+\frac{1}{4}\left(1-\frac{2-4\gamma\rho_0}{1-\gamma\rho_0}\right)^2\right)}. \tag{3.39}$$

Solving, Equation (3.39) as before the numeric results of energy are obtained for n and l. These results are presented in Table 3.5 for $\delta=-5, m=1/2, \alpha=5, \rho_0=1$, $\hbar=1, b=1.3, \gamma=0.01, a=-0.5$ parameters and the energy graph is drawn as function of r in Figure 3.11. The energy equation of Cornell potentials is compared when $\varepsilon(r)=0$ as in literature; the potentials are reduced to the simple form of the corresponding potentials. It is seen from the figure, the energy values of Cornell potential showed a decrease depending on the increase quantum number, but it showed an increase as the number of angular momentum increases. At the same time, since the energy changes in all quantum states are very close to each other, such as, E_n=-4.56077 in l_1=1, E_n=-4.54759 in l_2=2 and E_n=-4.52523 in l_2=2 for quantum state n=1. So, the energy changes in different momentum states have the same feature.

Table 3.5 The energy eigenvalues of the Cornell potential in Case 1 under $\delta=-5, m=1/2, \alpha=5, \hbar=1, \rho_0=1, b=1.3, \gamma=0.01, a=-0.5$.

State	l_1=1	l_2=2	l_3=3
n=1	-4.38239	-4.35797	-4.3155
n=2	-4.43733	-4.41664	-4.38095
n=3	-4.48451	-4.46684	-4.43654
n=4	-4.5253	-4.51009	-4.48415
n=5	-4.56077	-4.54759	-4.52523
n=6	-4.59179	-4.5803	-4.56089
n=7	-4.61905	-4.60897	-4.59202
n=8	-4.64311	-4.63423	-4.61935
n=9	-4.66444	-4.65659	-4.64345
n=10	-4.68343	-4.67645	-4.66481

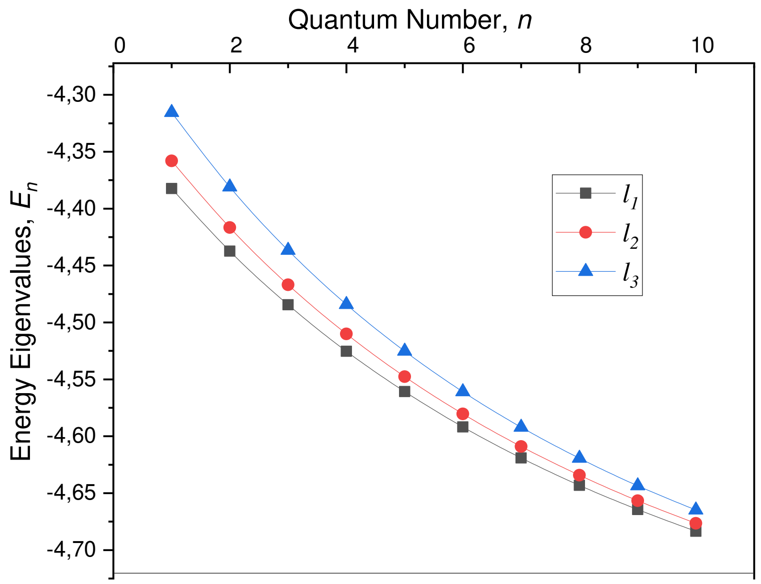

Figure 3.11 The graph of energy eigenvalues of the Cornell potential in Case 1 for $\delta=-5, m=1/2, \alpha=5, \hbar=1, \rho_0=1, b=1.3, \gamma=0.01, a=-0.5$.

The corresponding wave function is given by using Equation (2.15),

$$R[n,r]=\frac{1}{r}\left(N_{ln}\,2\mathrm{e}^{-r\sqrt{\xi_1}}\,r^{1+\frac{1}{2}\left(1-\frac{2-4\gamma\rho_0}{1-\gamma\rho_0}\right)+\sqrt{\xi_3+\frac{1}{4}\left(1-\frac{2-4\gamma\rho_0}{1-\gamma\rho_0}\right)^2}}\sqrt{\xi_1}\,L_n^{2\sqrt{\xi_3+\frac{1}{4}\left(1-\frac{2-4\gamma\rho_0}{1-\gamma\rho_0}\right)^2}}\right). \tag{3.40}$$

3.1.7 Woods-Saxon Potential

Woods-Saxon potential one of the useful models for determining single-particle energy levels of nuclei and nucleus-nucleus interaction [66]. The graph of potential is shown as function in Figure 3.11. Woods-Saxon potential is

$$V\left[r\right]=-\frac{V_0}{1+qe^{-\beta r}}$$

where q is the deformation parameter, V_0 is strength of potential and β is the screening parameter.

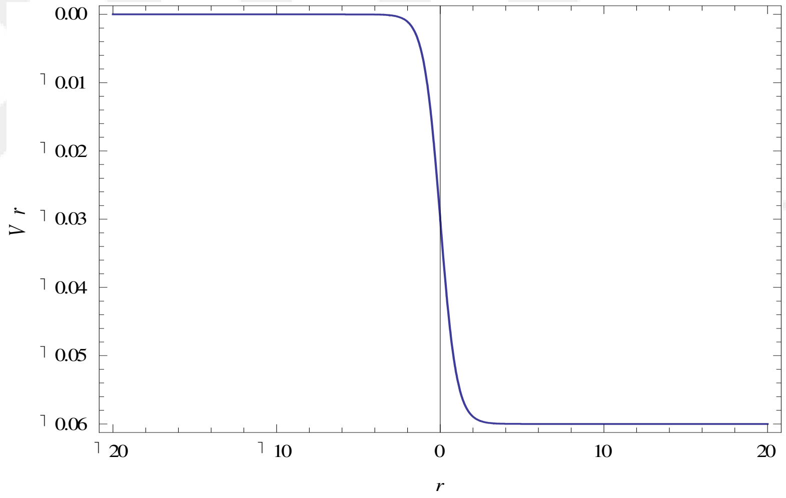

Figure 3. 12 Woods-Saxon potential for $V_0=0.06, \beta=2, q=1$.

The corresponding SE becomes,

$$R''\left[r\right]+\frac{1}{\hbar^2\left(1-\gamma\rho_0\right)}\left(-\frac{\hbar^2 l\left(l+1\right)}{r^2}+2m\left(E_n+\frac{V_0}{1+\mathrm{e}^{-r\beta}q}\right)\right)R\left[r\right]=0. \tag{3.41}$$

where the approximation

$$-\frac{\hbar^2 l\left(l+1\right)}{r^2}\approx\frac{\hbar^2 l\left(l+1\right)}{\left(1+\mathrm{e}^{-r\beta}q\right)^2}$$

is used and then Equation (3.41) becomes,

$$R''[r]+\frac{1}{1-\gamma\rho_0}\left(-\frac{\hbar^2 l(l+1)}{\left(1+\mathrm{e}^{-r\beta}q\right)^2}+2m\left(E_n+\frac{V_0}{1+\mathrm{e}^{-r\beta}q}\right)\right)R[r]=0. \tag{3.42}$$

By defining a variable of the form $r=e^{-s/\beta}$ the Equation (3.42) becomes,

$$\begin{aligned}&R''[r]+\frac{(1+qs)}{s(1+qs)}R'[r]+\\&\frac{\left(\hbar^2 l(l+1)-2E_n m-2E_n mq^2s^2-2mV_0+s(-4E_n mq-2mqV_0)\right)}{s^2(1+qs)^2\beta^2(-1+\gamma\rho_0)}R[r]=0.\end{aligned} \tag{3.43}$$

The parameters at this step are

$$\begin{aligned}\xi_1&=2E_n mq^2/\left(\beta^2(-1+\gamma\rho_0)\right)\\ \xi_2&=(-4E_n mq-2mqV_0)/\left(\beta^2(-1+\gamma\rho_0)\right)\\ \xi_3&=\left(\hbar^2 l(l+1)-2E_n m-2mV_0\right)/\left(\left(\beta^2(-1+\gamma\rho_0)\right)\right)\\ c_1&=1\\ c_2&=-q\\ c_3&=-q\\ c_4&=0\\ c_5&=q/2\\ c_6&=\frac{q^2}{4}+\xi_1\\ c_7&=-\xi_2\\ c_8&=-\xi_3\\ c_9&=\frac{q^2}{4}+\xi_1+q\xi_2+q^2\xi_3\\ c_{10}&=1+2\sqrt{\xi_3}\\ c_{11}&=2q+2\left(-q\sqrt{\xi_3}+\sqrt{\frac{q^2}{4}+\xi_1+q\xi_2+q^2\xi_3}\right)\\ c_{12}&=\sqrt{\xi_3}\\ c_{13}&=\frac{q}{2}+q\sqrt{\xi_3}-\sqrt{\frac{q^2}{4}+\xi_1+q\xi_2+q^2\xi_3},\end{aligned} \tag{3.44}$$

with a similar algebraic calculation used in previous steps, the energy equation is obtained.

$$\lambda = -nq - (-1+n)nq - \frac{1}{2}(1+2n)q - \xi_2 - 2q\xi_3 + 2\sqrt{\xi_3\left(\frac{q^2}{4} + \xi_1 + q\xi_2 + q^2\xi_3\right)} +$$

$$(1+2n)\left(-q\sqrt{\xi_3} + \sqrt{\frac{q^2}{4} + \xi_1 + q\xi_2 + q^2\xi_3}\right). \tag{3.45}$$

The numerical value of energy for n and l is given in Table 3.6 with fixed parameters $\gamma = 0.05, m = 1/2, \hbar = 1, V_0 = 0.06, \beta = 2, \rho_0 = -0.5$. The energy equation of Woods-Saxon potentials is compared when $\varepsilon(r) = 0$ as in literature; the potentials are reduced to the simple form of the corresponding potentials. The energy graph is presented as shown in Figure 3.13 As shown in the graph, the energy values increase positively depending on *n* and *l*. Since the energy values are very close to each other, it showed a overlapping for example, E_n*=3510.32* in l_1*=1,* E_n*=3506.26* in l_2*=2* and *En=3500.17* in l_3*=3* for *n=7* quantum state and energy increases a bit and increased slope is observed for all possible quantum states.

The corresponding wave function is

$$R[n,r] = N_{nl}\, s^{\sqrt{\xi_3}}\,(1+qs)^{\frac{q}{2}+q\sqrt{\xi_3}-\sqrt{\frac{q^2}{4}+\xi_1+q\xi_2+q^2\xi_3}}$$

$$ {}_2F_1\left(\begin{array}{l} -n, 1+1-2q+2\sqrt{\xi_3}+2(-q\sqrt{\xi_3}+\sqrt{\frac{q^2}{4}+\xi_1+q\xi_2+q^2\xi_3})+n; 2 \\ +2\sqrt{\xi_3}; -qr \end{array}\right) \tag{3.46}$$

Table 3.6 The energy eigenvalues of the Woods-Saxon potential in Case 1 under $\gamma = 0.05, m = 1/2, \hbar = 1, V_0 = 0.06, \beta = 2, \rho_0 = -5.$

State	l_1*=1*	l_2*=2*	l_3*=3*
n=1	138.287	133.988	126.944
n=2	388.086	383.957	377.593
n=3	762.758	758.673	752.462
n=4	1262.32	1258.25	1252.1
n=5	1886.76	1882.7	1876.58
n=6	2636.09	2632.04	2625.94
n=7	3510.32	3506.26	3500.17
n=8	4509.43	4505.38	4499.29
n=9	5633.43	5629.38	5623.3
n=10	6882.31	6878.27	6872.19

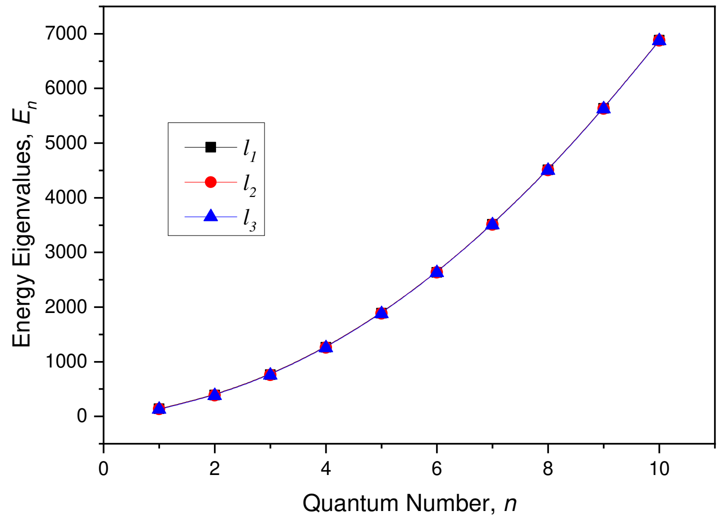

Figure 3. 13 The graph of energy eigenvalues of Woods-Saxon potential in Case 1 for $\gamma = 0.05, m = 1/2, \hbar = 1, V_0 = 0.06, \beta = 2, \rho_0 = -5$.

3.1.8 Pöschl-Teller Potential

The Pöschl-Teller Potential is used to describe the structure of the crystals. Also application of solution in this potential are crystals model expressed in solid state physic [67].The graph of potential is given in Figure 3.14.

Pöschl-Teller Potential is given by,

$$V[r] = -\frac{4\mathrm{e}^{-2ar}V_0}{\left(1+\mathrm{e}^{-2ar}q\right)^2},$$

where q is the deformation parameter, V_0 is strength of potential and α is the screening parameter.

The corresponding SE becomes,

$$R''[r] + \frac{2}{r(1-\gamma\rho_0)}R'[r] + \frac{1}{1-\gamma\rho_0}\left(-\frac{l(l+1)}{r^2} + \frac{2m(E_n + \frac{4\mathrm{e}^{2ar}V_0}{(\mathrm{e}^{2ar}+q)^2})}{\hbar^2} \right) R[r] = 0. \qquad (3.47)$$

Now using wave function $R[r] = \dfrac{U[r]}{r}$ then Equation (3.47) becomes

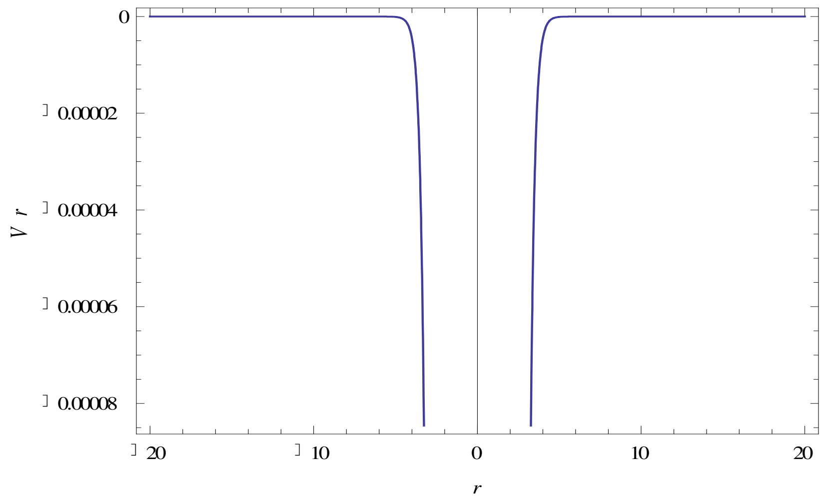

Figure 3.14 Pöschl-Teller potential for $V_0 = 0.5, q = 1$.

$$U''[r] + \frac{2\gamma\rho_0}{r(1-\gamma\rho_0)}U'[r] + \frac{1}{r^2(1-\gamma\rho_0)}\left(-l(1+l) + \frac{2mr^2(E_n + \frac{4e^{2ar}V_0}{(e^{2ar}+q)^2})}{\hbar^2} - 2\gamma\rho_0\right)U[r] = 0. \tag{3.48}$$

In this equation, when the following the approximation is used

$$\frac{4e^{2ar}V_0}{\left(e^{2ar}+q\right)^2} \approx \frac{4V_0}{r^2},$$

the Equation (3.48) is reduced to

$$U''[r] + \frac{2\gamma\rho_0}{r(1-\gamma\rho_0)}U'[r] + \frac{\left(-\hbar^2 l(1+l)r^2 + 2m\left(E_n r^4 + 4V_0\right)\right)}{\hbar^2 r^4(-1+\gamma\rho_0)}U[r] = 0. \tag{3.49}$$

By using transformation $r = \sqrt{s}$ the Equation (3.49) becomes

$$U''[s] + \frac{(1+\gamma\rho_0)}{2s(-1+\gamma\rho_0)}U'[s] - \frac{\left(\left(-\hbar^2 l(l+1) + 2E_n m\right)s + \frac{8mV_0}{s}\right)}{4\hbar^2 s^2(-1+\gamma\rho_0)}U[s] = 0. \tag{3.50}$$

Since the coefficient of $U[s]$ in the above equation $\frac{1}{s}$, do not provide solution of the equation by NU method, this coefficient is opened to power series by using Equation (3.36).

And then, Equation (3.50) takes the following form

$$R''[s]+\frac{(-2+4\gamma\rho_0)}{s(-1+\gamma\rho_0)}R'[s]+$$
$$\frac{\left(\hbar^2 l(l+1)-8mV_0-\frac{6E_n ms^2}{\delta^3}+\frac{16E_n ms}{\delta^2}-\frac{12E_n m}{\delta}+2\hbar^2\gamma\rho_0\right)}{\hbar^4 s^2(-1+\gamma\rho_0)}R[s]=0. \tag{3.51}$$

The parameters take

$$\xi_1=-\left(-\frac{6E_n m}{\delta^3}\right)/\left(\hbar^4(-1+\gamma\rho_0)\right)$$
$$\xi_2=\left(\frac{16E_n m}{\delta^2}\right)/\left(\hbar^4(-1+\gamma\rho_0)\right)$$
$$\xi_3=-\left(\hbar^2 l(l+1)-8mV_0-\frac{12E_n m}{\delta}+2\hbar^2\gamma\rho_0\right)/\left(\hbar^4(-1+\gamma\rho_0)\right)$$
$$c_1=(-2+4\gamma\rho_0)/(-1+\gamma\rho_0)$$
$$c_2=0, c_3=0$$
$$c_4=\frac{1}{2}(1-\frac{-2+4\gamma\rho_0}{-1+\gamma\rho_0}, c_5=0$$
$$c_6=\frac{6E_n m}{\hbar^4\delta^3(-1+\gamma\rho_0)}, c_7=-\frac{16E_n m}{\hbar^4\delta^2(-1+\gamma\rho_0)}$$
$$c_8=\frac{-\hbar^2 l(l+1)+8mV_0+\frac{12E_n m}{\delta}-2h^2\gamma\rho_0}{\hbar^4(-1+\gamma\rho_0)}+$$
$$\frac{1}{4}\left(1-\frac{-2+4\gamma\rho_0}{-1+\gamma\rho_0}\right)^2$$
$$c_9=\frac{6E_n m}{\hbar^4\delta^3(-1+\gamma\rho_0)}$$
$$c_{10}=1+2\sqrt{\frac{-\hbar^2 l(l+1)+8mV_0+\frac{12E_n m}{\delta}-2\hbar^2\gamma\rho_0}{\hbar^4(-1+\gamma\rho_0)}+\frac{1}{4}\left(1-\frac{-2+4\gamma\rho_0}{-1+\gamma\rho_0}\right)^2}$$
$$c_{11}=2\sqrt{6}\sqrt{\frac{E_n m}{\hbar^4\delta^3(-1+\gamma\rho_0)}}$$
$$c_{12}=\frac{1}{2}\left(1-\frac{-2+4\gamma\rho_0}{-1+\gamma\rho_0}\right)+$$
$$\sqrt{\frac{-\hbar^2 l(l+1)+8mV_0+\frac{12E_n m}{\delta}-2\hbar^2\gamma\rho_0}{\hbar^4(-1+\gamma\rho_0)}+\frac{1}{4}\left(1-\frac{-2+4\gamma\rho_0}{-1+\gamma\rho_0}\right)^2}$$

$$c_{13} = -\sqrt{6}\sqrt{\frac{E_n m}{\hbar^4 \delta^3 \left(-1+\gamma\rho_0\right)}}, \tag{3.52}$$

the energy equation is written

$$\lambda = \sqrt{6}\left(1+2n\right)\sqrt{\frac{E_n m}{\hbar^4 \delta^3 \left(-1+\gamma\rho_0\right)}} - \frac{16 E_n m}{\hbar^4 \delta^2 \left(-1+\gamma\rho_0\right)} + \sqrt{6}\sqrt{\frac{E_n m\left(\left(1-3\gamma\rho_0\right)^2 + \frac{4\left(-1+\gamma\rho_0\right)\left(-\hbar^2 l\left(l+1\right)+8mV_0+\frac{12E_n m}{\delta}-2\hbar^2\gamma\rho_0\right)}{\hbar^4}\right)}{\hbar^4\delta^3\left(-1+\gamma\rho_0\right)^3}}. \tag{3.53}$$

The numerical value of energy for *n* and *l* is given in Table 3.7 with appropriate parameters $\gamma = 0.6, m = 1/2, \hbar = 1, V_0 = 0.5, \delta = -0.03, \rho_0 = 10$. So energy equation and wave function of the Pöschl-Teller potential give the same results as literature for the case of $\varepsilon(r) = 0$ when using these parameters. The energy graph is shown in Figure 3.15 for given energy values. The energy values of Pöschl-Teller potential show a negative decrease when *n* and *l* increase. Since, the energy values appear to be close to each other in different momentum states, also energy changes showed a similar fluctuation in all momentum states , such as E_n*=-0.366285* in l_1*=1,*E_n*=-0.376564 in* l_2*=2,* E_n*=-0.392234* in l_3*=3* for *n =7.* When our result is compared with non velocity-dependent potential, it is seen that it is in full agreement with the literature complete harmony.

The wave function is

$$R[n,r] = \frac{1}{r}\left(N_{ln} 2\sqrt{6} e^{-\sqrt{6} r \sqrt{-\frac{E_n m}{\hbar^4\delta^3}}} r^{\frac{1}{2}+\sqrt{\frac{1}{4}-\frac{-h^2 l(l+1)+8mVo+\frac{12E_n m}{\delta}}{\hbar^4}}} L_n^{2\sqrt{\frac{1}{4}-\frac{-h^2 L(1+L)+8mVo+\frac{12E_n m}{\delta}}{\hbar^4}}} \sqrt{-\frac{E_n m}{\hbar^4\delta^3}} \right). \tag{3.54}$$

Table 3.7 The energy eigenvalues of the Pöschl-Teller potential in Case 1 under $\gamma = 0.6, m = 1/2, \hbar = 1, V_0 = 0.5, \delta = -0.03, \rho_0 = 10.$

State	$l_1=1$	$l_2=2$	$l_3=3$
n=1	-0.00923383	-0.0191414	-0.0400918
n=2	-0.0353182	-0.0454756	-0.0629481
n=3	-0.0749469	-0.0851717	-0.101656
n=4	-0.127888	-0.13814	-0.154215
n=5	-0.194099	-0.204365	-0.220231
n=6	-0.273566	-0.28384	-0.299586
n=7	-0.366285	-0.376564	-0.392234
n=8	-0.472254	-0.482536	-0.498156
n=9	-0.591471	-0.601756	-0.61734
n=10	-0.723935	-0.734222	-0.74978

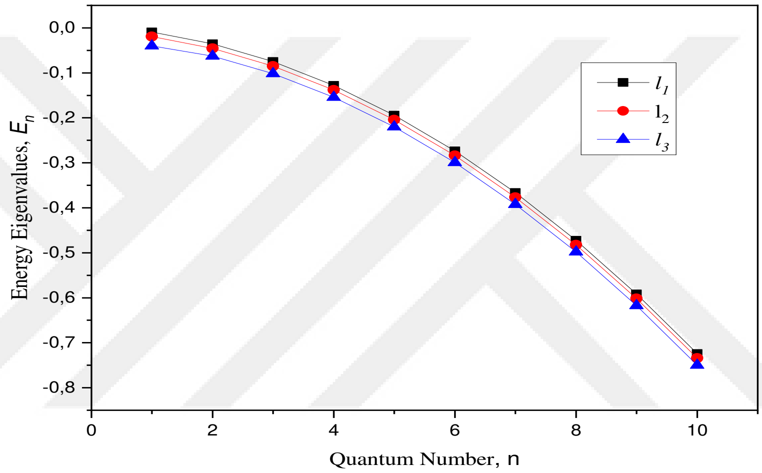

Figure 3.15 The graph of energy eigenvalues of the Pöschl-Teller potential in Case 1 for $\gamma = 0.6, m = 1/2, \hbar = 1, V_0 = 0.5, \delta = -0.03, \rho_0 = 10.$

3.2 Case 2: State of form factor $\varepsilon(r) = \gamma r$

In this frame, by taking form factor $\varepsilon(r) = \gamma\rho(r) = \gamma r$ the Schrödinger equation of Equation (2.14) becomes SE,

$$R''[r] + \frac{(-2 + r\gamma)}{r(-1 + r\gamma)} R'[r] + \frac{\left(-2E_n m r^2 + l(l+1)\hbar^2 + 2mr^2 V[r]\right)}{r^2(-1 + r\gamma)\hbar^2} R[r] = 0. \tag{3.55}$$

The solutions of energy eigenvalues and corresponding wave function were searched for various potentials by changing $V[r]$ in this equation.

3.2.1 Harmonic Oscillator

The SE with Harmonic Oscillator is transformed to

$$
\begin{aligned}
&R''[r]+\frac{(-2+r\gamma)}{r(-1+r\gamma)}R'[r]+\\
&\frac{\left(mr^2\left(-2E_n+mr^2w^2\right)+l\left(2m+\hbar^2\right)+l^2\left(2m+\hbar^2\right)\right)}{r^2(-1+r\gamma)\hbar^2}R[r]=0.
\end{aligned}
\tag{3.56}
$$

By letting $r=\alpha\tau$ using with wave function $R[r]=\frac{U[r]}{r}$ then Equation (3.56) is

$$
\begin{aligned}
&\frac{1}{\alpha^2}U''[\tau]+\frac{\gamma}{\alpha(-1+\alpha\gamma\tau)}U'[\tau]-\\
&\frac{\left(m\left(2l(l+1)-2E_n\alpha^2\tau^2+mw^2\alpha^4\tau^4\right)+\left(l+l^2+\alpha\gamma\tau\right)\hbar^2\right)}{\alpha^2\tau^2(-1+\alpha\gamma\tau)\hbar^2}U[\tau]=0.
\end{aligned}
\tag{3.57}
$$

Also defining a variable of the form $\tau\to\frac{1}{s}$, the Equation (3.57) yields,

$$
\begin{aligned}
&U''[s]+\frac{(2s-3\alpha\gamma)}{s(s-\alpha\gamma)}U'[s]+\\
&\frac{\left(\begin{array}{l}-\frac{2E_nm\alpha^2}{s}+\frac{m^2w^2\alpha^4}{s^3}+\alpha\gamma\hbar^2+\\ s^2\left(2l(1+l)m+l\hbar^2+l^2\hbar^2\right)-s\alpha\gamma\left(2l(1+l)m+l\hbar^2+l^2\hbar^2\right)\end{array}\right)}{s^2(s-\alpha\gamma)^2\hbar^2}U[s]=0.
\end{aligned}
\tag{3.58}
$$

The same procedure, the power series expansion of $\frac{1}{s}$ and $\frac{1}{s^3}$ is applied from Equation (3.36). By substituting Equation (3.36) into Equation (3.58) and the equation takes the following form

$$U''[s]+\frac{(2s-3\alpha\gamma)}{s\alpha\left(-1+\frac{s}{\alpha\gamma}\right)\gamma}U'[s]+ \tag{3.59}$$

$$\frac{\left(\begin{array}{l} s^2\left(2l(1+l)m-\frac{2E_n m\alpha^2}{\delta^3}-\frac{6m^2w^2\alpha^4}{\delta^3}\right)-\frac{6E_n m\alpha^4}{\delta}-\frac{2m^2w^2\alpha^4}{\delta} \\ +l\hbar^2+l^2\hbar^2+\alpha\gamma\hbar^2+s\left(\begin{array}{l}\frac{6E_n m\alpha^2}{\delta^2}+\frac{9m^2w^2\alpha^4}{\delta^2}- \\ \alpha\gamma\left(2l(l+1)m+l\hbar^2+l^2\hbar^2\right)\end{array}\right)\end{array}\right)}{s^2\alpha^2\left(-1+\frac{s}{\alpha\gamma}\right)^2\gamma^2\hbar^2}U[s]=0.$$

At this step, it can be obtained the parameters as

$$\begin{aligned}
\xi_1 &= -\left(2l(l+1)m-\frac{2E_n m\alpha^2}{\delta^3}-\frac{6m^2w^2\alpha^4}{\delta^3}\right)/\left((\alpha\gamma)^2\,2\hbar^2\right) \\
\xi_2 &= \left(\frac{6E_n m\alpha^2}{\delta^2}+\frac{9m^2w^2\alpha^4}{\delta^2}-\alpha\gamma\left(2l(l+1)m+l\hbar^2+l^2\hbar^2\right)\right)/\left((\alpha\gamma)^2\hbar^2\right) \\
\xi_3 &= -\left(-\frac{6E_n m\alpha^2}{\delta}-\frac{2m^2w^2\alpha^4}{\delta}\right)/\left((\alpha\gamma)^2\hbar^2\right) \\
c_1 &= -3, c_2=-2/(\alpha\gamma) \\
c_3 &= -1/(\alpha\gamma), c_4=2, c_5=0 \\
c_6 &= \xi_1, c_7=-\xi_2, c_8=4+\xi_3, c_9=\xi_1+\frac{\xi_2}{\alpha\gamma}+\frac{4+\xi_3}{\alpha^2\gamma^2} \\
c_{10} &= 1+2\sqrt{4+\xi_3} \\
c_{11} &= -\frac{2}{\alpha\gamma}+2\left(-\frac{\sqrt{4+\xi_3}}{\alpha\gamma}+\sqrt{\xi_1+\frac{\xi_2}{\alpha\gamma}+\frac{4+\xi_3}{\alpha^2\gamma^2}}\right) \\
c_{12} &= 2+\sqrt{4+\xi_3} \\
c_{13} &= \frac{\sqrt{4+\xi_3}}{\alpha\gamma}-\sqrt{\xi_1+\frac{\xi_2}{\alpha\gamma}+\frac{4+\xi_3}{\alpha^2\gamma^2}}.
\end{aligned} \tag{3.60}$$

the energy equation is

$$\lambda=-\frac{2n}{\alpha\gamma}-\frac{(-1+n)n}{\alpha\gamma}-\xi_2-\frac{2(4+\xi_3)}{\alpha\gamma}+2\sqrt{(4+\xi_3)\left(\xi_1+\frac{\xi_2}{\alpha\gamma}+\frac{4+\xi_3}{\alpha^2\gamma^2}\right)}+ \tag{3.61}$$

$$(1+2n)\left(-\frac{\sqrt{4+\xi_3}}{\alpha\gamma}+\sqrt{\xi_1+\frac{\xi_2}{\alpha\gamma}+\frac{4+\xi_3}{\alpha^2\gamma^2}}\right).$$

Due to Equation (3.61) has not analytical solution, numerical solution of this equation is obtained for n and l. The obtained results are given in the Table 3.8 below with fixed parameters $w = 10, \alpha = -0.48, \delta = 2, \gamma = -25, m = 1/2, \hbar = 1$ and the energy graph is drawn as in Figure 3.16. In figure, energy values of Harmonic oscillator have positive increased with increasing quantum number, also showed a positive increase in the case of momentum state, and there is also a noticeable fluctuation between these values. For example, the biggest energy value is taken $E_n=1762.7$ in $n=10$ and $l_3=3$ while the smallest value is E_n=107.356 in $n=10$ and l_1=1. So, this figure is very similar to literature in case $\varepsilon(r) = 0$.

The wave function is calculated by using Equation (2.15),

$$R[n,r] = \frac{1}{r}\begin{pmatrix} N_{nl}\, r^{2+\sqrt{4+\xi_3}} \left(1+\dfrac{r}{\alpha\gamma}\right)^{\frac{\sqrt{4+\xi_3}}{\alpha\gamma} - \sqrt{\xi_1 + \frac{\xi_2}{\alpha\gamma} + \frac{4+\xi_3}{\alpha^2\gamma^2}}} \\ {}_2F_1\left(-n, 1+2+2\sqrt{4+\xi_3}+n; 2+2\sqrt{4+\xi_3}; -\dfrac{r}{\alpha\gamma}\right) \end{pmatrix}. \tag{3.62}$$

Table 3.8 The energy eigenvalues of the Harmonic oscillator potential in Case 2 under $w = 10, \alpha = -0.48, \delta = 2, \gamma = -25, m = 1/2, \hbar = 1$.

State	$l_1=1$	$l_2=2$	$l_3=3$
n=1	107.356	329.756	690.442
n=2	164.752	385.736	735.66
n=3	237.31	458.242	802.715
n=4	325.335	546.819	888.612
n=5	429.118	651.434	992.077
n=6	548.93	772.199	1112.57
n=7	685.013	909.273	1249.89
n=8	837.587	1062.83	1403.98
n=9	1006.84	1233.03	1574.9
n=10	1192.95	1420.04	1762.7

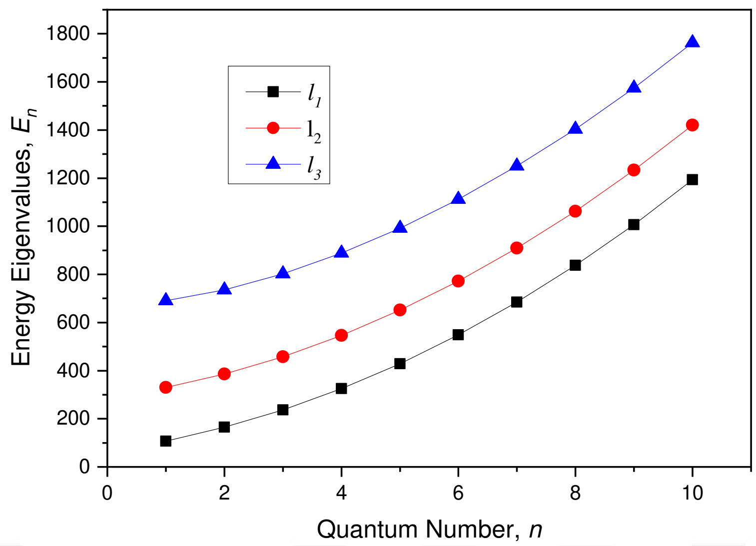

Figure 3.16 The graph of energy eigenvalues of the Harmonic oscillator potential in Case 2 for $w=10, \alpha=-0.48, \delta=2, \gamma=-25, m=1/2, \hbar=1$.

3.2.2 Coulomb Potential

Using this condition with the Coulomb potential and then with similar algebraic calculation, the corresponding SE becomes,

$$R''[s]+\frac{(2s-\gamma)}{s\gamma\left(-1+\frac{s}{\gamma}\right)}R'[s]+ \tag{3.63}$$

$$\frac{\left(\begin{array}{l}-2l(l+1)s^2\mu-2E_n\gamma\left(\frac{s^2}{\delta^3}-\frac{3s}{\delta^2}+\frac{3}{\delta}\right)\mu+2\mu(E_n+A\gamma)+\\ 2s\mu(-A+l(l+1)\gamma)\end{array}\right)}{s^2\gamma^2\hbar^2\left(-1+\frac{s}{\gamma}\right)^2}R[s]=0.$$

By using the parameters

$$\xi_1=-\left(-2l(l+1)\mu-\frac{2E_n\gamma\mu}{\delta^3}\right)/\left(\gamma^2\hbar^2\right)$$

$$\xi_2=\left(\frac{6E_n\gamma\mu}{\delta^2}+2\mu(-A+l(l+1)\gamma)\right)/\left(\gamma^2\hbar^2\right)$$

$$\xi_3=-\left(-\frac{6E_n\gamma\mu}{\delta}+2\mu(E_n+A\gamma)\right)/\left(\gamma^2\hbar^2\right)$$

$$
\begin{aligned}
c_1 &= -1 \\
c_2 &= -2/(\gamma) \\
c_3 &= 1/(\gamma) \\
c_4 &= 1 \\
c_5 &= 0 \\
c_6 &= \xi_1 \\
c_7 &= -\xi_2 \\
c_8 &= 1+\xi_3 \\
c_9 &= \xi_1 + \frac{\xi_2}{\gamma} + \frac{1+\xi_3}{\gamma^2} \\
c_{10} &= 1 + 2\sqrt{1+\xi_3} \\
c_{11} &= -\frac{2}{\gamma} + 2\left(-\frac{\sqrt{1+\xi_3}}{\gamma} + \sqrt{\xi_1 + \frac{\xi_2}{\gamma} + \frac{1+\xi_3}{\gamma^2}} \right) \\
c_{12} &= 1 + \sqrt{1+\xi_3} \\
c_{13} &= \frac{\sqrt{1+\xi_3}}{\gamma} - \sqrt{\xi_1 + \frac{\xi_2}{\gamma} + \frac{1+\xi_3}{\gamma^2}}.
\end{aligned}
\tag{3.64}
$$

using the same procedure as before, the energy spectrum is obtained for the system as,

$$
\begin{aligned}
\lambda = &-\frac{2n}{\gamma} - \frac{(-1+n)n}{\gamma} - \xi_2 - \frac{2(1+\xi_3)}{\gamma} + 2\sqrt{(1+\xi_3)\left(\xi_1 + \frac{\xi_2}{\gamma} + \frac{1+\xi_3}{\gamma^2} \right)} \\
&+(1+2n)\left(-\frac{\sqrt{1+\xi_3}}{\gamma} + \sqrt{\xi_1 + \frac{\xi_2}{\gamma} + \frac{1+\xi_3}{\gamma^2}} \right).
\end{aligned}
\tag{3.65}
$$

The numerical results of the energy for *n* and *l* are given in the Table 3.9 for $\gamma = 0.02$, $\delta = -2, \mu = 1/2, \hbar = 1, A = 50$ parameters by using above equation and energy graph is plotted as shown in Figure 3.17. As seen in figure, the energy values of Coulomb potential negative decreased when quantum number increases, on the other hand, the energy changes negative increase as momentum number increases. The energy changes in different quantum states are close to each other in different momentum states E_n=*-607570* is in l_1=*1*, E_n=*-58890*.5 in l_2=*2*, E_n=*-56083*.7 in l_3 =3, for *n =10*, and they showed a parallel slope. When the graph of energy compared with for non-velocity dependent potential, it is seen that is different with the literature. The reason of this, the form factor changes to *r*.

The wave function is given by using Equation (2.12),

$$R[n,r] = N_{nl} r^{1+\sqrt{1+\xi_3}} \left(1+\frac{r}{\gamma}\right)^{\frac{\sqrt{1+\xi_3}}{\gamma} - \sqrt{\xi_1+\frac{\xi_2}{\gamma}+\frac{1+\xi_3}{\gamma^2}}} \tag{3.66}$$

$$_2F_1\left(\begin{array}{l} -n, 1+1-\dfrac{2}{\gamma}+2\sqrt{1+\xi_3}+2\left(-\dfrac{\sqrt{1+\xi_3}}{\gamma}+\sqrt{\xi_1+\dfrac{\xi_2}{\gamma}+\dfrac{1+\xi_3}{\gamma^2}}\right)+n; \\ 2+2\sqrt{1+\xi_3}; -\dfrac{r}{\gamma} \end{array}\right).$$

Table 3.9 The energy eigenvalues of the Coulomb potential in Case 2 under $\gamma = 0.02, \delta = -2, \mu = 1/2, \hbar = 1, A = 50$.

State	$l_1=1$	$l_2=2$	$l_3=3$
n=1	-1454.71	-517.838	-155.961
n=2	-3594.43	-2056.21	-571.252
n=3	-6869.93	-5139.33	-2678.99
n=4	-11259.3	-9462.33	-6776.25
n=5	-16754.4	-14927.5	-12177.2
n=6	-23352.5	-21509.5	-18732.6
n=7	-31052.3	-29199.5	-26409.1
n=8	-39853.1	-37994.1	-35195.7
n=9	-49754.8	-47891.4	-45088.
n=10	-60757	-58890.5	-56083.7

These results are new and to the best of our knowledge, it has not been reported before in the available literature.

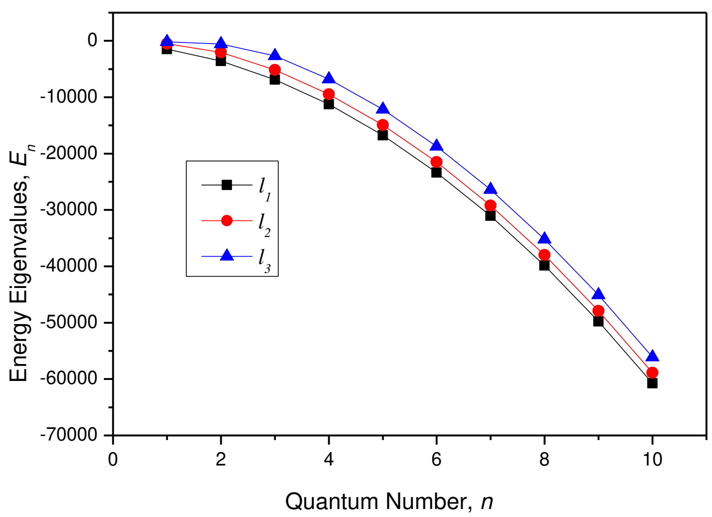

Figure 3.17 The graph of energy eigenvalues of the Coulomb potential in Case 2 for $\gamma = 0.02, \delta = -2, \mu = 1/2, \hbar = 1, A = 50$.

3.2.3 Hulthen Potential

The Schrödinger equation with Hulthen potential is transformed to

$$R''[r]+\frac{\left(\frac{2}{r}-\gamma\right)}{1-r\gamma}R'[r]+\frac{1}{1-r\gamma}\left(-\frac{l(1+l)}{r^2}+\frac{2m\left(E_n+\frac{K}{\left(-1+e^{r/\kappa}\right)\kappa}\right)}{\hbar^2}\right)R[r]=0. \tag{3.67}$$

By defining the new approximation,

$$\frac{K}{\left(-1+e^{r/\kappa}\right)\kappa}\approx\frac{K}{r^2\kappa},$$

and using wave function $R[r]=U[r]/r$, the Equation (3.67) is transformed to

$$U''[r]+\frac{\gamma}{1-r\gamma}U'[r]+\frac{1}{r^2(1-r\gamma)\hbar^2}\left(-l-l^2+2E_nr^2m+\frac{2Km}{\kappa\hbar^2}-r\gamma\hbar^2\right)U[r]=0. \tag{3.68}$$

And again, using the transformation, $r=1/s$ Equation (3.68) yields

$$U''[s]-\frac{(-2s+2\gamma)}{s(s-\gamma)}U'[s]- \tag{3.69}$$
$$-\frac{1}{s^2(s-\gamma)^2\hbar^2}\begin{pmatrix}2E_nm+\frac{2E_n\gamma m}{s}+s^2(l+l^2\\ -\frac{2K\mu}{\kappa\hbar^2})-\gamma^2\hbar^2+s(-l\gamma-l^2\gamma+\frac{2K\gamma m}{\kappa\hbar^2}+\gamma\hbar^2)\end{pmatrix}U[s]=0.$$

Equation (3.69) is solved in the same way by similar methods and power series expansion of Equation (3.36) was use. Substituting Equation (3.36) into the Equation (3.69) yields,

$$U''[s]+-\frac{(-2s+2\gamma)}{s\left(-1+\frac{s}{\gamma}\right)\gamma}U[s]+ \tag{3.70}$$
$$\frac{\begin{pmatrix}-2E_nm+\frac{6E_nm\gamma}{\delta}+s^2\left(l+l^2+\frac{2E_nm\gamma}{\delta^3}-\frac{2Km}{\kappa\hbar^2}\right)\\ -\gamma^2\hbar^2+s\left(-l\gamma-l^2\gamma-\frac{6E_nm\gamma}{\delta^2}+\frac{2Km\gamma}{\kappa\hbar^2}+\gamma\hbar^2\right)\end{pmatrix}}{s^2\left(-1+\frac{s}{\gamma}\right)^2\gamma^2\hbar^2}U[s]=0.$$

$$\xi_1 = \left(l + l^2 + \frac{2E_n \gamma m}{\delta^3} - \frac{2Km}{\kappa \hbar^2} \right) / \gamma^2 \hbar^2$$

$$\xi_2 = -\left(-l\gamma - l^2\gamma - \frac{6E_n \gamma m}{\delta^2} + \frac{2K\gamma m}{\kappa \hbar^2} + \gamma \hbar^2 \right) / \gamma^2 \hbar^2 \tag{3.71}$$

$$\xi_3 = \left(-2E_n m + \frac{6E_n \gamma m}{\delta} - \gamma^2 \hbar^2 \right) / \gamma^2 \hbar^2$$

$$c_1 = -2$$

$$c_2 = 2 / (\gamma)$$

$$c_3 = -1 / (\gamma)$$

$$c_4 = \frac{3}{2}$$

$$c_5 = \frac{2}{\gamma}$$

$$c_6 = \frac{4}{\gamma^2} + \frac{\left(l + l^2 + \frac{2E_n m\gamma}{\delta^3} - \frac{2Km}{\kappa \hbar^2} \right)\hbar^2}{\gamma^2}$$

$$c_7 = \frac{6}{\gamma} - \frac{\hbar^2 \left(l\gamma + l^2\gamma + \frac{6E_n m\gamma}{\delta^2} - \frac{2Km\gamma}{\kappa \hbar^2} - \gamma \hbar^2 \right)}{\gamma^2}$$

$$c_8 = \frac{9}{4} + \frac{\hbar^2 \left(-2E_n m + \frac{6E_n m\gamma}{\delta} - \gamma^2 \hbar^2 \right)}{\gamma^2}$$

$$c_9 = \left(\frac{4}{\gamma^2} + \frac{\left(l + l^2 + \frac{2E_n m\gamma}{\delta^3} - \frac{2Km}{\kappa \hbar^2} \right)\hbar^2}{\gamma^2} - \frac{\frac{6}{\gamma} - \frac{\hbar^2 \left(l\gamma + l^2\gamma + \frac{6E_n m\gamma}{\delta^2} - \frac{2Km\gamma}{\kappa \hbar^2} - \gamma \hbar^2 \right)}{\gamma^2}}{\gamma} + \frac{\frac{9}{4} + \frac{\hbar^2 \left(-2E_n m + \frac{6E_n m\gamma}{\delta} - \gamma^2 \hbar^2 \right)}{\gamma^2}}{\gamma^2} \right)$$

$$c_{10} = 1 + 2\sqrt{\frac{9}{4} + \frac{\hbar^2 \left(-2E_n m + \frac{6E_n m\gamma}{\delta} - \gamma^2 \hbar^2 \right)}{\gamma^2}}$$

$$
\begin{aligned}
c_{11} &= -\frac{2}{\gamma} + 2(-\frac{\sqrt{\frac{9}{4}+\frac{\hbar^2\left(-2E_n m+\frac{6E_n m\gamma}{\delta}-\gamma^2\hbar^2\right)}{\gamma^2}}}{\gamma} + \\
&\sqrt{\left(\frac{4}{\gamma^2}+\frac{\left(l+l^2+\frac{2E_n m\gamma}{\delta^3}-\frac{2Km}{\kappa\hbar^2}\right)\hbar^2}{\gamma^2} - \frac{\frac{6}{\gamma}-\frac{\hbar^2\left(l\gamma+l^2\gamma+\frac{6E_n m\gamma}{\delta^2}-\frac{2Km\gamma}{\kappa\hbar^2}-\gamma\hbar^2\right)}{\gamma^2}}{\gamma} + \frac{\frac{9}{4}+\frac{\hbar^2\left(-2E_n m+\frac{6E_n m\gamma}{\delta}-\gamma^2\hbar^2\right)}{\gamma^2}}{\gamma^2}\right)}
\end{aligned}
\tag{3.72}
$$

$$
c_{12} = \frac{3}{2} + \sqrt{\frac{9}{4}+\frac{\hbar^2\left(-2E_n m+\frac{6E_n m\gamma}{\delta}-\gamma^2\hbar^2\right)}{\gamma^2}}
$$

$$
\begin{aligned}
c_{13} &= \frac{2}{\gamma} + \frac{\sqrt{\frac{9}{4}+\frac{\hbar^2\left(-2E_n m+\frac{6E_n m\gamma}{\delta}-\gamma^2\hbar^2\right)}{\gamma^2}}}{\gamma} - \\
&\sqrt{\left(\frac{4}{\gamma^2}+\frac{\left(l+l^2+\frac{2E_n m\gamma}{\delta^3}-\frac{2Km}{\kappa\hbar^2}\right)\hbar^2}{\gamma^2} - \frac{\frac{6}{\gamma}-\frac{\hbar^2\left(l\gamma+l^2\gamma+\frac{6E_n m\gamma}{\delta^2}-\frac{2Km\gamma}{\kappa\hbar^2}-\gamma\hbar^2\right)}{\gamma^2}}{\gamma} + \frac{\frac{9}{4}+\frac{\hbar^2\left(-2E_n m+\frac{6E_n m\gamma}{\delta}-\gamma^2\hbar^2\right)}{\gamma^2}}{\gamma^2}\right)}.
\end{aligned}
$$

Energy equation is

$$\lambda = \frac{6}{\gamma} + \frac{2n}{\gamma} - \frac{(-1+n)n}{\gamma} - \frac{2(1+2n)}{\gamma} - \xi_2 - \frac{2\left(\frac{9}{4}+\xi_3\right)}{\gamma} + \tag{3.73}$$
$$2\sqrt{\left(\frac{9}{4}+\xi_3\right)\left(\frac{4}{\gamma^2}+\xi_1-\frac{\frac{6}{\gamma}-\xi_2}{\gamma}+\frac{\frac{9}{4}+\xi_3}{\gamma^2}\right)} +$$
$$(1+2n)\left(-\frac{\sqrt{\frac{9}{4}+\xi_3}}{\gamma}+\sqrt{\frac{4}{\gamma^2}+\xi_1-\frac{\frac{6}{\gamma}-\xi_2}{\gamma}+\frac{\frac{9}{4}+\xi_3}{\gamma^2}}\right).$$

The numerical results of the energy for n and l are obtained by using Eq. (3.73) these results are presented in the Table 3.10 for fixed parameters $K = 0.06, \kappa = 10, \gamma = 0.5, \delta = -0.05, m = 1/2\hbar = 1$. The energy graph is drawn as function of r in Figure 3.18. As seen in Figure, the energy values of Hulthen potential decreases due to the increasing quantum number however increases with increasing number of momentum. Otherwise, in the *n=1* quantum state, there is a positive decrease for example E_n= 0.0020192 while due to the increasing number of momentum, but in the *n=7* quantum state, there is a negative decrease for all momentum state. There is also a clear fluctuation between energy values. Similarly, if the graph is compared with the literature, there is a slight similarity for case non velocity-dependent potential.

Table 3.10 The energy eigenvalues of the Hulthen potential in Case 2 under $K = 0.06, \kappa = 10, \gamma = 0.5, \delta = -0.05, m = 1/2\hbar = 1$.

State	$l_1=1$	$l_2=2$	$l_3=3$
n=1	0.000427077	0.0020192	0.00322738
n=2	-0.00003044	0.00169187	0.00356193
n=3	-0.000649561	0.00113843	0.00336448
n=4	-0.0014313	0.000396832	0.00283101
n=5	-0.0023778	-0.000521942	0.00204403
n=6	-0.0034912	-0.00161469	0.00104029
n=7	-0.00477342	-0.00288077	-0.000162592
n=8	-0.00622603	-0.00432042	-0.00155561
n=9	-0.00785037	-0.00593413	-0.00313388
n=10	-0.00964749	-0.00772241	-0.00489458

The corresponding wave equation is

$$R[n,r]=\frac{1}{r}\left(\begin{array}{l} N_{nl}r^{\frac{3}{2}+\sqrt{\frac{9}{4}+\xi_3}}\left(1+\frac{r}{\gamma}\right)^{\frac{2}{\gamma}+\frac{\sqrt{\frac{9}{4}+\xi_3}}{\gamma}-\sqrt{\frac{4}{\gamma^2}+\xi_1-\frac{\frac{6}{\gamma}-\xi_2}{\gamma}+\frac{\frac{9}{4}+\xi_3}{\gamma^2}}} \\ {}_2F_1(-n,1+1-\frac{2}{\gamma}+2\sqrt{\frac{9}{4}+\xi_3}+2(-\frac{\sqrt{\frac{9}{4}+\xi_3}}{\gamma}+ \\ \sqrt{\frac{4}{\gamma^2}+\xi_1-\frac{\frac{6}{\gamma}-\xi_2}{\gamma}+\frac{\frac{9}{4}+\xi_3}{\gamma^2}})+n;2+2\sqrt{\frac{9}{4}+\xi_3};-\frac{r}{\gamma}) \end{array}\right). \tag{3.74}$$

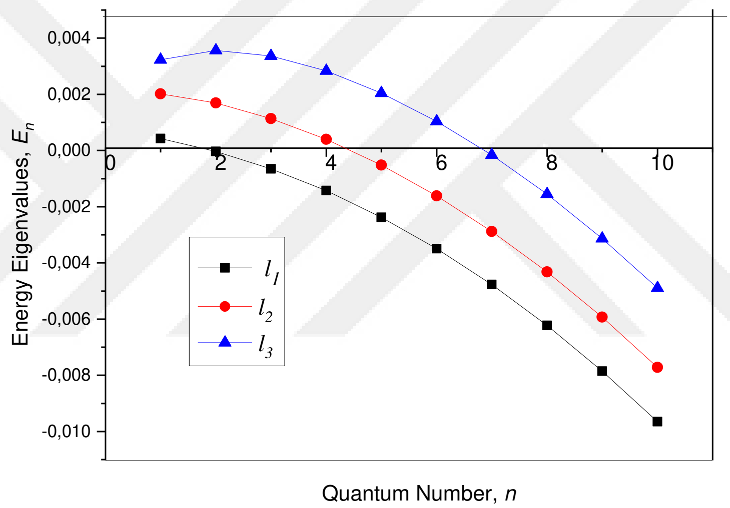

Figure 3.18 The graph of energy eigenvalues of the Hulthen potential in Case 2 for $K=0.06, \kappa=10, \gamma=0.5, \delta=-0.05, m=1/2\hbar=1$.

3.2.4 Kratzer Potential

The SE in the Kratzer potential case is

$$. \; R''[r]+\frac{\gamma}{-1+r\gamma}R'[r]+\frac{\left(-2E_n mr^2+l\left(l+1\right)\hbar^2+2mr^2V\left[r\right]\right)}{r^2\left(-1+r\gamma\right)\hbar^2}R\left[r\right]=0\,. \tag{3.75}$$

Taking a transformation equation of the form $r=1/s$ Equation (3.75) reduces to

$$R''[s]+\frac{(2s-\gamma)}{s(s-\gamma)}R'[s]+$$
$$\frac{1}{\hbar^2 s(s-\gamma)^2}\begin{pmatrix}-2Am+2E_n m-2Bm\gamma+\frac{2Am\gamma-2E_n m\gamma}{s}+\\ s^2\left(-l(l+1)\hbar^2-2mC\right)+s\left(2Bm+l(l+1)\gamma\hbar^2+2m\gamma C\right)\end{pmatrix}R[s]=0. \quad (3.76)$$

To solve the Equation (3.76) power series expansion of $\frac{1}{s}$ is determined by using Equation (3.36). And then substituting into Equation (3.76) and the equation take the following form

$$U''[s]+\frac{(2s-\gamma)}{s\left(-1+\frac{s}{\gamma}\right)\gamma}U'[s]+ \quad (3.77)$$
$$\frac{\begin{pmatrix}-2Am+2E_n m+2Am\gamma-2Bm\gamma-2E_n m\gamma\left(\frac{s^2}{\delta^3}-\frac{3s}{\delta^2}+\frac{3}{\delta}\right)\\ +s^2\left(-l(1+l)\hbar^2-2mC\right)+s\left(2Bm+l(1+l)\gamma\hbar^2+2m\gamma C\right)\end{pmatrix}}{s^2\left(-1+\frac{s}{\gamma}\right)^2\gamma^2\hbar^2}U[s]=0.$$

By defining parameters value

$$\begin{aligned}
&\xi_1=-\left(-\frac{2E_n m\gamma}{\delta^3}-l(l+1)\hbar^2-2mC\right)/\gamma^2\hbar^2 \\
&\xi_2=\left(\left(2Bm+l(l+1)\gamma\hbar^2+2m\gamma C\right)/\gamma^2\hbar^2\right) \\
&\xi_3=-\left(-2Am+2E_n m+2Am\gamma-2Bm\gamma-\frac{6E_n m\gamma}{\delta}\right)/\gamma^2\hbar^2 \\
&c_1=-1, c_2=-2/\gamma, c_3=-1/\gamma, c_4=1 \\
&c_5=0, c_6=\xi_1, c_7=-\xi_2, c_6=\xi_1 \\
&c_7=-\xi_2, c_8=1+\xi \\
&c_9=\xi_1+\frac{\xi_2}{\gamma}+\frac{1+\xi_3}{\gamma^2}, c_{10}=1+2\sqrt{1+\xi_3} \\
&c_{11}=-\frac{2}{\gamma}+2\left(-\frac{\sqrt{1+\xi_3}}{\gamma}+\sqrt{\xi_1+\frac{\xi_2}{\gamma}+\frac{1+\xi_3}{\gamma^2}}\right) \\
&c_{12}=1+\sqrt{1+\xi_3}, c_{13}=\frac{\sqrt{1+\xi_3}}{\gamma}-\sqrt{\xi_1+\frac{\xi_2}{\gamma}+\frac{1+\xi_3}{\gamma^2}},
\end{aligned} \quad (3.78)$$

the energy equation is

$$\lambda = -\frac{2n}{\gamma} - \frac{(-1+n)n}{\gamma} - \xi_2 - \frac{2(1+\xi_3)}{\gamma} + 2\sqrt{(1+\xi_3)\left(\xi_1 + \frac{\xi_2}{\gamma} + \frac{1+\xi_3}{\gamma^2}\right)} + (1+2n)\left(-\frac{\sqrt{1+\xi_3}}{\gamma} + \sqrt{\xi_1 + \frac{\xi_2}{\gamma} + \frac{1+\xi_3}{\gamma^2}}\right). \tag{3.79}$$

The numeric results of energy equation for *n* and *l* are given in Table 3.11 for suitable parameters $A = -0.05, B = 0.1, C = -0.05, \gamma = 50, \delta = 0.3, m = 1/2, \hbar = 1.$ and the energy graph is drawn as shown Figure 3.19. It is seen in graph, while the first two energy values of Kratzer potential have negative, *En*= -0.000915754 in *n=1*, *En*= -0.000182629 in *n=2*, they showed increased slope by taking positive values from the *n>6* case. In addition, there is a clear fluctuation in any energy values.

The corresponding wave function is evaluated.

$$R[n,r] = N_{nl} r^{1+\sqrt{1+\xi_3}} \left(1+\frac{r}{\gamma}\right)^{\frac{\sqrt{1+\xi_3}}{\gamma} - \sqrt{\xi_1 + \frac{\xi_2}{\gamma} + \frac{1+\xi_3}{\gamma^2}}} {}_2F_1\Big(-n, 1+1-\frac{2}{\gamma} + 2\sqrt{1+\xi_3} + 2\Big(-\frac{\sqrt{1+\xi_3}}{\gamma} + \sqrt{\xi_1 + \frac{\xi_2}{\gamma} + \frac{1+\xi_3}{\gamma^2}}\Big) + n; 2+2\sqrt{1+\xi_3}; -\frac{r}{\gamma}\Big). \tag{3.80}$$

Table 3.11 The energy eigenvalues of the Kratzer potential in Case 2 under $A = -0.05, B = 0.1, C = -0.05, \gamma = 50, \delta = 0.3, m = 1/2, \hbar = 1.$

State	$l_1=1$	$l_2=2$	$l_3=3$
n=1	-0.000915754	-0.00334366	-0.00569026
n=2	-0.000182629	-0.00300829	-0.00658579
n=3	0.000866024	-0.00212342	-0.00620772
n=4	0.00220047	-0.000871945	-0.00521287
n=5	0.00381186	0.000691688	-0.00379691
n=6	0.00569683	0.00254666	-0.00203464
n=7	0.00785388	0.00468363	0.0000403329
n=8	0.0102823	0.0070979	0.0024111
n=9	0.0129816	0.00978692	0.00506839
n=10	0.0159516	0.0127492	0.00800682

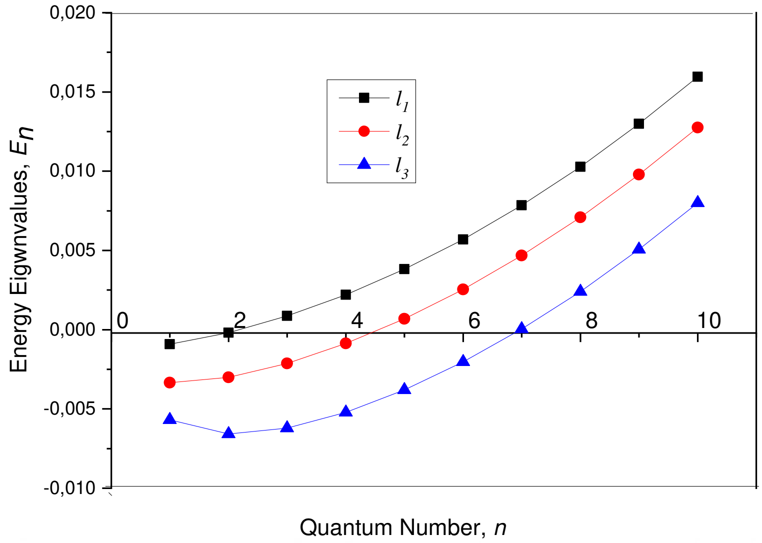

Figure 3.19 The graph of energy eigenvalues of the Kratzer potential in Case 2 for $A=-0.05, B=0.1, C=-0.05, \gamma=50, \delta=0.3, m=1/2, \hbar=1.$

3.2.5 Mie Potential

The SE can be written for Mie potential as

$$R''[r]+\frac{(-2+r\gamma)}{r(-1+r\gamma)}R'[r]+\frac{\left(-2E_n mr^2+a^2mV_0-2amrV_0+l(l+1)\hbar^2\right)}{r^2(-1+r\gamma)\hbar^2}R[r]=0. \tag{3.81}$$

Making use of new variable $r=1/s$ then Equation (3.81) is

$$R''[s]+\frac{1}{s\left(-1+\frac{s}{\gamma}\right)}R'[s]-\frac{\begin{pmatrix}-2E_n m\gamma+s^2\left(2amV_0-l\hbar^2\left(1+l+a^2mV_0\right)\right)+\\ s(2E_n m-2am\gamma V_0+l\gamma\hbar^2\left(1+l+a^2mV_0\right))\end{pmatrix}}{s^2\left(-1+\frac{s}{\gamma}\right)^2\gamma^2\hbar^2}R[s]=0. \tag{3.82}$$

The parameters take

$$\xi_1=-\left(2amV_0-l\left(1+l+a^2mV_0\right)\hbar^2\right)/\gamma^2\hbar^2$$

$$\xi_2 = \left(2E_n m - 2amV_0\gamma + l\left(1+l+a^2 mV_0\right)\gamma\hbar^2\right) / \left(\gamma^2\hbar^2\right)$$
$$\xi_3 = 2E_n m\gamma / \left(\gamma^2\hbar^2\right) \tag{3.83}$$
$$c_1 = -1, c_2 = 0, c_3 = -1/\gamma, c_4 = 1, c_5 = \frac{1}{\gamma}$$
$$c_6 = \frac{1}{\gamma^2} + \xi_1, c_7 = \frac{2}{\gamma} - \xi_2, c_8 = 1 + \xi_3, c_9 = \frac{1}{\gamma^2} + \xi_1 - \frac{\frac{2}{\gamma} - \xi_2}{\gamma} + \frac{1+\xi_3}{\gamma^2}$$
$$c_{10} = 1 + 2\sqrt{1+\xi_3}$$
$$c_{11} = -\frac{2}{\gamma} + 2\left(-\frac{\sqrt{1+\xi_3}}{\gamma} + \sqrt{\frac{1}{\gamma^2} + \xi_1 - \frac{\frac{2}{\gamma} - \xi_2}{\gamma} + \frac{1+\xi_3}{\gamma^2}}\right)$$
$$c_{12} = 1 + \sqrt{1+\xi_3}$$
$$c_{13} = \frac{\sqrt{1+\xi_3}}{\gamma} - \sqrt{\frac{1}{\gamma^2} + \xi_1 - \frac{\frac{2}{\gamma} - \xi_2}{\gamma} + \frac{1+\xi_3}{\gamma^2}},$$

energy equation is written

$$\lambda = \frac{2}{\gamma} - \frac{(-1+n)n}{\gamma} - \frac{1+2n}{\gamma} - \xi_2 - \frac{2(1+\xi_3)}{\gamma} + \tag{3.84}$$
$$2\sqrt{(1+\xi_3)\left(\frac{1}{\gamma^2} + \xi_1 - \frac{\frac{2}{\gamma} - \xi_2}{\gamma} + \frac{1+\xi_3}{\gamma^2}\right)} +$$
$$(1+2n)\left(-\frac{\sqrt{1+\xi_3}}{\gamma} + \sqrt{\frac{1}{\gamma^2} + \xi_1 - \frac{\frac{2}{\gamma} - \xi_2}{\gamma} + \frac{1+\xi_3}{\gamma^2}}\right).$$

The numerical results of the energy for n and l are evaluated by using Equation (3.88) and these results are given in the Table 3.12 with appropriate parameters $m = 1/2$, $a = 10, \gamma = 5, V_0 = 0.5, \hbar = 1$ and energy graph is plotted as function of r in Figure 3.20. The energy values of Mie potential show an increasing trend with increasing quantum number. Similarly, a positive increase is observed depending on the momentum number.

The wave function is

$$R[n,r] = N_{nl} r^{1+\sqrt{1+\xi_3}} \left(1+\frac{r}{\gamma}\right)^{\frac{1}{\gamma}+\frac{\sqrt{1+\varepsilon 3}}{\gamma}-\sqrt{\frac{1}{\gamma^2}+\xi_1-\frac{\frac{2}{\gamma}-\xi_2}{\gamma}+\frac{1+\xi_3}{\gamma^2}}} \tag{3.85}$$

$$ {}_2F_1\left(\begin{array}{l} -n, 1+-\frac{2}{\gamma}+2\sqrt{1+\xi_3}+2\left(-\frac{\sqrt{1+\xi_3}}{\gamma}+\sqrt{\frac{1}{\gamma^2}+\xi_1-\frac{\frac{2}{\gamma}-\xi_2}{\gamma}+\frac{1+\xi_3}{\gamma^2}}\right)+n; \\ 2+2\sqrt{1+\xi_3}; -\frac{r}{\gamma} \end{array} \right)$$

Table 3.12 The energy eigenvalues of the Mie potential in Case 2 under $m = 1/2, a = 10, \gamma = 5, V_0 = 0.5, \hbar = 1$.

State	l_1=1	l_2=2	l_3=3
n=1	734.15	1231.64	1688.9
n=2	1135.32	1793.21	2382.08
n=3	1590.36	2401.45	3114.4
n=4	2101.69	3062.38	3895.54
n=5	2670.24	3778.46	4729.49
n=6	3296.42	4550.85	5618.24
n=7	3980.49	5380.24	6562.92
n=8	4722.56	6267.01	7564.22
n=9	5522.73	7211.41	8622.59
n=10	6381.04	8213.61	9738.32

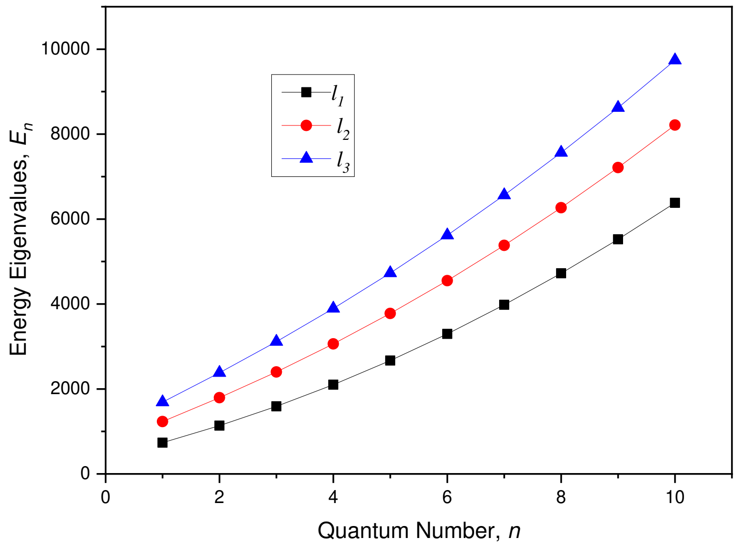

Figure 3.20 The graph of energy eigenvalues of Mie potential in Case 2 for $m = 1/2, a = 10, \gamma = 5, V_0 = 0.5, \hbar = 1$.

3.2.6 Cornell Potential

In this case the SE takes the form

$$R''[r]+\frac{(-2+r\gamma)}{r(-1+r\gamma)}R'[r]+ \\ \frac{\left(-2mr^2\left(E_n-\frac{b}{r}+ar\right)+l\left(2m+\hbar^2\right)+l^2\left(2m+\hbar^2\right)\right)}{r^2(-1+r\gamma)\hbar^2}R[r]=0. \tag{3.86}$$

By using transformation $r=\alpha\tau$ and then substituting into the Equation (3.86) is

$$R''[\tau]+\frac{(-2+\alpha\gamma\tau)}{\tau(-1+\alpha\gamma\tau)}R'[\tau]+ \\ \frac{\left(-2m\alpha\tau\left(-b+\alpha\tau\left(E_n+a\alpha\tau\right)\right)+l\left(2m+\hbar^2\right)+l^2\left(2m+\hbar^2\right)\right)}{\tau^2(-1+\alpha\gamma\tau)\hbar^2}R[\tau]=0. \tag{3.87}$$

In order to solve Equation (3.87) by using NU, then by performing the change of new variable $\tau=1/s$ Equation (3.87) becomes

$$R''[s]+\frac{\alpha\gamma\rho_0}{s(s-\alpha\gamma\rho_0)}R'[s]- \\ \frac{\left(2bm\alpha-\frac{2E_nm\alpha^2}{s}-\frac{2am\alpha^3}{s^2}+s\left(l\left(2m+\hbar^2\right)+l^2\left(2m+\hbar^2\right)\right)\right)}{s^2(s-\alpha\gamma\rho_0)^2}R[s]=0. \tag{3.88}$$

where, the power series expansion of $\frac{1}{s}$ and $\frac{1}{s^2}$ .is written from Equation (3.36)

By substituting Equation (3.36) into Equation (3.88) yields the following equation

$$R''[s]+\frac{1}{s\left(-1+\frac{s}{\alpha\gamma\rho_0}\right)}R'[s]- \\ \frac{\left(\begin{array}{l}-2E_nm\alpha^2\left(\frac{s^2}{\delta^3}-\frac{3s}{\delta^2}+\frac{3}{\delta}\right)- \\ 2am\alpha^3\left(\frac{3s^2}{\delta^3}-\frac{8s}{\delta^2}+\frac{6}{\delta}\right)+2b\alpha\mu+s\left(l\left(2m+\hbar^2\right)+l^2\left(2m+\hbar^2\right)\right)\end{array}\right)}{s^2\alpha^2\gamma^2\left(-1+\frac{s}{\alpha\gamma\rho_0}\right)^2\rho_0^2}R[s]=0. \tag{3.89}$$

The parameters take

$$\xi_1 = -\left(-\frac{2E_n m\alpha^2}{\delta^3} - \frac{6am\alpha^3}{\delta^3}\right) / \left(\alpha^2\gamma^2\right) \tag{3.90}$$

$$\xi_2 = \left(\frac{6E_n m\alpha^2}{\delta^2} + \frac{16am\alpha^3}{\delta^2} + l\left(2m+\hbar^2\right) + l^2\left(2m+\hbar^2\right)\right) / \left(\alpha^2\gamma^2\right)$$

$$\xi_3 = -\left(-\frac{2E_n m\alpha^2}{\delta^3} - \frac{6am\alpha^3}{\delta^3}\right) / \left(\alpha^2\gamma^2\right)$$

$$c_1 = -1, c_2 = 0, c_3 = -1/\left(\alpha\gamma\right), c_4 = 1, c_5 = \frac{1}{\alpha\gamma}, c_6 = \frac{1}{\alpha^2\gamma^2} + \xi_1, c_7 = \frac{2}{\alpha\gamma} - \xi_2,$$

$$c_8 = 1+\xi_3, c_9 = \frac{1}{\alpha^2\gamma^2} + \xi_1 - \frac{\frac{2}{\alpha\gamma} - \xi_2}{\alpha\gamma} + \frac{1+\xi_3}{\alpha^2\gamma^2}, c_{10} = 1 + 2\sqrt{1+\xi_3}$$

$$c_{11} = -\frac{2}{\alpha\gamma} + 2\left(-\frac{\sqrt{1+\xi_3}}{\alpha\gamma} + \sqrt{\frac{1}{\alpha^2\gamma^2} + \xi_1 - \frac{\frac{2}{\alpha\gamma} - \xi_2}{\alpha\gamma} + \frac{1+\xi_3}{\alpha^2\gamma^2}}\right)$$

$$-\frac{2}{\alpha\gamma} + 2\left(-\frac{\sqrt{1+\xi_3}}{\alpha\gamma} + \sqrt{\frac{1}{\alpha^2\gamma^2} + \xi_1 - \frac{\frac{2}{\alpha\gamma} - \xi_2}{\alpha\gamma} + \frac{1+\xi_3}{\alpha^2\gamma^2}}\right)$$

$$c_{12} = 1 + \sqrt{1+\xi_3}, c_{13} = \frac{1}{\alpha\gamma} + \frac{\sqrt{1+\xi_3}}{\alpha\gamma} - \sqrt{\frac{1}{\alpha^2\gamma^2} + \xi_1 - \frac{\frac{2}{\alpha\gamma} - \xi_2}{\alpha\gamma} + \frac{1+\xi_3}{\alpha^2\gamma^2}},$$

the energy equation is

$$\begin{aligned}\lambda = {} & \frac{2}{\alpha\gamma} - \frac{\left(-1+n\right)n}{\alpha\gamma} - \frac{1+2n}{\alpha\gamma} - \xi_2 - \frac{2\left(1+\xi_3\right)}{\alpha\gamma} + \\ & 2\sqrt{\left(1+\xi_3\right)\left(\frac{1}{\alpha^2\gamma^2} + \xi_1 - \frac{\frac{2}{\alpha\gamma} - \xi_2}{\alpha\gamma} + \frac{1+\xi_3}{\alpha^2\gamma^2}\right)} \\ & + \left(1+2n\right)\left(-\frac{\sqrt{1+\xi_3}}{\alpha\gamma} + \sqrt{\frac{1}{\alpha^2\gamma^2} + \xi_1 - \frac{\frac{2}{\alpha\gamma} - \xi_2}{\alpha\gamma} + \frac{1+\xi_3}{\alpha^2\gamma^2}}\right).\end{aligned} \tag{3.91}$$

The numeric results of energy for n and l are obtained from Equation (3.91) these results are given in Table 3.13 with suitable parameters $\delta = -5, m = 1/2, \alpha = 5, \hbar = 1,$

$b = 1.3, \gamma = 0.01, a = -0.05$. The energy graph is drawn as shown in Figure 3.21. In graph of energy, while the energy values decrease negatively with the increase in the quantum number, but, increases negatively with the increasing number of momentum number. Also since the energy values of Cornell potential are very close to each other in different momentum states as, E_n=*-15294.5* in l_1=*1*, E_n=*-15259.9* in l_2=*2* and E_n=*-15207.8* in l_3 *=3* for *n=7* quantum state, the energy changes show the same change for almost every momentum number .

The corresponding wave function,

$$R[n,r] = N_{nl} r^{1+\sqrt{1+\xi_3}} \left(1+\frac{r}{\gamma}\right)^{\frac{1}{\gamma}+\frac{\sqrt{1+\xi_3}}{\gamma}-\sqrt{\frac{1}{\gamma^2}+\varepsilon 1-\frac{\frac{2}{\gamma}-\xi_2}{\gamma}+\frac{1+\xi_3}{\gamma^2}}} \tag{3.92}$$

$$ {}_2F_1\left(\begin{array}{l} -n, 1+1-\dfrac{2}{\gamma}+2\sqrt{1+\xi_3} \\ +2\left(-\dfrac{\sqrt{1+\xi_3}}{\gamma}+\sqrt{\dfrac{1}{\gamma^2}+\xi_1-\dfrac{\frac{2}{\gamma}-\xi_2}{\gamma}+\dfrac{1+\xi_3}{\gamma^2}}\right) \\ +n; 2+2\sqrt{1+\xi_3}; -\dfrac{r}{\gamma} \end{array}\right).$$

Table 3.13 The energy eigenvalues of the Cornell potential in Case 2 under $\delta = -5, m = 1/2, \alpha = 5, \hbar = 1, b = 1.3, \gamma = 0.01, a = -0.05$.

State	l_1=*1*	l_2=*2*	l_3=*3*
n=1	-399.716	-355.359	-278.914
n=2	-1512.22	-1475.5	-1419.42
n=3	-3167.78	-3132.26	-3078.58
n=4	-5373.18	-5338.1	-5285.25
n=5	-8129.3	-8094.43	-8041.98
n=6	-11436.4	-11401.6	-11349.4
n=7	-15294.5	-15259.9	-15207.8
n=8	-19703.8	-19669.2	-19617.2
n=9	-24664.2	-24629.6	-24577.6
n=10	-30175.7	-30141.1	-30089.2

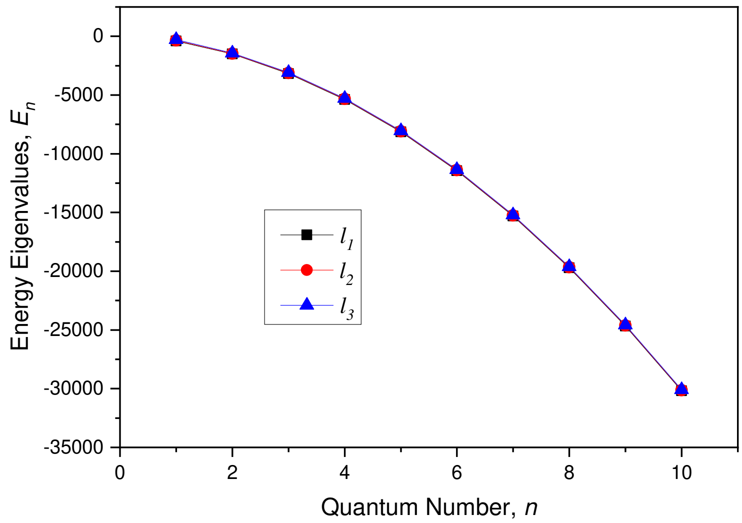

Figure 3.21 The graph of energy eigenvalues of Cornell potential in Case 2 for $\delta = -5, m = 1/2, \alpha = 5, \hbar = 1, b = 1.3, \gamma = 0.01, a = -0.05.$

3.2.7 Woods-Saxon Potential

The Schrödinger equation with Woods-Saxon potential takes the form,

$$R''[r] + \frac{\left(\frac{2}{r} - \gamma\right)}{1 - r\gamma} R'[r] + \frac{1}{1 - r\gamma}\left(\frac{2E_n m}{\hbar^2} - \frac{l(l+1)}{r^2} + \frac{2mV_0}{\hbar^2\left(1 + \mathrm{e}^{-r\beta} q\right)}\right) R[r] = 0 \tag{3.93}$$

where the approximation

$$\frac{2mV_0}{\hbar^2\left(1 + \mathrm{e}^{-r\beta} q\right)} \approx \frac{2mV_0}{\hbar^2 r^2}$$

is expressed.

A change of new variable of the form $r = 1/s$ substituting into the Equation (3.93) yields,

$$R''[s] + \frac{\gamma}{s(s-\gamma)} R'[s] - \\ \left(\frac{2E_n m + \left(-\hbar^2 l(l+1) + 2mV_0\right)s^2 - \frac{2E_n m\gamma}{s} + s\left(\hbar^2 l(l+1)\gamma - 2mV_0\gamma\right)}{\hbar^2 s^2 (s-\gamma)^2}\right) R[s] = 0. \tag{3.94}$$

To obtain the solution of Equation (3.94) in the same way by similar methods as before, power series expansion from Equation (3.36) is written.

Substituting this expansion into Equation (3.94) takes the following form

$$R''[s]\frac{R'[s]}{s\left(-1+\frac{s}{\gamma}\right)}+\frac{\left(\begin{array}{l}2E_n m+s^2\left(-\hbar^2 l(l+1)+2mV_0-\frac{2E_n m\gamma}{\delta^3}\right)+\\ s\left(\hbar^2 l(l+1)\gamma-2mV_0\gamma+\frac{6E_n m\gamma}{\delta^2}\right)-\frac{6E_n m\gamma}{\delta}\end{array}\right)}{s^2\gamma^2\hbar^2\left(-1+\frac{s}{\gamma}\right)^2}R[s]=0. \tag{3.95}$$

The parameters at this step are

$$\xi_1=-\left(\frac{-\hbar^2 l(l+1)+2mV_0-\frac{2E_n m\gamma}{\delta^3}}{\hbar^2\gamma^2}\right) \tag{3.96}$$

$$\xi_2=\left(\frac{\hbar^2 l(l+1)\gamma-2mV_0\gamma+\frac{6E_n m\gamma}{\delta^2}}{\hbar^2\gamma^2}\right),\xi_3=-\frac{\left(2E_n m-\frac{6E_n m\gamma}{\delta}\right)}{\hbar^2\gamma^2}$$

$$c_1=-1,c_2=0,c_3=-1/\gamma,c_4=1$$

$$c_5=\frac{1}{\gamma},c_6=\frac{1}{\gamma^2}+\xi_1,c_7=\frac{2}{\gamma}-\xi_2,c_8=1+\xi_3$$

$$c_9=\frac{1}{\gamma^2}+\xi_1-\frac{\frac{2}{\gamma}-\xi_2}{\gamma}+\frac{1+\xi_3}{\gamma^2},c_{10}=1+2\sqrt{1+\xi_3}$$

$$c_{11}=-\frac{2}{\gamma}+2\left(-\frac{\sqrt{1+\xi_3}}{\gamma}+\sqrt{\frac{1}{\gamma^2}+\xi_1-\frac{\frac{2}{\gamma}-\xi_2}{\gamma}+\frac{1+\xi_3}{\gamma^2}}\right),c_{12}=1+\sqrt{1+\xi_3}$$

$$c_{13}=\frac{\sqrt{1+\xi_3}}{\gamma}-\sqrt{\frac{1}{\gamma^2}+\xi_1-\frac{\frac{2}{\gamma}-\xi_2}{\gamma}+\frac{1+\xi_3}{\gamma^2}},$$

energy equation is obtained after comparison

$$\lambda=\frac{2}{\gamma}-\frac{(-1+n)n}{\gamma}-\frac{1+2n}{\gamma}-\xi_2-\frac{2(1+\xi_3)}{\gamma}+2\sqrt{(1+\xi_3)\left(\frac{1}{\gamma^2}+\xi_1-\frac{\frac{2}{\gamma}-\xi_2}{\gamma}+\frac{1+\xi_3}{\gamma^2}\right)}+ \tag{3.97}$$

$$(1+2n)\left(-\frac{\sqrt{1+\xi_3}}{\gamma}+\sqrt{\frac{1}{\gamma^2}+\xi_1-\frac{\frac{2}{\gamma}-\xi_2}{\gamma}+\frac{1+\xi_3}{\gamma^2}}\right).$$

The numeric solutions of the energy equation are calculated and obtained results are presented Table 3.14 for n and l with appropriate parameters $m=1/2$, $\gamma=0.05$, $\hbar=1, V_0=0.06, \delta=-0.005$. The energy graphs are plotted as function of r in Figure 3.22. As seen in figure, the energy decreases positively with the increasing the quantum number, also it increases positively with the increasing number of momentum. It is seen that energy takes the biggest value is $E_n=22.3383$ in $l_3=1$ and $n=10$ and the lowest value is, $E_n=0.538297$ in $l_3=3$ and $n=1$. Further, since the energy values are very close to each other, they were overlapped at the same point.
The wave function can be obtained from Equation (2.15) as

$$R[r,n]=N_{nl}r^{1+\sqrt{1+\xi_3}}\left(1+\frac{r}{\gamma}\right)^{\frac{1}{\gamma}+\frac{\sqrt{1+\xi_3}}{\gamma}-\sqrt{\frac{1}{\gamma^2}+\xi_1-\frac{\frac{2}{\gamma}-\xi_2}{\gamma}+\frac{1+\xi_3}{\gamma^2}}} \tag{3.98}$$

$${}_2F_1\left(\begin{array}{l}-n,1+1-\frac{2}{\gamma}+2\sqrt{1+\xi_3}+2\left(-\frac{\sqrt{1+\xi_3}}{\gamma}+\sqrt{\frac{1}{\gamma^2}+\xi_1-\frac{\frac{2}{\gamma}-\xi_2}{\gamma}+\frac{1+\xi_3}{\gamma^2}}\right)+\\ n;2+2\sqrt{1+\xi_3};-\frac{r}{\gamma}\end{array}\right)$$

Table 3.14 The energy eigenvalues of the Woods-Saxon potential in Case 2 under $m=1/2, \gamma=0.05, \hbar=1, V_0=0.06, \delta=-0.005$.

State	*l_1=1*	*l_2=2*	*l_3=3*
n=1	0.538297	0.615996	0.715073
n=2	1.34016	1.42965	1.552
n=3	2.53843	2.63263	2.76616
n=4	4.13497	4.23141	4.37078
n=5	6.13025	6.22791	6.37061
n=6	8.52441	8.62279	8.76754
n=7	11.3175	11.4163	11.5624
n=8	14.5095	14.6087	14.7557
n=9	18.1006	18.2	18.3476
n=10	22.0906	22.1901	22.3383

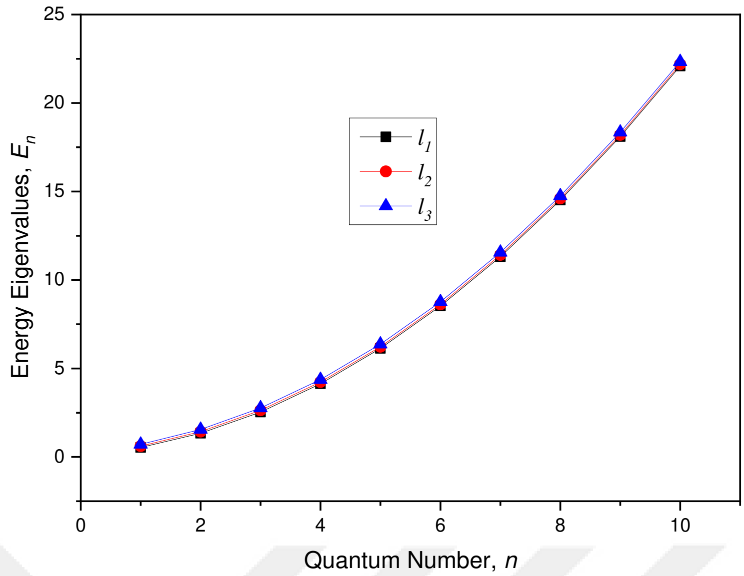

Figure 3.22 The graph of energy eigenvalues of Woods- Saxon potential in Case 2 for $m = 1/2, \gamma = 0.05, \hbar = 1, V_0 = 0.06, \delta = -0.005$.

3.2.8 Pöschl-Teller Potential

The SE is written for Pöschl-Teller potential in Equation (3.14)

$$R''[r] + \frac{\left(\frac{2}{r} - \gamma\right)}{1 - r\gamma} R'[r] + \frac{1}{1 - r\gamma}\left(-\frac{l(l+1)}{r^2} + \frac{2m(E_n + \frac{4e^{2ar}V_0}{(e^{2ar}+q)^2})}{\hbar^2} \right) R[r] = 0. \quad (3.99)$$

Here the approximation is expressed

$$\frac{4e^{2ar}V_0}{\left(e^{2ar}+q\right)^2} \approx \frac{4V_0}{r^2}$$

and by defining wave function $R[r] = \frac{U[r]}{r}$ then Equation (3.99) is

$$U''[r] + \frac{\gamma}{1 - r\gamma} U'[r] + \frac{1}{\hbar^2 r^2 (1 - r\gamma)} \left(\frac{2mr^2(E_n + \frac{4V_0}{r^2})}{\hbar^2} - \hbar^2\left(l + l^2 + r\gamma\right) \right) U[r] = 0. \quad (3.100)$$

By defining transformation $r = 1/s$ the Equation (3.100) yields

$$U''[s]+\frac{(2s-3\gamma)}{s(s-\gamma)}U'[s]+\frac{\begin{pmatrix}2E_nm+\left(-\hbar^4 l(l+1)+8mV_0\right)s^2-\frac{2E_nm\gamma}{s}+\\ \hbar^4\gamma^2+s\left(-\hbar^4\gamma+\hbar^4 l(l+1)\gamma-8mV_0\gamma\right)\end{pmatrix}}{\hbar^4 s^2(s-\gamma)^2}U[s]=0. \tag{3.101}$$

To solve of the above equation $\frac{1}{s}$, is opened to power series from Equation (3.36) and then Equation (3.101) takes the following form

$$U''[s]+\frac{(2s-3\gamma)}{s(-1+\frac{s}{\gamma})\gamma}U'[s]+\frac{\begin{pmatrix}2E_nm-\frac{6E_nm\gamma}{\delta}+\gamma^2\hbar^4+s^2(8mV_0-\frac{2E_nm\gamma}{\delta^3}-l(l+1)\hbar^4)\\ +s(-8mV_0\gamma+\frac{6E_nm\gamma}{\delta^2}-\gamma\hbar^4+l(l+1)\gamma\hbar^4)\end{pmatrix}}{s^2(-1+\frac{s}{\gamma})^2\hbar^4}U'[s]=0. \tag{3.102}$$

By using parameters

$$\begin{aligned}
&\xi_1=-\left(-\hbar^4 l(l+1)+8mV_0-\frac{2E_nm\gamma}{\delta^3}\right)/\gamma^2\hbar^4\\
&\xi_2=\left(-\hbar^4\gamma+\hbar^4 l(l+1)\gamma-8mV_0\gamma+\frac{6E_nm\gamma}{\delta^2}\right)/\gamma^2\hbar^4\\
&\xi_3=-\left(2E_nm+\hbar^4\gamma^2-\frac{6E_nm\gamma}{\delta}\right)/\gamma^2\hbar^4\\
&c_1=-3, c_2=-2/\gamma, c_3=-\frac{1}{\gamma}, c_4=2\\
&c_5=0, c_6=\xi_1, c_7=\xi_2, c_8=4+\xi_3\\
&c_9=\xi_1+\frac{\xi_2}{\gamma}+\frac{4+\xi_3}{\gamma^2}, c_{10}=1+2\sqrt{4+}\xi_3\\
&c_{11}=-\frac{2}{\gamma}+2\left(-\frac{\sqrt{4+\xi_3}}{\gamma}+\sqrt{\xi_1+\frac{\xi_2}{\gamma}+\frac{4+\xi_3}{\gamma^2}}\right)\\
&c_{12}=2+\sqrt{4+}\xi_3, c_{13}=\frac{\sqrt{4+\xi_3}}{\gamma}-\sqrt{\xi_1+\frac{\xi_2}{\gamma}+\frac{4+\xi_3}{\gamma^2}},
\end{aligned} \tag{3.103}$$

the energy equation is

$$\lambda = \frac{2n}{\gamma} - \frac{(-1+n)n}{\gamma} - \xi_2 - \frac{2(4+\xi_3)}{\gamma} + 2\sqrt{(4+\xi_3)\left(\xi_1 + \frac{\xi_2}{\gamma} + \frac{4+\xi_3}{\gamma^2}\right)} + (1+2n)\left(-\frac{\sqrt{4+\xi_3}}{\gamma} + \sqrt{\xi_1 + \frac{\xi_2}{\gamma} + \frac{4+\xi_3}{\gamma^2}}\right). \tag{3.104}$$

The numeric solutions of the energy equation are evaluated and obtained results are given in Table 3.15 for n and l with fixed $\gamma = 0.6, \delta = -0.03, m = 1/2, \hbar = 1, V_0 = 0.5$ parameters. The energy graph is drawn in Figure 3.23. In figure, while the energy values take the both negative and positive values up to the *n=5* quantum state, they have taken a negative value for each momentum state from *n>6* quantum state. The energy values of Pöschl-Teller potential show decreased slope. In addition, there is a clear fluctuation in energy values in figure.

The wave function is

$$R[n,r] = \frac{1}{r}\left(N_{nl} r^{2+\sqrt{4+\xi_3}} \left(1+\frac{r}{\gamma}\right)^{\frac{\sqrt{4+\xi_3}}{\gamma} - \sqrt{\varepsilon 1 + \frac{\xi_2}{\gamma} + \frac{4+\xi_3}{\gamma^2}}} \; {}_2F_1\left(-n, 1+1-\frac{2}{\gamma} + 2\sqrt{4+\xi_3} + 2\left(-\frac{\sqrt{4+\xi_3}}{\gamma} + \sqrt{\xi_1 + \frac{\xi_2}{\gamma} + \frac{4+\xi_3}{\gamma^2}}\right) + n; 2+2\sqrt{4+\xi_3}; -\frac{r}{\gamma} \right) \right). \tag{3.105}$$

Table 3.15 The energy eigenvalues of the Pöschl-Teller potential in Case 2 under $\gamma = 0.6, \delta = -0.03, m = 1/2, \hbar = 1, V_0 = 0.5$.

State	$l_1=1$	$l_2=2$	$l_3=3$
n=1	-0.0000749559	0.000173107	0.000452206
n=2	-0.000164271	0.000103741	0.000448073
n=3	-0.000279116	0.00000984964	0.000377361
n=4	-0.000419053	-0.000135035	0.000263187
n=5	-0.000583972	-0.000296175	0.000114692
n=6	-0.000773872	-0.000483463	-0.0000640056
n=7	-0.000988795	-0.00069647	-0.000270864
n=8	-0.0012288	-0.000934999	-0.000504803
n=9	-0.00149395	-0.00119897	-0.000765222
n=10	-0.00178431	-0.00148836	-0.00105178

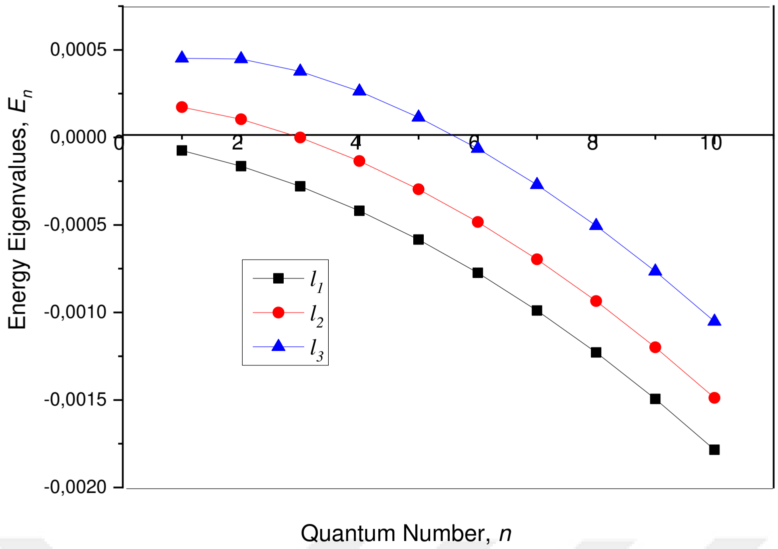

Figure 3.23 The graph of energy eigenvalues of Pöschl-Teller potential in Case 2 for $\gamma = 0.6, \delta = -0.03, m = 1/2, \hbar = 1, V_0 = 0.5.$

3.3 Case 3: State of form factor $\varepsilon(r) = \gamma r^2$

In case, the form factor $\varepsilon(r) = \gamma\rho(r) = \gamma r^2$ is taken with SE,

$$R''[r] + \frac{2}{r}R'[r] + \frac{\left(-2E_n mr^2 + l(l+1)\hbar^2 + 2mr^2V[r]\right)}{r^2\left(-1 + r^2\gamma\right)\hbar^2}R[r] = 0 \tag{3.106}$$

and then solutions were investigated for potentials.

3.3.1 Harmonic Oscillator

The SE can be expressed with Harmonic potential as,

$$\frac{1}{r^3\mu\hbar^2}r^2\left(1 - r^2\gamma\right)\mu\hbar^2R''[r] - \frac{m\left(-2E_n r^2\mu + mr^4w^2\mu + l\left(2\mu + \hbar^2\right) + l^2\left(2\mu + \hbar^2\right)\right)R[r]}{r^3\mu\hbar^2} = 0. \tag{3.107}$$

By performing the change of new variable $r \to \alpha\tau$ Equation (3.107) becomes,

$$\frac{R''[\tau]}{\alpha^2}+\frac{m\left(\mu\left(2l(l+1)-2E_n\alpha^2\tau^2+mw^2\alpha^4\tau^4\right)+l(l+1)\hbar^2\right)}{\alpha^2\mu\tau^2\left(-1+\alpha^2\gamma\tau^2\right)\hbar^2}R[\tau]=0. \quad (3.108)$$

and now the coordinate transformations, $\tau\to 1/y$

$$R''[y]+\frac{2}{y}R'[y]+\frac{m\left((2l(l+1)-\frac{2E_n\alpha^2}{y^2}+\frac{mw^2\alpha^4}{y^4})\mu+l(l+1)\hbar^2\right)}{y^2(-1+\frac{\alpha^2\gamma}{y^2})\mu\hbar^2}R[y]=0. \quad (3.109)$$

Then again with similar algebraic calculation and new defining transformation $y=\sqrt{s}$ the Equation (3.109) becomes

$$R''[s]+\frac{3\left(-s+\alpha^2\gamma\right)}{2s\alpha^2\left(1-\frac{s}{\alpha^2\gamma}\right)\gamma}R'[s]+ \quad (3.110)$$

$$\frac{\left(\begin{array}{l}-m^2w^2\alpha^4-2E_nm\alpha^4\gamma+m^2w^2\alpha^6\gamma\left(\frac{s^2}{\delta^3}-\frac{3s}{\delta^2}+\frac{3}{\delta}\right)+\\ s^2\left(-2l(l+1)m-l(l+1)\hbar^2\right)\\ +s\left(2E_nm\alpha^2+\alpha^2\gamma\left(2l(l+1)m+l(l+1)\hbar^2\right)\right)\end{array}\right)}{4y^2\alpha^2\left(1-\frac{s}{\alpha^2\gamma}\right)^2\gamma\hbar^2}R[s]=0.$$

By defining the following parameters

$$\xi_1=-\left(-2l(l+1)m+\frac{m^2w^2\alpha^6\gamma}{\delta^3}-l(l+1)\hbar^2\right)/\left(4\hbar^2\alpha^2\gamma\right)$$

$$\xi_2=\left(2E_nm\alpha^2-\frac{3m^2w^2\alpha^6\gamma}{\delta^2}+\alpha^2\gamma\left(2l(l+1)m+l(l+1)\hbar^2\right)\right)/\left(4\hbar^2\alpha^2\gamma\right)$$

$$\xi_3=-\left(-m^2w^2\alpha^4-2E_nm\alpha^4\gamma+\frac{3m^2w^2\alpha^6\gamma}{\delta}\right)/\left(4\hbar^2\alpha^2\gamma\right)$$

$$c_1=-3/2$$

$$c_2=3/2$$

$$c_3=2/\left(\alpha^2\gamma\right)$$

$$c_4=\frac{5}{4}$$

$$c_6 = \frac{1}{4}\left(-\frac{4}{\alpha^2\gamma} + \frac{3\alpha^2\gamma}{2}\right)^2 + \xi_1 \tag{3.111}$$

$$c_7 = \frac{5}{4}\left(-\frac{4}{\alpha^2\gamma} + \frac{3\alpha^2\gamma}{2}\right) - \xi_2$$

$$c_8 = \frac{25}{16} + \xi_3 c_9 = \frac{1}{4}\left(-\frac{4}{\alpha^2\gamma} + \frac{3\alpha^2\gamma}{2}\right)^2 + \xi_1 + \frac{2\left(\frac{5}{4}\left(-\frac{4}{\alpha^2\gamma} + \frac{3\alpha^2\gamma}{2}\right) - \xi_2\right)}{\alpha^2\gamma} + \frac{4\left(\frac{25}{16} + \xi_3\right)}{\alpha^4\gamma^2}$$

$$c_{10} = 1 + 2\sqrt{\frac{25}{16} + \xi_3}$$

$$c_{11} = \frac{4}{\alpha^2\gamma} + 2\left(\frac{2\sqrt{\frac{25}{16} + \xi_3}}{\alpha^2\gamma} + \left(\sqrt{\begin{array}{l}\frac{1}{4}\left(-\frac{4}{\alpha^2\gamma} + \frac{3\alpha^2\gamma}{2}\right)^2 \\ +\xi_1 + \frac{2\left(\frac{5}{4}\left(-\frac{4}{\alpha^2\gamma} + \frac{3\alpha^2\gamma}{2}\right) - \xi_2\right)}{\alpha^2\gamma} + \frac{4\left(\frac{25}{16} + \xi_3\right)}{\alpha^4\gamma^2}\end{array}}\right)\right)$$

$$c_{12} = \frac{5}{4} + \sqrt{\frac{25}{16} + \xi_3}$$

$$c_{13} = \frac{1}{2}\left(-\frac{4}{\alpha^2\gamma} + \frac{3\alpha^2\gamma}{2}\right) - \frac{2\sqrt{\frac{25}{16} + \xi_3}}{\alpha^2\gamma} - \left(\sqrt{\begin{array}{l}\frac{1}{4}\left(-\frac{4}{\alpha^2\gamma} + \frac{3\alpha^2\gamma}{2}\right)^2 + \xi_1 \\ + \frac{2\left(\frac{5}{4}\left(-\frac{4}{\alpha^2\gamma} + \frac{3\alpha^2\gamma}{2}\right) - \xi_2\right)}{\alpha^2\gamma} + \frac{4\left(\frac{25}{16} + \xi_3\right)}{\alpha^4\gamma^2}\end{array}}\right).$$

the energy equation is written from Equation (2.12) as

$$
\begin{aligned}
\lambda = {} & \frac{2(-1+n)n}{\alpha^2\gamma}+\frac{3}{2}n\alpha^2\gamma+\frac{5}{4}\left(-\frac{4}{\alpha^2\gamma}+\frac{3\alpha^2\gamma}{2}\right)- \\
& \frac{1}{2}(1+2n)\left(-\frac{4}{\alpha^2\gamma}+\frac{3\alpha^2\gamma}{2}\right)-\xi_2+\frac{4\left(\frac{25}{16}+\xi_3\right)}{\alpha^2\gamma}+ \\
& 2\sqrt{\left(\frac{25}{16}+\xi_3\right)\left(\frac{1}{4}\left(-\frac{4}{\alpha^2\gamma}+\frac{3\alpha^2\gamma}{2}\right)^2+\xi_1+\frac{2\left(\frac{5}{4}\left(-\frac{4}{\alpha^2\gamma}+\frac{3\alpha^2\gamma}{2}\right)-\xi_2\right)}{\alpha^2\gamma}+\frac{4\left(\frac{25}{16}+\xi_3\right)}{\alpha^4\gamma^2}\right)}+ \\
& (1+2n)\left(\frac{2\sqrt{\frac{25}{16}+\xi_3}}{\alpha^2\gamma}+\sqrt{\frac{1}{4}\left(-\frac{4}{\alpha^2\gamma}+\frac{3\alpha^2\gamma}{2}\right)^2+\xi_1+\frac{2\left(\frac{5}{4}\left(-\frac{4}{\alpha^2\gamma}+\frac{3\alpha^2\gamma}{2}\right)-\xi_2\right)}{\alpha^2\gamma}+\frac{4\left(\frac{25}{16}+\xi_3\right)}{\alpha^4\gamma^2}}\right).
\end{aligned}
\tag{3.112}
$$

The numeric results of Eq. (3.112) are given for n and l in Table 3.16 with suitable parameters $w = 10, \alpha = -0.48, \delta = 0.5, \gamma = -25, m = 1/2, \hbar = 1$ and energy graph is drawn as shown in Figure 3.24. Looking at the energy values of Harmonic oscillator potential in figure, the energy values showed a positive decrease with the increase in both the n and l numbers. At the same time, it is observed that the energy values overlapped because the energy values are very close to each other in different momentum states. For example, E_n=33409.3 in $l_1=1$, E_n=33062.6 in $l_2=2$…etc.

Table 3.16 The energy eigenvalues of the Harmonic oscillator potential in Case 3 under $w=10, \alpha=-0.48, \delta=0.5, \gamma=-25, m=1/2, \hbar=1$.

State	$l_1=1$	$l_2=2$	$l_3=3$
n=1	33409.3	33062.6	32539.1
n=2	29181.2	28873.6	28409.2
n=3	25315.9	25045.8	24637.8
n=4	21804.7	21570.2	21215.8
n=5	18637.4	18436.3	18132.3
n=6	15801.6	15631.6	15374.4
n=7	13283.1	13141.6	12927.2
n=8	11065.4	10949.6	10773.6
n=9	9129.93	9036.76	8894.77
n=10	7456.15	7382.62	7270.08

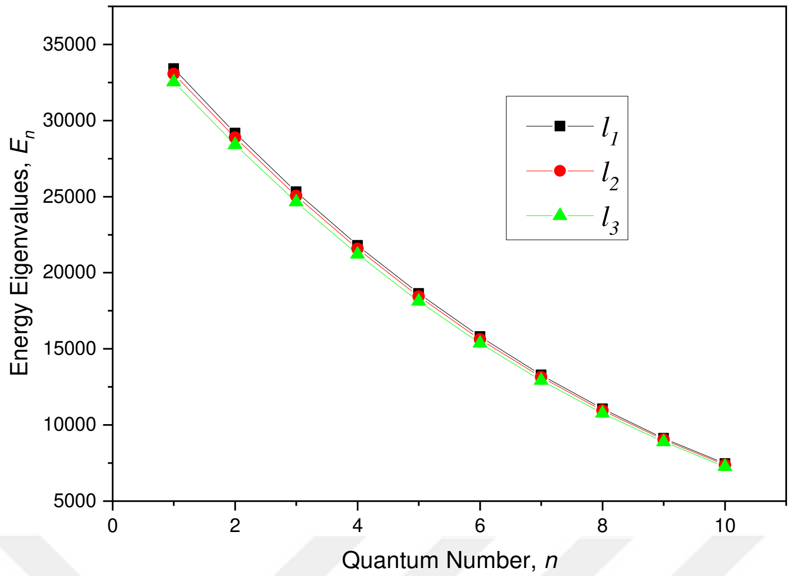

Figure 3.24 The graph of energy eigenvalues of Harmonic oscillator potential in Case 3 for $w = 10, \alpha = -0.48, \delta = 0.5, \gamma = -25, m = 1/2, \hbar = 1$.

The wave function is calculated

$$R[n,r] = \frac{1}{r}\left(\begin{array}{l} N_{nl} r^{\frac{5}{4}+\sqrt{\frac{25}{16}+\xi_3}} \left(1-\frac{2r}{\alpha^2\gamma}\right)^{\frac{1}{2}\left(-\frac{4}{\alpha^2\gamma}+\frac{3\alpha^2\gamma}{2}\right)-\frac{2\sqrt{\frac{25}{16}+\xi_3}}{\alpha^2\gamma}-\sqrt{\frac{1}{4}\left(-\frac{4}{\alpha^2\gamma}+\frac{3\alpha^2\gamma}{2}\right)^2+\xi_1+\frac{2\left(\frac{5}{4}\left(-\frac{4}{\alpha^2\gamma}+\frac{3\alpha^2\gamma}{2}\right)-\xi_2\right)}{\alpha^2\gamma}+\frac{4\left(\frac{25}{16}+\xi_3\right)}{\alpha^4\gamma^2}}} \\ {}_2F_1(-n, 1+1+\frac{4}{\alpha^2\gamma}+2\sqrt{\frac{25}{16}+\xi_3}+ \\ 2\left(\frac{2\sqrt{\frac{25}{16}+\xi_3}}{\alpha^2\gamma}+\sqrt{\frac{1}{4}\left(-\frac{4}{\alpha^2\gamma}+\frac{3\alpha^2\gamma}{2}\right)^2+\xi_1+\frac{2\left(\frac{5}{4}\left(-\frac{4}{\alpha^2\gamma}+\frac{3\alpha^2\gamma}{2}\right)-\xi_2\right)}{\alpha^2\gamma}+\frac{4\left(\frac{25}{16}+\xi_3\right)}{\alpha^4\gamma^2}}\right) \\ +n; +2\sqrt{\frac{25}{16}+\xi_3}; \frac{2r}{\alpha^2\gamma}) \end{array} \right) \tag{3.113}$$

3.3.2 Hulthen Potential

In this case the SE can be written,

$$R''[r]+\frac{2(-1+r^2\gamma)}{r(1-r^2\gamma)}R'[r]-\frac{1}{1-r^2\gamma}\left(-\frac{l(l+1)}{r^2}+\frac{2(E_n+\frac{K}{(-1+e^{r/\kappa})\kappa})\mu}{\hbar^2}\right)R[r]=0. \tag{3.114}$$

The approximation

$$\frac{K}{\left(-1+e^{r/\kappa}\right)\kappa}\approx\frac{K}{r^2\kappa}$$

is proposed for Hulthen potential

$$\left(1-r^2\gamma\right)R''[r]+\left(\frac{2}{r}-2r\gamma\right)R'[r]+\left(-\frac{l(l+1)}{r^2}+\frac{2\left(E_n+\frac{K}{r^2\kappa}\right)\mu}{\hbar^2}\right)R[r]=0. \tag{3.115}$$

.

By defining transformation $r=\sqrt{s}$ and then substituting into the above equation yields

$$R''[s]+\frac{3(-1+s\gamma)}{2s(-1+s\gamma)}R'[s]+\frac{\begin{pmatrix}2K\mu-2E_ns^2\gamma\kappa\mu-l(l+1)\kappa\hbar^2+\\ s\left(-2K\gamma\mu+2E_n\kappa\mu+l(l+1)\gamma\kappa\hbar^2\right)\end{pmatrix}}{4s^2(-1+s\gamma)^2\kappa\hbar^2}R[s]=0. \tag{3.116}$$

The parameters at this step are

$$\xi_1=-2E_n\gamma\kappa/\left(4\kappa\hbar^2\right)$$
$$\xi_2=\left(-2K\gamma\mu+2E_n\kappa\mu+l(l+1)\gamma\kappa\hbar^2\right)/\left(4\kappa\hbar^2\right)$$
$$\xi_3=-\left(-l(l+1)\kappa\hbar^2+2K\mu\right)/\left(4\kappa\hbar^2\right)$$
$$c_1=-3/2,c_2=-3\gamma/2,c_3=-\gamma/2,c_4=\frac{5}{4},c_5=-\frac{\gamma}{4},c_6=\frac{\gamma^2}{16}+\frac{E_n\gamma}{2\hbar^2}$$
$$c_7=-\frac{5\gamma}{8}-\frac{-2K\gamma\mu+2En\kappa\mu+l(l+1)\gamma\kappa\hbar^2}{4\kappa\hbar^2},c_8=\frac{25}{16}+\frac{-2K\mu+l(l+1)\kappa\hbar^2}{4\kappa\hbar^2}$$
$$c_9=\frac{\gamma^2}{16}+\frac{E_n\gamma}{2\hbar^2}+\frac{1}{4}\gamma^2\left(\frac{25}{16}+\frac{-2K\mu+l(l+1)\kappa\hbar^2}{4\kappa\hbar^2}\right)$$
$$-\frac{1}{2}\gamma\left(-\frac{5\gamma}{8}-\frac{-2K\gamma\mu+2E_n\kappa\mu+l(l+1)\gamma\kappa\hbar^2}{4\kappa\hbar^2}\right)$$
$$c_{10}=1+2\sqrt{\frac{25}{16}+\frac{-2K\mu+l(l+1)\kappa\hbar^2}{4\kappa\hbar^2}}$$

$$c_{11}=-\gamma+2(-\frac{1}{2}\gamma\sqrt{\frac{25}{16}+\frac{-2K\mu+l\left(l+1\right)\kappa\hbar^2}{4\kappa\hbar^2}}+\sqrt{\begin{pmatrix}\frac{\gamma^2}{16}+\frac{E_n\gamma}{2\hbar^2}+\frac{1}{4}\gamma^2\left(\frac{25}{16}+\frac{-2K\mu+l\left(l+1\right)\kappa\hbar^2}{4\kappa\hbar^2}\right)\\-\frac{1}{2}\gamma-\frac{5\gamma}{8}-\frac{-2K\gamma\mu+2E_n\kappa\mu+l\left(l+1\right)\gamma\kappa\hbar^2}{4\kappa\hbar^2})\end{pmatrix}} \tag{3.117}$$

$$c_{12}=\frac{5}{4}+\sqrt{\frac{25}{16}+\frac{-2K\mu+l\left(l+1\right)\kappa\hbar^2}{4\kappa\hbar^2}}$$

$$c_{13}=-\frac{\gamma}{4}+\frac{1}{2}\gamma\sqrt{\frac{25}{16}+\frac{-2K\mu+l\left(l+1\right)\kappa\hbar^2}{4\kappa\hbar^2}}+\sqrt{\frac{\gamma^2}{16}+\frac{E_n\gamma}{2\hbar^2}+\frac{1}{4}\gamma^2\left(\frac{25}{16}+\frac{-2K\mu+l\left(l+1\right)\kappa\hbar^2}{4\kappa\hbar^2}\right)-\frac{1}{2}\gamma\left(-\frac{5\gamma}{8}-\frac{-2K\gamma\mu+2En\kappa\mu+l\left(l+1\right)\gamma\kappa\hbar^2}{4\kappa\hbar^2}\right)},$$

using Equation (2.12), the energy equation can be calculated

$$\begin{aligned}\lambda=&\frac{1}{16\kappa\hbar^2}(16K\gamma\mu-\kappa(8E_n\mu+\hbar^2(\gamma(31+8L\left(1+l\right)+\\&4n\left(2+2n+\sqrt{25+4l\left(l+1\right)-\frac{8K\mu}{\kappa\hbar^2}}\right)\\&+2\sqrt{25+4l\left(l+1\right)-\frac{8K\mu}{\kappa\hbar^2}})-\\&2\sqrt{\frac{\gamma\left(-24K\gamma\mu+16E_n\kappa\left(2+\mu\right)+\left(49+12l\left(l+1\right)\right)\gamma\kappa\hbar^2\right)}{\kappa\hbar^2}}\\&-4n\sqrt{\frac{\gamma\left(-24K\gamma\mu+16E_n\kappa\left(2+\mu\right)+\left(49+12l\left(l+1\right)\right)\gamma\kappa\hbar^2\right)}{\kappa\hbar^2}}\\&-\sqrt{\frac{\gamma\left(-8K\mu+\left(25+4l\left(l+1\right)\right)\kappa\hbar^2\right)\left(-24K\gamma\mu+16E_n\kappa\left(2+\mu\right)+\left(49+12l\left(l+1\right)\right)\gamma\kappa\hbar^2\right)}{\kappa^2\hbar^4}}))).\end{aligned} \tag{3.118}$$

The numerical results of the energy are given in the Table 3.118 by using Equation (3.118) for n and l with fixed parameters $K=0.006, \kappa=10, \gamma=0.5, \hbar=1$, $\delta=-0.5, m=1/2.$ The energy graph is drawn in Figure 3.25. In graph, energy values increase positively with increasing quantum and momentum number. Since the change in different momentum states is almost the same, therefore, the energy changes in these situations also show parallel behavior.

The wave function can be obtained

$$R[n,r]=N_{nl}r^{\frac{5}{4}+\sqrt{\frac{25}{16}+\xi_3}}\left(1+\frac{r\gamma}{2}\right)^{-\frac{\gamma}{4}+\frac{1}{2}\gamma\sqrt{\frac{25}{16}+\xi_3}-\sqrt{\frac{\gamma^2}{16}+\xi_1-\frac{1}{2}\gamma\left(-\frac{5\gamma}{8}-\xi_2\right)+\frac{1}{4}\gamma^2\left(\frac{25}{16}+\xi_3\right)}} \tag{3.119}$$

$${}_2F_1\left(\begin{array}{l}-n,1+1-\gamma+2\sqrt{\frac{25}{16}+\xi_3}+2(-\frac{1}{2}\gamma\sqrt{\frac{25}{16}+\xi_3}+\\ \sqrt{\frac{\gamma^2}{16}+\xi_1-\frac{1}{2}\gamma\left(-\frac{5\gamma}{8}-\xi_2\right)+\frac{1}{4}\gamma^2\left(\frac{25}{16}+\xi_3\right)})+n;2+2\sqrt{\frac{25}{16}+\xi_3};\\ -\frac{r\gamma}{2}\end{array}\right)$$

Table 3.17 The energy eigenvalues of the Hulthen potential in Case 3 under $K=0.06,\kappa=10,\gamma=0.5,\delta=-0.05,m=1/2,\hbar=1$.

State	$l_1=1$	$l_2=2$	$l_3=3$
n=1	148.107	177.144	216.064
n=2	271.45	311.802	364.673
n=3	430.667	482.307	549.081
n=4	625.766	688.684	769.34
n=5	856.752	930.943	1025.47
n=6	1123.62	1209.09	1317.48
n=7	1426.39	1523.11	1645.37
n=8	1765.03	1873.03	2009.14
n=9	2139.57	2258.83	2408.81
n=10	2550.0	2680.52	2844.35

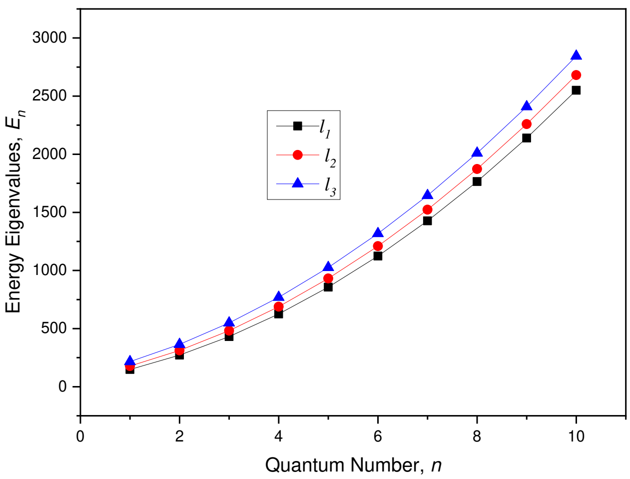

Figure 3. 25 The graph of energy eigenvalues of Hulthen potential in Case 3 for $K=0.06,\kappa=10,\gamma=0.5,\delta=-0.05,m=1/2,\hbar=1$.

3.3.3 Woods-Saxon Potential

Thus situated the SE has the form

$$\hbar^2\left(1-r^2\gamma\right)R''\left[r\right]+\frac{2\hbar^2\left(-1+r^2\gamma\right)}{r}R'\left[r\right]+\left(-2E_nm+\frac{l\left(l+1\right)}{r^2}\hbar^2-\frac{2mV_0}{\left(1+\mathrm{e}^{-r\beta}q\right)}\right)R\left[r\right]=0. \tag{3.120}$$

Using the approximation

$$\frac{2mV_0}{\hbar^2\left(1+\mathrm{e}^{-r\beta}q\right)}\approx\frac{2mV_0}{\hbar^2r^2}$$

then,

$$R''\left[r\right]+\frac{2\left(-1+r^2\gamma\right)}{r\left(1-r^2\gamma\right)}R'\left[r\right]-\frac{1}{1-r^2\gamma}\left(\frac{2E_nm}{\hbar^2}-\frac{l\left(l+1\right)}{r^2}+\frac{2mV_0}{\hbar^2r^2}\right)R\left[r\right]=0. \tag{3.121}$$

And then using new variable $r=\sqrt{s}$ the Equation (3.120) yields

$$R''\left[s\right]+\frac{3\left(-1+s\gamma\right)}{2s\left(-1+s\gamma\right)}R'\left[s\right]+ \tag{3.122}$$

$$\frac{\left(-\hbar^2l\left(l+1\right)+2mV_0-2E_nms^2\gamma+s\left(2E\ m+\hbar^2l\left(l+1\right)\gamma-2mV_0\gamma\right)\right)}{4\hbar^2s^2\left(-1+s\gamma\right)}R\left[s\right]=0.$$

The parameters take

$$\xi_1=2mE_n\gamma/4\hbar^2$$
$$\xi_2=\left(2E_nm+\hbar^2l\left(l+1\right)\gamma-2mV_0\gamma\right)/4\hbar^2$$
$$\xi_3=\left(\hbar^2l\left(l+1\right)-2mV_0\right)/4\hbar^2$$
$$c_1=-3/2,c_2=-3\gamma/2,c_3=-2\gamma$$
$$c_4=\frac{1}{5},c_5=\frac{5\gamma}{4},c_6=\frac{25\gamma^2}{16}+\xi_1,c_7=\frac{\gamma}{2}-\xi_2,c_8=\frac{1}{25}+\xi_3$$
$$c_9=\frac{25\gamma^2}{16}+\xi_1-2\gamma\left(\frac{\gamma}{2}-\right)\xi_2+4\gamma^2\left(\frac{1}{25}+\xi_3\right),c_{10}=\frac{11}{10}+2\sqrt{\frac{1}{25}+\xi_3}$$
$$c_{11}=-4\gamma+2\left(-2\gamma\sqrt{\frac{1}{25}+\xi_3}+\sqrt{\frac{25\gamma^2}{16}+\xi_1-2\gamma\left(\frac{\gamma}{2}-\xi_2\right)+4\gamma^2\left(\frac{1}{25}+\xi_3\right)}\right)$$
$$c_{12}=\frac{1}{5}+\sqrt{\frac{1}{25}+\xi}$$

$$c_{13} = \frac{5\gamma}{4} + 2\gamma\sqrt{\frac{1}{25} + \xi_3} - \sqrt{\frac{25\gamma^2}{16} + \xi_1 - 2\gamma\left(\frac{\gamma}{2} - \xi_2\right) + 4\gamma^2\left(\frac{1}{25} + \xi_3\right)}, \tag{3.123}$$

the energy equation is obtained

$$\begin{aligned}\lambda = {} & \frac{\gamma}{2} - \frac{3n\gamma}{2} - 2(-1+n)n\gamma - \frac{5}{4}(1+2n)\gamma - \xi_2 - 4\gamma\left(\frac{1}{25} + \xi_3\right) \\ & +2\sqrt{\left(\frac{1}{25} + \xi_3\right)\left(\frac{25\gamma^2}{16} + \xi_1 - 2\gamma\left(\frac{\gamma}{2} - \xi_2\right) + 4\gamma^2\left(\frac{1}{25} + \xi_3\right)\right)} + \\ & (1+2n)\left(-2\gamma\sqrt{\frac{1}{25} + \xi_3} + \sqrt{\frac{25\gamma^2}{16} + \xi_1 - 2\gamma\left(\frac{\gamma}{2} - \xi_2\right) + 4\gamma^2\left(\frac{1}{25} + \xi_3\right)}\right),\end{aligned} \tag{3.124}$$

The numeric solutions of the energy are calculated by using above equation and obtained results for n and l are given in Table 3.18 with appropriate parameters $m = 1/2$, $\gamma = 0.05$, $\hbar = 1$, $V_0 = 0.06$ and energy graph is presented in Figure 3.26. The energy values of Woods-Saxon potential show a parallel increase positively based on the quantum and momentum state. While the change in energy is not so much in the first $n=1$ quantum state, $l_1=1$, $E_n= 0.378428$ and $l_2=2$, $E_n=0.422159$, this change has increased markedly for different momentum states with the increasing number of quantum.

Table 3.18 The energy eigenvalues of the Woods-Saxon potential in Case 3 under $m = 1/2, \gamma = 0.05, \hbar = 1, V_0 = 0.06$.

State	$l_1=1$	$l_2=2$	$l_3=3$
n=1	0.378428	0.422159	0.424604
n=2	0.959159	1.09973	1.18399
n=3	1.75636	2.00113	2.18159
n=4	2.76854	3.12004	3.40214
n=5	3.99534	4.45469	4.84096
n=6	5.43663	6.00438	6.49618
n=7	7.09233	7.76881	8.36695
n=8	8.96244	9.74784	10.4528
n=9	11.0469	11.9414	12.7535
n=10	13.3458	14.3494	15.2689

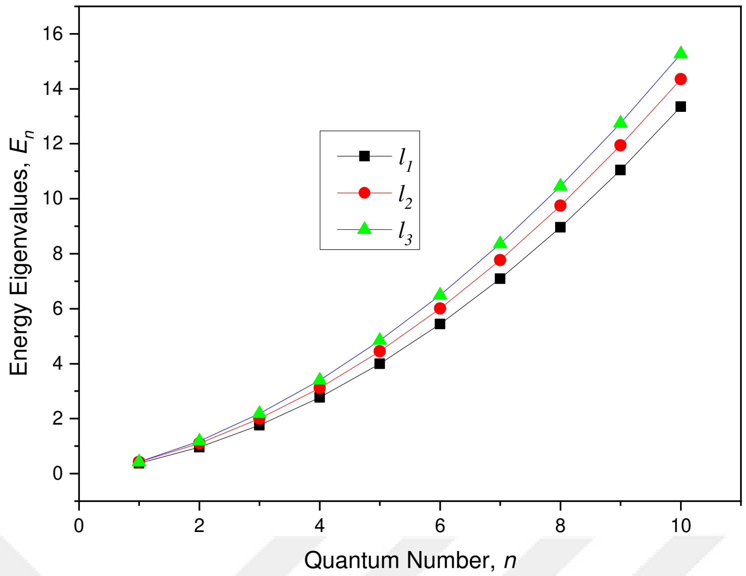

Figure 3.26 The graph of energy eigenvalues of Woods-Saxon potential in Case 3 for $m=1/2, \gamma=0.05, \hbar=1, V_0=0.06$.

The wave function has the form of

$$R[n,r]=N_{nl}r^{\frac{1}{5}+\sqrt{\frac{1}{25}+\xi_3}}\left(1+2r\gamma\right)^{\frac{5\gamma}{4}+2\gamma\sqrt{\frac{1}{25}+\xi_3}-\sqrt{\frac{25\gamma^2}{16}+\xi_1-2\gamma\left(\frac{\gamma}{2}-\xi_2\right)+4\gamma^2\left(\frac{1}{25}+\xi_3\right)}}$$
$${}_2F_1\left(\begin{array}{l}-n,1+-\frac{11}{10}-4\gamma+2\sqrt{\frac{1}{25}+\xi_3}+2(-2\gamma\sqrt{\frac{1}{25}+\xi_3}+\\ \sqrt{\frac{25\gamma^2}{16}+\xi_1-2\gamma\left(\frac{\gamma}{2}-\xi 2\right)+4\gamma^2(\frac{1}{25}+\xi_3))}\\ +n;\frac{1}{10}+2\sqrt{\frac{1}{25}+\xi_3};-2r\gamma.\end{array}\right) \tag{3.125}$$

3.3.4 Pöschl-Teller Potential

In this case the SE has the form

$$R''[r]-\frac{2\left(-1+r^2\gamma\right)}{r\left(1-r^2\gamma\right)}R'[r]+\frac{1}{1-r^2\gamma}\left(\frac{2E_n m}{\hbar^2}-\frac{l}{r^2}-\frac{l^2}{r^2}+\frac{8e^{2ar}mV_0}{\hbar^2\left(e^{2ar}+q\right)^2}\right)R[r]=0. \tag{3.126}$$

By considering the approximation

$$\frac{2mV_0}{\hbar^2\left(1+\mathrm{e}^{-r\beta}q\right)} \approx \frac{2mV_0}{\hbar^2 r^2},$$

and then using new variable $r = \alpha\tau$ with wave function $R[r] = \dfrac{U[r]}{r}$ the Equation (3.126) yields

$$\frac{1}{\alpha^2}U''[\tau] + \frac{\left(-2m\left(4V_0 + E_n\alpha^2\tau^2\right) + l(l+1)\hbar^2\right)}{\hbar^2\alpha^2\tau^2\left(-1+\alpha^2\gamma\tau^2\right)}U[\tau] = 0. \tag{3.127}$$

and again, the coordinate transformations $\tau \to 1/y$ yields

$$\frac{\hbar^2 y^2\left(y^2-\alpha^2\gamma\right)}{\hbar^2 y^3\left(y^2-\alpha^2\gamma\right)}U''[y] + \frac{+\left(2m\left(4y^2V_0 + E_n\alpha^2\right) - l(l+1)y^2\hbar^2\right)}{\hbar^2 y^3\left(y^2-\alpha^2\gamma\right)}U[y] = 0. \tag{3.128}$$

So, by performing the change of new variable $y \to \sqrt{s}$ Equation (3.128) becomes

$$U''[s] + \frac{3\left(s-\alpha^2\gamma\right)}{2s\alpha^2\left(-1+\dfrac{s}{\alpha^2\gamma}\right)\gamma}U'[s] + \frac{\begin{pmatrix}-2E_n m\alpha^4\gamma + s^2\left(8mV_0 - l(l+1)\hbar\right) + \\ s\left(2E_n m\alpha^2 - 8mV_0\alpha^2\gamma + l(1+l)\alpha^2\gamma\hbar\right)\end{pmatrix}}{4h^2 s^2\alpha^4\left(-1+\dfrac{s}{\alpha^2\gamma}\right)^2\gamma^2}U[s] = 0. \tag{3.129}$$

By using the following parameters values

$$\xi_1 = -\left(8mV_0 - l(1+l)\hbar\right)/\left(4\gamma^2\alpha^4\hbar^2\right)$$
$$\xi_2 = \left(2E_n m\alpha^2 - 8mV_0\alpha^2\gamma + l(1+l)\alpha^2\gamma\hbar\right)/\left(4\gamma^2\alpha^4\hbar^2\right)$$
$$\xi_3 = -\left(-2E_n m\alpha^4\gamma\right)/\left(4\gamma^2\alpha^4\hbar^2\right)$$
$$c_1 = -3/2, c_2 = -3/2\alpha^2\gamma$$
$$c_3 = -2/(\alpha^2\gamma, c_4 = \frac{5}{4}, c_5 = \frac{1}{2}\left(\frac{4}{\alpha^2\gamma} - \frac{3\alpha^2\gamma}{2}\right)$$
$$c_5 = \frac{1}{2}\left(\frac{4}{\alpha^2\gamma} - \frac{3\alpha^2\gamma}{2}\right), c_6 = \frac{1}{4}\left(\frac{4}{\alpha^2\gamma} - \frac{3\alpha^2\gamma}{2}\right)^2 + \xi_1$$
$$c_7 = \frac{5}{4}\left(\frac{4}{\alpha^2\gamma} - \frac{3\alpha^2\gamma}{2}\right) - \xi_2, c_8 = \frac{25}{16} + \xi_3$$
$$c_9 = \frac{1}{4}\left(\frac{4}{\alpha^2\gamma} - \frac{3\alpha^2\gamma}{2}\right)^2 + \xi_1 - \frac{2\left(\frac{5}{4}\left(\frac{4}{\alpha^2\gamma} - \frac{3\alpha^2\gamma}{2}\right) - \xi_2\right)}{\alpha^2\gamma} + \frac{4\left(\frac{25}{16} + \xi_3\right)}{\alpha^4\gamma^2}$$

$$c_{10} = 1 + 2\sqrt{\frac{25}{16} + \xi_3}$$

$$c_{11} = -\frac{4}{\alpha^2\gamma} + 2(-\frac{2\sqrt{\frac{25}{16}+\xi_3}}{\alpha^2\gamma} + \sqrt{\frac{1}{4}\left(\frac{4}{\alpha^2\gamma} - \frac{3\alpha^2\gamma}{2}\right)^2 + \xi_1 - \frac{2\left(\frac{5}{4}\left(\frac{4}{\alpha^2\gamma} - \frac{3\alpha^2\gamma}{2}\right) - \xi_2\right)}{\alpha^2\gamma} + \frac{4\left(\frac{25}{16}+\xi_3\right)}{\alpha^4\gamma^2}})$$

$$c_{12} = \frac{5}{4} + \sqrt{\frac{25}{16} + \xi_3} \tag{3.130}$$

$$c_{13} = \frac{1}{2}\left(\frac{4}{\alpha^2\gamma} - \frac{3\alpha^2\gamma}{2}\right) + \frac{2\sqrt{\frac{25}{16}+\xi_3}}{\alpha^2\gamma} - \sqrt{\frac{1}{4}\left(\frac{4}{\alpha^2\gamma} - \frac{3\alpha^2\gamma}{2}\right)^2 + \xi_1 - \frac{2\left(\frac{5}{4}\left(\frac{4}{\alpha^2\gamma} - \frac{3\alpha^2\gamma}{2}\right) - \xi_2\right)}{\alpha^2\gamma} + \frac{4\left(\frac{25}{16}+\xi_3\right)}{\alpha^4\gamma^2}}$$

the energy equation is obtained

$$\lambda = -\frac{2(-1+n)n}{\alpha^2\gamma} - \frac{3}{2}n\alpha^2\gamma + \frac{5}{4}\left(\frac{4}{\alpha^2\gamma} - \frac{3\alpha^2\gamma}{2}\right) - \frac{1}{2}(1+2n)\left(\frac{4}{\alpha^2\gamma} - \frac{3\alpha^2\gamma}{2}\right) - \xi_2 - \frac{4\left(\frac{25}{16}+\xi_3\right)}{\alpha^2\gamma} + 2\sqrt{\left(\frac{25}{16}+\xi_3\right)\left(\frac{1}{4}\left(\frac{4}{\alpha^2\gamma} - \frac{3\alpha^2\gamma}{2}\right)^2 + \xi_1 - \frac{2\left(\frac{5}{4}\left(\frac{4}{\alpha^2\gamma} - \frac{3\alpha^2\gamma}{2}\right) - \xi_2\right)}{\alpha^2\gamma} + \frac{4\left(\frac{25}{16}+\xi_3\right)}{\alpha^4\gamma^2}\right)} + (1+2n)\left(-\frac{2\sqrt{\frac{25}{16}+\xi_3}}{\alpha^2\gamma} + \sqrt{\frac{1}{4}\left(\frac{4}{\alpha^2\gamma} - \frac{3\alpha^2\gamma}{2}\right)^2 + \xi_1 - \frac{2\left(\frac{5}{4}\left(\frac{4}{\alpha^2\gamma} - \frac{3\alpha^2\gamma}{2}\right) - \xi_2\right)}{\alpha^2\gamma} + \frac{4\left(\frac{25}{16}+\xi_3\right)}{\alpha^4\gamma^2}}\right). \tag{3.131}$$

The numeric solutions of the energy are given in Table 3.19 for parameters $\gamma = 0.06$, $m = 1/2\,, \hbar = 1, \mathrm{V}_0 = 0.5, \alpha = -0.004$. The energy graph is shown in Figure 3.27. As seen in figure, the energy change of Pöschl-Teller potential shows similarly to Woods-Saxon potential.

The corresponding wave equation is calculated

$$R[n,r] = \frac{1}{r}\left(\begin{array}{l} N_{nl} r^{\frac{5}{4}+\sqrt{\frac{25}{16}+\xi_3}} \left(1+\frac{2r}{\alpha^2\gamma}\right)^{\frac{1}{2}\left(\frac{4}{\alpha^2\gamma}-\frac{3\alpha^2\gamma}{2}\right)+\frac{2\sqrt{\frac{25}{16}+\xi_3}}{\alpha^2\gamma}-\sqrt{\frac{1}{4}\left(\frac{4}{\alpha^2\gamma}-\frac{3\alpha^2\gamma}{2}\right)^2+\xi_1-\frac{2\left(\frac{5}{4}\left(\frac{4}{\alpha^2\gamma}-\frac{3\alpha^2\gamma}{2}\right)-\xi_2\right)}{\alpha^2\gamma}+\frac{4\left(\frac{25}{16}+\xi_3\right)}{\alpha^4\gamma^2}}} \\ {}_2F_1(-n, 1+1-\frac{4}{\alpha^2\gamma}+2\sqrt{\frac{25}{16}+\xi_3}+2(-\frac{2\sqrt{\frac{25}{16}+\xi_3}}{\alpha^2\gamma}+ \\ \sqrt{\frac{1}{4}\left(\frac{4}{\alpha^2\gamma}-\frac{3\alpha^2\gamma}{2}\right)^2+\xi_1-\frac{2\left(\frac{5}{4}\left(\frac{4}{\alpha^2\gamma}-\frac{3\alpha^2\gamma}{2}\right)-\xi_2\right)}{\alpha^2\gamma}+\frac{4\left(\frac{25}{16}+\xi_3\right)}{\alpha^4\gamma^2}})+ \\ n; 2+2\sqrt{\frac{25}{16}+\xi_3}; -\frac{2r}{\alpha^2\gamma}) \end{array} \right) \tag{3.132}$$

Table 3.19 The energy eigenvalues of the Pöschl-Teller potential in Case 3 under $\gamma = 0.6, m = 1/2, \hbar = 1, V_0 = 0.5, \alpha = -0.004$.

State	*l_1=1*	*l_2=2*	*l_3=3*
n=1	205.812	240.913	281.607
n=2	443.595	498.247	560.564
n=3	776.278	850.564	934.549
n=4	1203.95	1297.9	1403.56
n=5	1726.64	1840.25	1967.61
n=6	2344.35	2477.63	2626.68
n=7	3057.08	3210.05	3380.79
n=8	3864.84	4037.49	4229.92
n=9	4767.63	4959.96	5174.09
n=10	5765.45	5977.46	6213.28

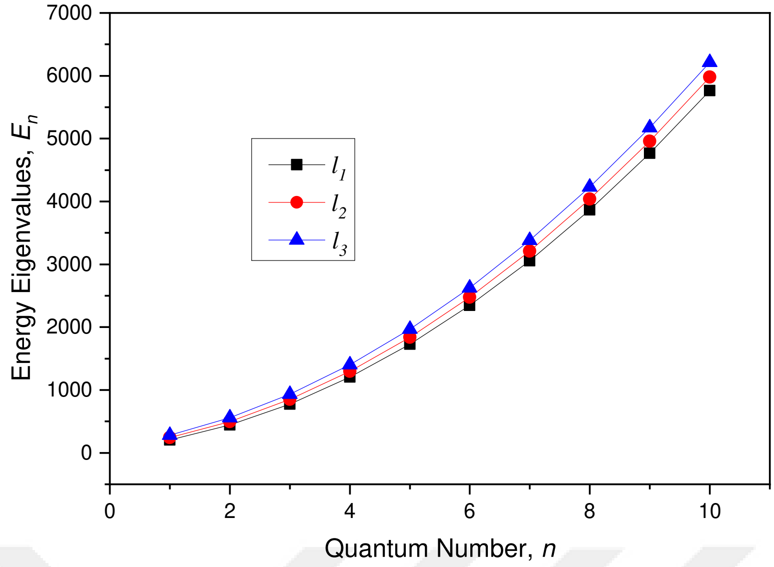

Figure 3.27 The graph of energy eigenvalues of Pöschl-Teller potential in Case 3 for $\gamma = 0.6, m = 1/2, \hbar = 1, V_0 = 0.5, \alpha = -0.004$.

CHAPTER 4

CONCLUSION

In this thesis, the influence of the velocity-dependent on the solution of non-relativistic SE has been investigated and energy spectrums are calculated for Harmonic oscillator, Coulomb, Kratzer, Mie, Hulthen, Cornell, Woods-Saxon and Pöschl-Teller potentials for any quantum states within the framework of the NU. The corresponding velocity-dependent term $\varepsilon(r)$ is considered in different case for these potentials in accordance to the types of potentials.

As a result of studies, the energy eigenvalues and eigenfunctions of the proposed potentials are analyzed. First, solutions for the value $\varepsilon(r) = \gamma\rho_0$ of the form factor have been made for Harmonic oscillator, Coulomb Kratzer, Mie, Hulthen, Cornell, Woods-Saxon and Pöschl-Teller potentials. Of the potentials mentioned above, the obtained energy spectrums were calculated analytically for Harmonic oscillator, and numerically for Coulomb, Kratzer, Mie, Hulthen Cornell, Woods-Saxon and Pöschl-Teller potentials. The determined wave functions and the calculated energy eigenvalues are in similar form of corresponding functions in the case of non-velocity-dependent in the literature.

Although we obtained the energy equation analytically for Coulomb, Kratzer, Mie, Hulthen, Cornell, Woods-Saxon and Pöschl-Teller potentials, due to the insufficiency of the used computer program, the appropriate constants for some parameters were selected and numerical values of the energy were presented as tables. Energy graphs were plotted for these values.

During the study, solutions were made for all potentials by using form factor $\varepsilon(r) = \gamma r$ condition. In the same way, the energy eigenvalues and corresponding wave functions are obtained for all potentials. The calculated wave functions and energy spectrums for the proposed potentials are slightly different compared to the literature and only give the same results in case $\varepsilon(r) = 0$. While expecting the energy equation to come out analytically here, since the equation was formed in very complex structures the numerical value of the energy was given by taking fixed parameters because of the insufficiency of the computer program. The values of energy are presented as tables and energy graphs are drawn for these potentials. These results are new and have never been reported in the literature before to the best of our knowledge.

In the last part of studies, the solutions of non-relativistic SE have been investigated with the case of the velocity-dependent term $\varepsilon(r) = \gamma r^2$ for the considered potentials. However energy spectrums have been calculated only Harmonic oscillator, Hulthen, Woods-Saxon and Pöschl-Teller potentials. The solution of the Harmonic oscillator is show similarities with a slight difference when compared with the literature. Other potentials have not been solved in the literature so far and these potential have only been investigated in our study. At the same time, the calculated wave function and energy spectrums are for Hulthen, Woods-Saxon and Pöschl-Teller potentials when $\varepsilon(r) = 0$ as in literature, the potentials are reduced to the simple form of the corresponding potentials. Similarly values of energy here are numerical and the results are shown as tables. In additionally, energy graphs are plotted for these potentials. The reason for calculating the energy equation numerically is that the equation is very complex structure and used calculating program is inefficient.

In this thesis, it is presented that the velocity-dependent potentials with different forms have definitely an effect on the energy eigenvalues of the system under consideration. Apart from our work in different studies can be done in the future. For example in addition to this study, the solution of the effect velocity-dependent potentials on the solution of relativistic wave equation for physical potential is determined for obtaining energy spectrum by using different methods. Also the solvable systems can be increased in the solution of the effect velocity-dependent potentials on the solution of relativistic wave equation and investigate the superiority of correspondence method on the methods in literature.

REFERENCES

[1] Kreiger, J. B. (1967). Use of the WKB Method for Obtaining Energy Values, *The Journal of Chemical Physics*. **47(8)**, 2942-2945.

[2] Schiff, L. I. (1968). *Quantum Mechanic.* 3nd edition. McGraw-Hill: New York.

[3] Griffiths, D. J. (1995). *Introduction to Quantum Mechanic*. Prentice Hall.

[4] Cooper, F., Freedman, B. (1983). Aspect of Supersymmetric Quantum Mechanics, *Annals of Physics*. **146(2)**, 262-288.

[5] Mlodinow, L. D., Shatz, M. P. (1984). Solving the Schrödinger Equation with use of 1/N Perturbation Theory, *Journal of Mathematical Physics*. **25(4)**, 943-950.

[6] Akdaş, M., Sever, R. (2004). Exact Supersymmetric Solution of Schrodinger Equation for Central Confining Potentials by using the Nikiforov-Uvarov Method, *Journal of Molecular Structure Theochem*. 7**10(1-3)**, 223-228.

[7] Tang, A. Z., Chan, F. T. (1987). Sifted 1/N Expansion for the Hulthen Potential, *Physical Review A*. **35(2)**, 911.

[8] Drigo, E., Ricotta, R. M. (1995). Supersymetry, Variational Method and Hulthen Potential, *Modern Physics Letters A*. **10(22)**, 1613-1618.

[9] Varshni, Y. P. (2004). SUSY Super Potentials for a Confined Hulthen Potential, *Modern Physics Letters A*. **19(37)**, 2757-2764.

[10] Gönül, B., Ozer, O., Cançelik, Y., Koçak, M. (2000). Hamiltonian Hierarchy and the Hulthen Potential, *Physics Letters A*. **275**, 238-243.

[11] Fakhri, H., Chenaghlou, A. (2004). Extented Supersymmetry for the Bound States of the Generalized Hulthen Potential Hierarchy, *Journal of Physics A: Mathematical and General*. **37(35)**, 8545.

[12] Bayrak, O., Boztosun, I. (2006). Analytical Solutions to the Hulthen and the Morse Potentials by using the Asymptotic Iteration Method, *Journal of Molecular Structure Theochem*. **802**, 17-21.

[13] Çiftçi, H., Hall, R. L,. Saad, N. (2003). Asymptotic Iteration Method for Eigenvalue Problems, *Journal of Physics A: Mathematical and General*. **36(47)**, 11807.

[14] Çiftçi, H., Hall, R. L**.,** Saad, N. (2005). Construction of Exact Solutions to Eigenvalue Problems by the Asymptotic Iteration Method, *Journal of Physics A: Mathematical and General.* **38(5)**, 1147.

[15] Bayrak, O., Boztosun, I. (2007). The Pseudospin Symmetric Solution of the Morse Potential for Any State*, Journal of Physics A: Mathematical and Theoretical.* ***40(36)****, 1119.*

[16] Ikhdair, S. M., Sever, R. (2007). Exact Solution of Radial Schrödinger Equation for Some Physical Potentials, *Central European Journal of Physics.* **5(7)**, 516-527.

[17] Ikhdair, S. M., Sever, R. (2007). Exact Polynomial Eigensolutions of the Schrödinger Equation for the Pseudoharmonic Potential, *Journal of Molecular Structure Theochem.* **806**, 155.

[18] Tezcan, C., Sever, R. (2009). A General Approach for the Exact Solution of the Schrödinger Equation, *International Journal of Theoretical Physics.* **48(27)**, 337–350.

[19] Goldman, I. I., Krivchenkov, V. D. (1961). *Problems in Quantum Mechanics*. Pergamon Press: New York.

[20] Weissman, Y., Jortner, J. (1979). The Isotonic Oscillator, *Physics Letters A.* **70**, 177-179.

[21] Sever, R., Bucurgat, M., Tezcan, C., Yeşiltaş, Ö. (2008). Bound State Solution of Schrödinger Equation for Mie potential, *Journal of Mathematical Chemistry*. **43**, 749-755.

[22] Maitland, G. C., Rigby, M., Smith, E. B., Wakeham, W. A. (1987). *Intermolecular Forces.* Oxford Univ Press: Oxford.

[23] Ikot, A. N., Hassanabadi, H., Akpan, I. O., Abbey, T. M. (2016). Exact Solution of Schrödinger Equation with Improved Ring-Shaped Non-Spherical

Harmonic Oscillator and Coulomb Potential, *Communications in Theoretical Physics*. **65(5)**, 569-574.

[24] Bayrak, O., Açıksöz, E. (2015). Corrected Analytical Solution of the Generalized Woods-Saxon Potential for Arbitrary States, *Physica Scripta.* **90(1)**, 015302.

[25] Jian-You, G., Zheng, F. Z., Xu, F. X. (2002). Solution of the Relativistic Dirac Woods-Saxon Problem, *Physical Review A*. **66(6)**, 062105.

[26] Maghsoodi, E., Hassanabadi, H., Zarrinkamar, S. (2013). Exact Solution of Dirac Equation with the Pöschl-Teller Potential Double-Ring-Shaped Coulomb Potential via the Nikiforov-Uvarov Method, *Chinese Physics B*. **22(3)**, 03032.

[27] Hassanabadi, H., Ikot, A. N., Zarrinkamar, S. (2014). Exact Solution of Klein-Gordon Equation with the Pöschl-Teller Potential Double-Ring-Shaped Coulomb Potential, *Acta Physica Polonica A*. **3**,126.

[28] Kisslinger, L. S. (1955). Scattering of Mesons by Light Nuclei, *Physical Review*. **98(3)**, 761.

[29] Sharma, R. D., Green, A. E. S. (1967). Velocity-Dependent OBEP and Nucleon-Nucleon Scattering Phase Shift in the Born Approximation, *Nuclear Physics B*. **3(1)**, 33-46.

[30] Serra, L. I., Lipparini, E. (1997). Spin Response of Unpolarized Quantum Dots, *Europhysics Letters.* **40(6),** 667.

[31] MPi, M. B., Gatica, S. M., Hernandez, E. S., Navarro, J. (1997). Structure and Energetics of Mixed He-He Drops, *Physical Review B.* **56**, 8997.

[32] Salti, M., Aydoğdu, O. (2017). Spin (Pseudospin) Doublet in View of Energy-Dependent Potential, *Turkish Journal of Physics.* 41-12.

[33] Sett, G. C., Talukdar, B. (1989). Phase-Function Method for Velocity-Dependent Potentials, *Pramana*. **33(3)**, 381-389.

[34] Nelson, B., Sheeks, B. (1982). Path Integration for Velocity-Dependent Potentials, *Communications in Mathematical Phys*ics. **84(4)**, 515-530.

[35] Razavy, M., Field G., Levinger J. S. (1962). Analytical Solutions for Velocity-Dependent Nuclear Potential, *Physical Review*. 125-269.

[36] Lodhi, M.A.K. (1969). Single-Particle Energy Levels Based on the Velocity-Dependent Potential, *Physical Review*. **182**, 1061.

[37] Lodhi, M.A.K. (1970). Spin-Orbit Splitting Effect on Single-Particle Energy Levels Based on Velocity-Dependent Potential, *Physical Review C*. **1**, 365.

[38] Green, A. E. S., Darewych G., Berezdivin, R. (1967). Morse Function and Velocity-Dependent Nuclear Potentials, *Physical Review*. **157**, 929.

[39] Miller, L. D., Green A. E. S. (1969). Independent-Particle-Model Energy-Level Formula, *Physical Review.* **184**, 1012.

[40] Jaghoub, M. I. (2001). S-Wave Bound and Scattering State Wave Functions for A Velocity-Dependent Kisslinger Potential, *European Physical Journal A-Hadrons and Nuclei.* **11(2)**, 175-183.

[41] Jaghoub, M. I. (2002). Bound and Scattering Wave Functions for a Velocity-Dependent Kisslinger Potential for l>0, *The European Physical Journal A-Hadrons and Nuclei.* **13(3)**, 349-354.

[42] Jaghoub, M. I. (2002). Perturbation Theory for Velocity-Dependent Potentials, *The European Physical Journal A-Hadrons and Nuclei*. **15(4)**, 443-448.

[43] Jaghoub, M. I. (2006). Perturbation Theory for Isotropic Velocity-Dependent Potentials Bound-States Case, *The European Physical Journal A-Hadrons and Nuclei.* **27(1)**, 99-103.

[44] Jaghoub, M. I. (2006). Perturbation Theory for Isotropic Velocity-Dependent Potentials Bound-States Case, *Physical Review A.* **74(3)**, 032702.

[45] Soylu, A., Bayrak, O., Boztosun, I. (2012). Effect of the Velocity-Dependent Potentials on the Energy Eigenvalues of the Morse Potential, *Central European Journal of Physics.* **10(4)**, 953-959.

[46] Bayrak, O., Soylu A., Boztosun, I. (2011). Effect of the Velocity-Dependent Potentials on the Bound State Energy Eigenvalues, *Chinese Physics Letters.* **28(4)**, 040304.

[47] Lodhi, M.A.K. (1970). Spin-Orbit Splitting Effect On Single-Particle Energy Levels Based on Velocity-Dependent Potential, *Physical Review. C*. **1**, 365.

[48] Lodhi, M.A.K. (1972). Single-Particle States of Heavy and Super Heavy Nuclei in a Velocity-Dependent potential, *Zeitschrift für Noturforschung.* **27(12)**, 1862-183.

[49] Moreno, G. A., Barrachina, R. O. (2008). A Velocity-dependent Potential of a Rigid Body in a Rotating Frame, *American Journal of Physics*. **79**, 1146-1149.

[50] Green, A. E. S., Rio, D. E., Ueda, T. (1981). Analytic Velocity-Dependent Potential for Bound and Scattering States of Electrons and Atoms, *Physical Review A*. **24**, 6.

[51] Green, A. E. S., Darewvch, G., Berezdivin, R. (1967). Morse Function and Velocity-Dependent Nuclear Potentials, *Physical Review*. **157**, 4.

[52] Miller, L. D., Green, A. E. S. (1969). Independent-Particle-Model Energy-Level Formula, *Physical Review*. 1**84**, 1012.

[53] Nikiforov, A. V., Uvarov, V. B. (1988). *Special Functions of Mathematical Physics*. Birkhauser: Bassel.

[54] Büyükılıç, F., Egrifes, H., Demirhan, D. (1997). Solution of the Schrodinger Equation for Two Different Molecular Potentials by the Nikiforov-Uvarov Method, *Theoretical Chemistry Accounts*. **98**,192-196.

[55] Akdas, M., Sever, R. (2004). Exact Supersymmetric Solution of Schrodinger Equation for Central Confining Potentials by using the Nikiforov-Uvarov Method, *Journal of Molecular Structure Theochem*. 7**10**, 223.

[56] Berkdemir, C., Han, J. (2005). Any ℓ-State Solutions of the Morse Potential through the Pekeris Approximation and Nikiforov-Uvarov Method, *Chemical Physics Letter*s. **409(4-6)**, 203-207.

[57] Berkdemir, C. (2009). A Novel Angle-Dependent Potential and Its Exact Solution, *Journal of Mathematical Chemistry*. **46 (1)**, 139-154.

[58] Tezcan, C., Sever, R. (2009). A general Approach for the Exact Solution of the Schrödinger Equation, *International Journal of Theoretical Physics*. **48 (2)**, 337-350.

[59] Berkdemir, C. (2012). *Application of the Nikiforov-Uvarov Method in Quantum Mechanic*. Theoretical Concept of Quantum Mechanics. 11.

[60] Hulthen, L. (1942). On the Virtual State of the Deuteron, *Physical Review*. **61(9-10)**, 671.

[61] Pekeris, C. L. (1934). The Rotation-Vibration Coupling in Diatomic Molecules, *Physical Review*. **45(2)**, 98.

[62] Kratzer, A. (1920). Die Ultraroten Rotationsspektren der Alogenwasserstoffe, *Zeitschrift für Physik.* **3**, 289-307.

[63] Mie, G. (1903). Zur Kinetischen Theorie der Einatomigen, *Körper Annalen der Physik.* **316(8)**, 657-697.

[64] Hamzavi, M., Rajabi, A. A. (2013). Bound Dirac States for Pseudoscalar Cornell Potential: 3+1 Dimensions, *Chinese Physics C*. **37(10)**, 103102.

[65] Taylor Series www.Wikipedia .org, 6.12.2019.

[66] Woods, R. D., Saxon, D. S. (1954). Diffuse Surface Optical Model for Nucleon-Nuclei Scattering, *Physical Review*. **95(2)**, 577.

[67] Pöschl, G., Teller, E. (1933). Bemerkungen zur Quantenmechanik des Anharmonischen Oszillators, *Zeitschrift für Physik*. **83(3-4)**, 143-151.

CURRICULUM VITAE

PERSONAL INFORMATION

Name, Surname: Yıldız BERK ATEŞ

Nationality: Turkish

Birth Date and Place: 1983 / İslahiye

email: yildiz. berk@hotmail.com

EDUCATION INFORMATION

M.Sc. (2011) University of Bülent Ecevit, Physics

B.Sc. (2009) University of Bülent Ecevit, Physics

PUBLICATIONS

SCI:

Y. B. Ateş, E. Olğar U. S. Okorie, A. N. Ikot, "Analytical Solution of Schrödinger Equation for Isotropic Velocity-Dependent Potentials'', Physica Scripta, Vol. 94, No. 11., August. 2019.